The Role of Direct Carboxyl-terminal Truncated HBx Target Genes in Hepatocellular Carcinoma

ZHU, Ranxu

A Thesis Submitted in Partial Fulfillment

of the Requirements for the Degree of

Docotor of Philosophy

in

Medical Sciences

The Chinese University of Hong Kong

September 2011

ProQuest LLC.
789 East Eisenhower Parkway
P.O. Box 1346
Ann Arbor, MI 48106 - 1346

ABSTRACT

Chronic hepatitis B virus (HBV) infection is a major cause of hepatocellular carcinoma (HCC) and the X protein of HBV (HBx) is highly implicated in hepatocarcinogenesis. Recently HBx has been shown to act as coregulator of cancer-related genes by interacting with DNA-bound transcription factor (TF). The carboxyl-terminal truncated forms of HBx (tHBx), rather than the full-length counterpart, have been shown to frequently express in HCC tissues and possess oncogenic abilities *in vitro* and *in vivo*. tHBxΔ35 (deletion of 35aa carboxyl-amino acids) is one of the truncated oncoproteins naturally generated by cytidine deaminases in HCC tissues. However, how tHBxΔ35 exerts oncogenic effects is poorly understood.

In this study, we used genome-wide location analysis and functional studies to elucidate the role of direct tHBxΔ35 target genes in the development of HCC. tHBxΔ35 was cloned from the serum of an HCC patient infected with HBV genotype C. Ectopic expression of tHBxΔ35 in 2 immortal human liver cell lines (MIHA and LO2) significantly increased cell proliferation compared with vector-control cells as shown by MTS and colony formation assays ($p<0.05$). To characterize direct targets of tHBxΔ35 that confer oncogenic properties, chromatin immunoprecipitation (ChIP) coupled with human promoter arrays were performed. These analyses identified 347 and 485 target genes in tHBxΔ35-expressing MIHA and LO2 cells ($p<0.001$), respectively, of which 42 genes were common in both cell lines. Notably, gene

ontology analysis of these target genes revealed an enrichment of negative regulators of cell proliferation ($p<0.005$). Quantitative ChIP-PCR and RT-PCR analyses further demonstrated that one of the common target genes, *growth arrest specific 2* (*GAS2*) was directly repressed by tHBxΔ35 in liver cells and down-regulated in a subset (22/54) of HBV-associated HCCs compared with the non-tumor tissues.

Ectopic GAS2 expression in SK-Hep1 HCC cells significantly decreased cell growth by MTS and colony formation assays ($p<0.05$). The GAS2-induced growth inhibition was mediated by apoptosis as shown by increase in sub-G1 population and induction of caspase-3 and PARP cleavage. Treatment with a chemotherapy drug etoposide further enhanced the apoptotic effect of GAS2. Conversely, siRNA-mediated knockdown of *GAS2* and etoposide treatment synergistically decreased caspase-3 and PARP cleavage in MIHA and HepG2 cells. Furthermore, TF binding site analysis revealed highly significant over-representation of POU3F2 binding sites in tHBxΔ35-bound loci ($p<1E-53$) including the *GAS2* promoter.

In conclusion, our genome-wide binding analysis of tHBx revealed direct repression of *GAS2*, which may provide a selective growth advantage for precancerous cells. POU3F2 may function as a previously unidentified TF partner of tHBx in exerting its oncogenic properties.

摘　　要

慢性乙型肝炎病毒(HBV)感染是原發性肝細胞癌的一個主要病因。HBV 中的 HBx 蛋白被廣泛地顯示在肝癌的形成中。近年來，HBx 通過與 DNA 結合的轉錄因數相互作用而被顯示充當癌症相關基因的協調因數。羧基末端被截斷的 HBx, 而不是完整的 HBx,頻繁地被發現在 HCC 組織裏，並在體內外顯現出致癌基因的能力。tHBxΔ35(羧基末端被截斷 35 個氨基酸的 HBx)在 HCC 組織裏是被胞苷脫氨酶自然水解所產生的癌基因蛋白。然而，tHBxΔ35 如何發揮致癌效應卻很少被人理解。

在我們的研究中，我們用全基因組定位分析和功能研究來闡述 tHBxΔ35 直接的靶基因在 HCC 發展中的作用。tHBxΔ35 基因是從感染 HBV 基因型 C 的病人血清中克隆出來的。通過用 MTS 和集落形成鑒定方法，高表達于兩個永生化肝細胞株（MIHA 和 LO2）的 tHBxΔ35 相對於對照組細胞明顯地增加細胞的增殖能力(p<0.05)。為了顯示 tHBxΔ35 致癌基因特性的直接靶基因的特徵，我們採用了人類啟動子免疫共沉澱鑒定技術。分析鑒定出了分別表達在 MIHA 和 LO2 細胞株的 tHBxΔ35 的 347 個和 485 個靶基因(p<0.001)，其中有 42 個靶基因共同顯示在兩個細胞株。值得注意的是，這些共同靶基因的本位基因分析揭示了為細胞增殖的負性調節因數的雲集(p<0.005)。定量 ChIP-PCR 和 RT-PCR 分析進一步闡述了作為共同靶基因之一的特異性生長捕獲基因 2(*GAS2*)，在肝細胞株中直接被 tHBxΔ35 所抑制，並且 GAS2 的表達在 HBV 相關的 HCC 中相對於非腫瘤組織，有一部分被下調(22/54)。

通過用 MTS 和集落形成鑒定方法，在肝癌細胞株 SK-Hep1 中高表達的 GAS2 明顯地減少細胞的增殖(p<0.05)。由 GAS2 所誘導地生長抑制的凋亡被通過在 sub-G1 種群中的增加和凋亡蛋白酶 caspase-3 與 PARP 誘導的水解所證明。化療藥物 etoposide 的處理進一步增加了 GAS2 的凋亡效應。相反地，在兩個細胞株中，如果用 siRNA 基因敲除 *GAS2*, etoposide 則減少凋亡蛋白酶 caspase-3 與 PARP 的水解。另外，轉錄因數結合位點的分析揭示了 POU3F2 非常顯著有代表性地結合在 tHBxΔ35 結合的基因座上(p<1E-53)，並且還同時結合 *GAS2* 的啟動子。

總之，我們的 tHBxΔ35 全基因組結合分析揭示了 *GAS2* 的直接抑制作用，這可能為癌前細胞提供選擇性的生長優勢。POU3F2 可能充當在 tHBxΔ35 執行致癌特性時的尚未鑒定的轉錄因數伴侶。

ACKNOWLEDGEMENTS

I would like to express my highly sincere appreciation to my supervisor, Professor Henry Chan, for his tremendous support throughout my study. I benefit a lot from his patient guidance, thoughtful ideas and instructive suggestion. I am also motivated by his profound inspirations.

I would also like to express my special gratitude to my co-supervisor, Prof. Alfred Cheng, for his instruction with great patience. As I was a beginner in the field of medical science, he spent abundant time and energy teaching me about the basically biological skills and scientific thinking. And he also helped me overcome lots of difficulties in the experiments for his patient guidance.

I attribute my Doctor degree to their cautious direction and encouragement. Without them, I am not competent in my project and thesis.

Special thanks must be dedicated to Prof. Yangchao Chen in The Chinese University of Hong Kong for his assistant in lentivirus generation. I wish to thank Prof. Yutaka Kondo in Aichi Cancer Center Research Institute, Japan, for his generous provision of GAS2-expression vector. Thanks also go to Prof. Paul Lai of the Department Surgery for providing the clinical specimens. I would also like to express my thanks to Prof. Jun Yu and Prof. Vincent Wong for their helpful advice.

I am thankful to the team members of the Institute of Digestive Disease, Miss Suki Lau, Dr Xiaoxing Li, Dr Martin Chan, Dr William Wu, Dr Paul Cheung, Mr. Eagle Chu, for their immense support and unconditional technical assistance.

Finally, my gratitude is devoted to my colleagues in Institute of Digestive Disease and in Room 415, Cancer Center, who have given me countless help and helpful advice, and most importantly, the warm and fragrant friendship during the years of my study.

LIST OF FIGURES

Figure 1.1 The genomic structure of HBV 19

Figure 1.2 Schematic structure of hepatitis B virus.....20

Figure 1.3 Structure of HBx protein.....22

Figure 1.4 Transduction signal pathways affected by HBx.....26

Figure 1.5 A working model for the regulatory network of P53-dependent apoptosis induced by GAS2.....34

Figure 2.1 A schematic diagram of a lentivirus Vector, pRRL-cPPT-CMV-X-IRES- EGFP-PRE-SIN.....43

Figure 3.1 Expression of HBxΔ35 protein in lentivirus-infected LO2 and MIHA cells.....73

Figure 3.2 Western blot analysis of HBxΔ35 protein expression in LO2 and MIHA cells infected with lenti-HBxΔ35 or lenti-CTRL.....74

Figure 3.3 COOH-terminal truncated HBx (HBxΔ35) increased the growth rate of non- tumorigenic liver cell lines.....75

Figure 3.4 Effect of HBxΔ35 on colony formation.....76

Figure 3.5 Identification of common direct targets of HBxΔ35 in LO2 and MIHA hepatocytes.....78

Figure 3.6 Confirmation of authenticity of ChIP assay.....79

Figure 3.7 Quantitative RT-PCR analysis of HBxΔ35 target genes in MIHA and LO2 cells.....81

Figure 3.8 Enrichment map demonstrating the HBxΔ35 binding region in the *GAS2* proximal promoter of the LO2 and MIHA cells.....83

Figure 3.9 Confirmation of *GAS2* as HBxΔ35 target gene by quantitative and conventional ChIP-PCR assays in LO2 and MIHA cells.....84

Figure 3.10 Expression of *GAS2* mRNA and protein in lenti-HBxΔ35 and lenti-CTRL -infected MIHA cells.....86

Figure 3.11 Western blot analysis of GAS2 expression in liver and HCC cell lines 88

Figure 3.12 Effect of GAS2 overexpression on HCC cell growth.....89

Figure 3.13 Effect of GAS2 on cell cycle progression.....91

Figure 3.14 Ectopic overexpression of *GAS2* enhanced susceptibility to cell apoptosis 94

Figure 3.15 Overexpression of GAS2 increased the expression of apoptosis markers in HCC cells treated by etoposide.....95

Figure 3.16 Effect of siRNA on GAS2 expression in MIHA and HepG2 cells.....97

Figure 3.17 siRNA-mediated silencing of *GAS2* decreased the expression of apoptosis markers in MIHA and HepG2 cells treated with etoposide...98

Figure 3.18 siRNA-mediated knockdown of P53 in SK-hep1 cells.....100

Figure 3.19 Effect of P53 on GAS2-induced apoptosis in HCC cells.....101

Figure 3.20 Expression of *GAS2* transcripts in HCC specimens as determined by real-time RT-PCR.....104

Figure 4.1 Identification of potential transcription factor partners of HBxΔ35 by promoter binding site analysis.....117

Figure 5.1 A working model of transcriptional repression by C-terminal truncated HBx.....122

LIST OF TABLES

Table 2.1 Demographic information of 54 patients diagnosed wit HCC.....40

Table 2.2 Antibodies used in Western Blot.....48

Table 2.3 Sequence of Primers used in Real-time PCR& semi quantitative-PCR... 58

Table 2.4 Sequence of Primers for RT-PCR.....65

Table 2.5 Sequence of Primers for real-time and conventional ChIP-PCR.....67

LIST OF ABBREVIATIONS

7-AAD	7-Amino-actinomycin D
aa	Amino acid
BSA	Bovine serum albumin
BCLC	Barcelona Clinic Liver Cancer
BCP	Basal core promoter
cDNA	Complementary DNA
ChIP-chip	Chromatin immunoprecipitation microarray
CMV	Cytomegalovirus (human)
CO_2	Carbon dioxide
cPPT	HIV-1 central polypurine tract
C-tHBx	Carboxyl-terminal truncated HBx
CREB	cAMP-response-element- binding protein
DDB1	Damage-specific DNA binding protein
DMEM	Dulbecco's modified Eagle's medium
DMSO	Dimethyl sulfoxide
DNA	Deoxyribonucleic acid
dNTP	Deoxynucleotide triphosphates
E. coli	Escherichia coli
EGFP	Enhanced green fluorescent protein
4E-BPs	eIF4E-binding proteins
FACS	Fluorescence-activated cell sorting analysis
FBS	Fetal bovine serum
GAS2	Growth arrest-specific gene 2
HBcAg	Hepatitis B virus core protein
HBeAg	Hepatitis B virus e antigen
HBsAg	Hepatitis B virus surface portein
HBV	Hepatitis B virus
HBx	Hepatitis B virus X protein

HBxΔ35	3'- deleted Δ35aa of HBx
HCC	Hepatocarcinoma
HCV	Hepatitis C virus
IRES	The internal ribosome entry site of the encephalomyocarditis virus
IL-8	Interleukin 8
kb	Kilo base pair
LTR (ΔU3)	Deletion in the HIV-1 LTR U3 sequence
MAPK	Mitogen-activated protein kinase
miRNA	MicroRNA
MMS	Methyl methanesulfonate
mRNA	Messager RNA
MTS	[3-(4,5-dimethythiazol-2-yl)-5-(3- carboxymethoxy-phenyl)-2-(4-sulfophenyl)-2H-tetrazolium assay
N	Normal tissue
NAFLD	Nonalcoholic fatty liver disease
NASH	Nonalcoholic steatohepatitis
NF- κB	Nuclear factor kappa B
NT	Adjacnt non-tumor tissue
ORF	Open reading frames
PARP	Poly (ADP-ribose) polymerase
PBS	Phosphate buffered saline
PBST	Phosphate buffered saline Tween-20
PCNA	Proliferating cell nuclear antigen
PCR	Polymerase chain reaction
PE	Phycoerthrin
PI	Propidium Iodide
PKC	Protein kinase C
PRE	Posttranscriptional regulatory element (human hepatitis virus)
RISC	RNA-induced silencing complex

RNA	Ribonucleic acid
RRE	HIV Rev response element
RSV	Rous sarcoma virus and HIV chimeric long terminal repeat
RT-PCR	Reverse transcription-PCR
SAPK/JNK	Stress-activated protein kinase/NH2-terminal-Jun kinase
SDS	Sodium dodecylsulfate
TACE	Transarterial chemoembolization
TAE	Transcatheter arterial embolization
TBE	Tris-boric acid-EDTA
TBST	Tris-buffered saline-Tween 20
TF	Transcription factor
TSS	Transcription start site
UTR	Untranslational region
VEGF	Vascular endothelial growth factors
WHO	World Health Organization

TABLE OF CONTENTS

ABSTRACT i
摘　　要 iii
ACKNOWLEDGEMENTS v
LIST OF FIGURES vii
LIST OF TABLES ix
LIST OF ABBREVIATIONS x
TABLE OF CONTENTS xiii
CHAPTER ONE-INTRODUCTION 1
1.1 Hepatocellular carcinoma 1
1.1.1 Epidemiology 1
1.1.2 Etiology 3
1.1.3 Prevention and therapy 9
1.1.4 Gene therapy 12
1.2 Hepatitis B Virus 14
1.2.1 Epidemiology of Hepatitis B Virus Infection 14
1.2.2 HBV Genotypes and Their Significances 15
1.2.3 Morphology and Genome of Hepatitis B Virus 17
1.3 Hepatitis B Virus X Protein 21
1.3.1 Structure of HBx protein 21
1.3.2 HBx activates various signal transduction pathways 23
1.3.3 Significance of COOH-terminal Truncated HBx in Liver Tumors 27
1.4 Growth arrest-specific gene 2 (GAS2) 29
1.4.1 Definition and function of GAS2 29
1.4.2 GAS2 and p53-dependent apoptosis 31
1.4.3 GAS2 and cancer 35
1.5 Hypothesis and objectives of the Study 37
CHAPTER TWO- METHODOLOGY 38
2.1 Cell cultures 38
2.2 Patients and clinical specimens 39
2.3 Vector construction and lentivirus production 42
2.4 Generation of Lentivirus 44
2.5 Lentivirus Infection 44
2.6 Plasmids and transfection 45
2.7 Western Blot Analysis 46
2.8 Counting Cell 49
2.9 Proliferation Assay 49
2.10 Colony Formation Assay 50
2.11 Chromatin Immunoprecipitation Microarry (ChIP-chip) 51
2.11.1 Chromatin Immunoprecipitation (ChIP) 51
2.11.2 Microarray hybridization 54
2.11.3 Data Analysis and Identification of In vivo DNA Binding Sites 54
2.12 RNA Extraction 55
2.13 Reverse transcription (RT) 56

2.14 Quantitative RT-polymerase chain reaction (Real-time PCR) 57
2.15 Semi-quantitative polymerase chain reaction (PCR) 63
2.15.1 RT-PCR 63
2.15.2 Real-time ChIP-PCR 66
2.15.3 Conventional ChIP-PCR 66
2.16 Flow cytometry 68
2.17 Annexin V Apoptosis Assay 69
2.18 Statistical analysis 70
CHAPTER THREE- RESULTS 71
3.1 **Oncogenic ability of carboxyl-terminal truncated HBx** 71
3.2 **Identification of direct target genes of HBxΔ35 in human hepatocytes** 77
3.2.1 Genome-wide location analysis of HBxΔ35 binding sites 77
3.2.2 Validation of HBxΔ35 target genes in hepatocyte cell lines 80
3.3 Confirmation of GAS2 as a direct transcriptional target of HBxΔ35 82
3.3.1 Binding of HBxΔ35 in GAS2 gene promoter 82
3.3.2 HBxΔ35 down-regulates GAS2 mRNA and protein levels 85
3.4 Functional characterization of GAS2 in HCC development 87
3.4.1 Ectopic overexpression of GAS2 suppresses HCC cell proliferation 87
3.4.2 Ectopic overexpression of GAS2 alters cell cycle progression in HCC cells 90
3.4.3 Ectopic overexpression of GAS2 enhances susceptibility to apoptosis 92
3.4.4 Knockdown of GAS2 reduces apoptosis 96
3.4.5 GAS2-induced apoptosis is P53-dependent 99
3.5 Correlation between GAS2 expression and carboxyl-terminal HBx truncation in HCC specimens 102
CHAPTER FOUR- DISCUSSION 105
4.1 Oncogenic properties of COOH-terminal truncated (Δ35) HBx 105
4.2 Anti-oncogenic properties of Growth arrest specifc 2 (GAS2) in HCC 109
4.3 Clinical significance of GAS2 down-regulation by COOH-terminal truncated HBx in HCC 113
4.4 Future Studies 115
4.5 Limitation of the present study 118
CHAPTER FIVE- CONCLUSION 121
REFERENCES 123
PUBLICATIONS 142

CHAPTER ONE-INTRODUCTION

1.1 Hepatocellular carcinoma

1.1.1 Epidemiology

Liver cancer is the fifth most common tumor among men and the eighth in women worldwide, presenting approximately 5.7% of all new cancer cases. Liver cancer has become a major health problem in low-income countries, 82% of liver cancer cases worldwide occurred in eastern and southeastern Asia and sub-Saharan Africa such as Cameroon and Mozambique. Particularly, the highest incidence rate of liver cancer is recorded in China (55% of the world total). Although the liver cancer incidence is at low or intermediate levels in most developed areas of the world, including North America and most of Europe, there is an increasing trend recently. Globally, men have higher liver cancer rates than women with the sex ratio (male: female) around 2.4, and the difference is much greater in the high-risk areas. More importantly, liver cancer also becomes the third leading cause of cancer-related death in men worldwide due to its very poor prognosis, with the mortality nearly equivalent to the incidence rate (Boyle and Levin et al., 2008; Parkin et al., 2005; Parkin et al., 2006).

Hepatocellular carcinoma (HCC) is a primary malignant neoplasm derived from hepatocytes and accounts for about 80% of all primary liver cancers. Other tumour types in liver cancer including intrahepatic cholangiocarcinoma, hepatoblastoma and angiosarcoma are relatively rare compared to HCC. Since HCC is the predominant

primary liver cancer in most countries, the global variations in the rates of liver cancer discussed above can be regarded as a broadly accurate reflection of trends in HCC incidence (Boyle and Levin et al., 2008; Ahmed et al., 2008). The global age distribution of HCC varies by region, incidence rate, gender, and possibly by etiology (Parkin et al., 2002). In most high-risk Asian populations (e.g., Hong Kong), the highest age-specific rates occur among people aged 75 and older, which is similar to that in the Western most low-risk populations. In contrast, the age-specific rates of men in high-risk African populations (e.g., Gambia, Mali) tend to peak in the 60-65 years, while that of women peak between 65 and 70 years. The peak of age-specific rate in South Africa and Egypt is over the age of 85, which shows more similarity to low-risk population areas than high-risk African populations. These variations of age-specific patterns are likely related to the differences in the dominant hepatitis virus in the population, the age at viral infection as well as the existence of other risk factors (World Health Organization, 2008).

1.1.2 Etiology

HCC is such a complex disease that its origin is still unclear. According to the data of epidemiology, HCC is considered to be associated with many risk factors and cofactors (Gomaa et al., 2008; Di Bisceglie et al., 2002). Approximately 70%–90% of patients with HCC have an available case history of chronic liver disease and hepatic cirrhosis, with major risk factors including chronic infection with hepatitis B virus (HBV), hepatitis C virus (HCV), alcoholic liver disease, and nonalcoholic steato-hepatitis (NASH) (El-Serag et al., 2007, Poon et al., 2009). Additional risk factors for developing HCC include intake of aflatoxin-contaminated food, diabetes, obesity, certain hereditary conditions such as hemochromatosis, and some metabolic disorders (El-Serag et al., 2007; Montalto et al., 2002; Gomaa et al., 2008).

1.1.2.1 Virus Hepatitis

The major risk factors of HCC is, chronic virus hepatitis with hepatitis B virus (HBV) or hepatitis C virus (HCV) infection, which accounts for 80–90% of all HCC worldwide (Bosch et al., 2005). To date, it has been estimated that HBV is responsible for 50%–80% of HCC cases worldwide, whereas 10%–25% of HCC cases are thought to be a result of HCV infection (Block et al., 2003; Anthony et al., 2001). HBV is more prevalent, and the patterns of HBV infection by HBX worldwide largely affect the distribution of HCC incidence. HBV is the major risk factor of HCC in Africa, Asia (except for Japan), and the western Pacific region (Parkin et al., 2006). Hepato-

carcinogenesis induced by HBV results from chronic inflammation and repeated cellular regeneration with the HCC typically being diagnosed after 25–30 years of infection. It has been estimated that the lifetime risk of HCC for a person with a chronic HBV infection is between 10% and 25% (Lee et al., 1997; Seeger et al., 2000). Moreover, the majority of HBV-related HCC (between 70% and 90%) was derived from liver cirrhosis (El-Serag et al., 2007).

On the other hand, HCV infection is found in variable proportion of HCC cases in different regions. HCV accounts for 80–90% of HCC cases in Japan and 44–66% in Italy, while the highest prevalence locates in northern and middle Africa. Hence, HCV constitutes the major HCC risk factor in Japan, Western countries and some of Africa (Fasani et al., 1999; Stroffolini et al., 1999; Yoshizawa et al., 2002; Parkin et al., 2006). HCV infection causes chronic inflammation, proliferation, and cirrhosis of the liver (But et al., 2008). The liver cirrhosis caused by HCV almost exclusively results in liver cancer, which was 17-fold higher risk in developing HCC than only HCV infection, although this risk varies depending on the degree of liver fibrosis at the time of HCV infection (Donato et al., 2002).

Furthermore, co-infections with HBV and HCV may produce a cumulative effect on the development of HCC that varies from additive to multiplicative. Thus, globally, the burden of liver cancer attributable to viral infections is likely to be close to 90%.

1.1.2.2 Cirrhosis

Cirrhosis is present in about 80–90% of HCC and has a preceded role in the development of HCC (Colombo et al., 1991; Tiribelli et al., 1989). In western countries, about 70–90% of HCC are evolved from macronodular cirrhosis, while in eastern Asia and West Africa, the proportion of patients with pre-existing hepatic cirrhosis evolved into HCC appears to be much lower. The common causes of cirrhosis have been considered as key risk factors for HCC, such as virus hepatitis mentioned above, alcoholic liver disease, non-alcoholic fatty liver disease (NAFLD) and some metabolic disorders.

1.1.2.3 Aflatoxin-contaminated food

Aflatoxin B1 is a kind of hepatocarcinogenic mycotoxins which is produced by some aspergillus species. They can contaminate a large number of traditional foods, including grains, corn, cassava, peanuts, and fermented soy beans, particularly in parts of sub-Saharan Africa and Southeast Asia, as well as in many parts of Latin America with high moisture climate. Hence, these areas also have the high incidence areas of HCC. Aflatoxin B1 can bind to DNA to induce DNA mutations, particularly the tumor suppressor *p53* gene, resulting in down-regulation of p53 in 30–60% of all HCCs in these areas (Zhang et al., 2005). In addition, it has been found that individuals with HBV infection and intake of aflatoxin have an even higher risk of liver cancer compared with individual risk factor, suggesting a synergistic effect between HBV and aflatoxin (Qian et al., 1994).

1.1.2.4. Heavy Alcohol

Heavy alcohol intake, defined as ingestion of >50–70 g/day for prolonged periods, is a well-established HCC risk factor. Although it is reported that alcohol does not have a carcinogenic effect in itself, prolonged alcohol intake can increase the risk for the cirrhosis, a major risk factor for HCC. On the other hand, some evidence show that heavy alcohol ingestion can increase the risk of HCC induced by HCV or HBV infection by actively promoting the formation of cirrhosis. One study demonstrated that among heavy alcohol drinkers, HCC risk increased in a linear fashion at intake >60 g alcohol on a daily basis and the risk rate was doubled with simultaneous HCV infection (Donato et al., 2002).

1.1.2.5 Non-alcoholic fatty liver disease

Nonalcoholic fatty liver disease (NAFLD) is one of the most common liver diseases in the developed countries, with the incidence rate of 20% (Bedogni et al., 2005). The hepatic histology of NAFLD is similar to alcoholic hepatitis including the changes of disease progression. NAFLD may undergo a serial of variation ranging from simple fat to fat with inflammation, fat with ballooning degeneration, and nonalcoholic steatohepatitis (NASH) that is the severest stage of NAFLD (Falck-Ytter et al., 2001, Angulo et al., 1999). Contemporary survey data indicate that NAFLD is closely associated with metabolic syndrome, particularly diabetes (type Ⅱ) and obesity (Bugianesi et al., 2007). NAFLD frequently occurs in diabetic patients with morbidly obese (Adams et al., 2005). Furthermore, NASH has been shown to enhance the risk

for developing cirrhosis and HCC, since it is closely linked with metabolic syndrome (Bugianesi et al., 2005). Therefore, NAFLD is emerging as an important risk factor in the development of cirrhosis and HCC in many developed countries, irrespective of age (Sanyal et al., 2009).

1.1.2.6. Diabetes

Type Ⅱ diabetes mellitus is considered to be an important risk factor for both chronic liver disease and HCC possibly by facilitating the development of NAFLD and NASH. Data emerging from epidemiologic studies have shown the correlation between longer duration of diabetes and the increased risk of HCC that type II diabetes doubled the risk of developing HCC (Stroffolini et al., 1999; El-Serag et al., 2004). For example, an U.S. population-based study has reported that diabetes (type Ⅱ) is an independent risk factor for HCC having a two-to three-fold higher risk for HCC. In a Japanese case–control study, evidence also shows that diabetes increases the risk of HCC (Ohishi et al., 2008; Davila et al., 2005). Moreover, diabetes and obesity are demonstrated in the development of nonalcoholic steatohepatitis (NASH), which is thought to cause the occurrence of HCC by progression to cirrhosis.

1.1.2.7. Obesity

In many developed countries, the increasing incidence of HCC occurs frequently accompanied with obesity and type II diabetes. It is reported that more than 90% of all obese persons (BMI>30 kg/m2) and more than 70% of all type II diabetes patients

have some extent of fatty liver disease (Neuschwander-Tetri et al., 2003). The effect of obesity on HCC risk is revealed by a large prospective cohort study in U.S.A, where the mortality rates of HCC among men and women with a BMI >35 are 4.5 and 1.7 fold than normal-weight individuals, respectively (Calle et al., 2003). There is also similar observation in Sweden and Denmark that HCC risk has a 2–3-fold increase in obese men and women compared to individuals with normal figure (Moller et al., 1994; Wolk et al., 2001). Furthermore, there is evidence of a synergistic effect on HCC risk among obesity individuals with concomitant either HBV or HCV infection. Obesity results in more than twofold excess risk of HCC among persons with HBV infection compared to persons negative for both HBV and HCV infection. When obesity and diabetes occurred together, the combination enhances greatly 100-fold excess HCC risk with concomitant presence of either HBV or HCV infection.

1.1.3 Prevention and therapy

Since the major etiology of HCC was chronic viral hepatitis, the most feasible measures of preventing HCC are the inhibition of HBV and HCV infections. The safe and affordable HBV vaccines were introduced since 1984, and the mass HBV vaccination projects have been executed in 164 of 190 WHO member countries. The survey report on these vaccination programs has illustrated that these vaccines can be efficient to decrease the incidence rate of HBV infection, and vaccination of neonates will cause a sharp reduction in the incidence of HCC worldwide (Ni et al., 2001). An investigation from Taiwan followed up for 21 years indicated that the incidence rates of HCC among adolescents between 6 and 19 ages with vaccination were far less than that of those same-aged adolescents without vaccination (Chang et al., 2009).

However, the vaccine against HCV is not available, maybe due to the synthetic difficulties of the high mutation rate of HCV RNA. Therefore, the prevention measures of HCV are focused on the control of transmission in medical and public health care in developing countries. Infection-control interventions include monitoring potential blood and organ donors for hepatitis before transfusion, sterilization of needles and surgical instruments as well as other supplies, avoidance of the unsafe medical practice and so on. At the same time, strengthening public education and social health awareness of HCV infection is an effective measure to prevent the incidence of HCC induced by HCV. These preventive strategies will

reduce greatly the occurrence of HCV-induced HCC (Ohki et al., 2008; Lok et al., 2009; Chen et al., 2008). In addition, the preventive measures against other risk factors for HCC, such as aflatoxin-contaminated foods, heavy alcohol use, diabetes mellitus, obesity, were also critical, particularly in patients accompany with chronic viral hepatitis. Avoidance of individual exposure to aflatoxin and heavy alcohol, active treatment of diabetes mellitus, and loss weight will decrease the occurrence of HCC.

The treatment of HCC is determined by the extent of pathogenetic condition (tumor stages) and the impaired liver function as well as physical status (Lau WY and Lai EC, 2008).The most frequently-used staging system is the Barcelona Clinic Liver Cancer (BCLC) staging system which reflects the extent of pathogenetic condition. The liver function is embodied in the adverse criteria of ascites, serum albumin and bilirubin concentration and so on. Therapies for HCC can be divided into two categories: surgical interventions (tumor resection and liver transplantation) and non-surgical interventions (percutaneous local ablative, transarterial chemoembolization or transcatheter arterial embolization; chemotherapy; gene therapy and so on).According to the BCLC staging system, the curative treatment including resection, liver transplantation, and percutaneous local ablative treatment is predominantly appropriate for patients without clinical symptom at the early stage of HCCs (both stage A).Transarterial chemoembolization (TACE) or transcatheter arterial embolization (TAE) is primarily applied to the unresectable patients or asymptomatic patients

with multinodular HCC (intermediate, or stage B, some of stage C). The chemo-therapy with sorafenib is recommended as the only treatment for patients with advanced HCC (stage C)—especially those with metastatic or extrahepatic tumors. However, some studies in the recent years have shown that a chemotherapy regimen combining cisplatin, doxorubicin, interferon and 5-fluorouracil may prompt the therapeutic effect, although these studies in patients with single or combined therapy show no evidence of improvement in survival rate of HCC. The patients with terminal stage of HCC (stage D) are treated for the best supportive care (Bruix et al., 2005; Forner et al., 2010). The protocol of HCC determined by BCLC staging system is proven to benefit the survival of patients with early-stage HCC (Farinati et al., 1999).

However, due to the limitation of therapeutic options for advanced HCCs, a host of experimental strategies are being adopted, including gene and immune therapies based on mutation gene correction, prodrug activation, antiangiogenic genes (Mohr et al., 2002; Geissler et al., 2003; Mohr et al., 2004) and genetic modify oncolytic viruses therapy (Pei Z et al., 2004).

1.1.4 Gene therapy

Since the simple clinical therapeutic protocol on advanced hepatocellular carcinoma is not very effective, hope has focused on a lost of experimental strategies, including the gene therapy.

Irrespective of the etiologic agent, malignant transformation of hepatic cell may occur through hepatic excessive proliferation and abnormal cell differentiation induced by the ceaseless stimulus from chronic liver injury, regeneration, inflammation and immune response. This may lead to genetic variation including the unbalanced activity of cellular oncogene and tumor-suppressor gene, as well as the defects of DNA repair systems (Ozturk et al., 1999; Bergsland et al., 2001; Thorgeirsson et al., 2002; Yu et al., 2004).

Gene therapy is a novel and promising therapeutic option that can alter and modify the abnormal genes by the introduction of genetic materials into cells so as to generate a therapeutic effect against genetic variation (Sangro et al., 2003).To date, a number of gene therapy methods have been applied to treat liver cancer including inhibition of tumoral vascularization, inactivation of oncogenes, restoration of tumor suppressor gene function, selective prodrug activation against the tumor, stimulation of anti-tumoral immunity (Sangro et al., 2002). Some gene therapy methods targeting angiogenesis have been proven to benefit the treatment of HCC with high vessel

density. These approaches include the suppression of vascular endothelial growth factors (VEGF) expression by antisense oligonucleotides; the clearance of the angiogenesis by the formation of soluble VEGF receptor, Flt-1, which can segregate the circulating VEGF; and local generation of endostatin and angiostatin (Saleh et al., 1996; Goldman et al., 1998; Griscelli et al., 1998). The tumor suppressor gene is a protective gene that normally limits the excessive growth of cell. Tumor suppressor genes play a major role in regulating the development of cell differentiation and proliferation. When DNA damage occurs in a cell, some tumor suppressor genes can prohibit the cell from propagating till the damaged DNA is repaired. Furthermore, in the context of irreparable harm, specific tumor suppressor genes can activate the death program of "cell suicide". When tumor suppressor genes are altered, the impaired cells go on dividing and accumulating in the presence of DNA damages, which can eventually result in the formation of a neoplastic cell. So, the tumor suppressor gene is found frequently to be altered in the many tumors, such as *p53*. Transferring a wild-type *p53* gene into *p53*-mutated HCC cells can restore the function of the altered gene *p53* and inhibit the cell growth (Xu et al., 1996).

1.2 Hepatitis B Virus

1.2.1 Epidemiology of Hepatitis B Virus Infection

HBV is a serious global public health problem. According to the survey of the World Health Organization (WHO), more than 2 billion people have been infected and 350 million individuals suffer with chronic HBV infected diseases. In a world, the most prevalent distribution of HBV infection occurs in Asia, Sub-Saharan Africa, Amazon, some areas of Middle East, Indian subcontinent, and some southern parts of Eastern and Central Europe, especially with the majority of cases seen in China (>50%). It is reported that 500,000–1.2 million persons die of HBV-related liver disease every year. Chronic HBV infection can lead to acute and chronic virus hepatitis, cirrhosis, HCC (Goldstein et al., 2005; Lavanchy et al., 2004; WHO, 2000).

HBV is transmitted via infected blood or body fluids including semen and saliva. The transmission of hepatitis B infection is divided into two patterns: vertical transmission and horizontal transmission. Vertical transmission is one manner of perinatal transmission from the highly HBV infectious mother to her neonates, which is the predominant way for HBV infection in Asian countries and some endemic areas (Kane et al., 1995; Kim et al., 1994). Horizontal transmission is the other manner of transmission by behavioral exposure to HBV including sexual behavior, blood transmission, and close contact with infected patients, which is prevalent in developed countries (CDC, 1995; CDC, 2006).

1.2.2 HBV Genotypes and Their Significances

To date, according to phylogenetic clustering analysis based on complete viral sequences and nucleotide divergence, HBV is divided into at least 10 HBV genotypes (A to J) with an inter-genotype divergence of ≥8% and several different subgenotypes (A1-A5, B1-B7, C1-C5, D1-D5, F1-F4) with an inter-subgenotype divergence between 4% and 8%, respectively (Lin et al., 2011; McMahon et al., 2009; Kurbanov et al., 2010; Cao et al., 2009). The geographic distributions of HBV genotypes and subgenotypes are characterized as following: Genotype A highly lies in sub-Saharan Africa (subgenotype A1/Aa), Northern Europe (subgenotype A2/Ae), and Western Africa (subgenotype A3/Ac). Genotypes B and C are universally seen in Asia. Recently, genotype B is divided into B1–B7 subgenotypes. Among them, B1-B5, B7 are found in East Asia, particularly, B2 is common in China, and B6 is isolated in native populations living in the Arctic, such as Alaska, Northern Canada and Greenland. Genotype C (subtypes C1–C5), mainly occurs in East and Southeast Asia, especially subgenotype C2/Ce commonly exists in Eastern Asia (Korea, Japan) and North China. Genotype D with subtypes D1–D5 is found in the Mediterranean region, Africa, India, and Europe. Genotype E is confined in West Africa. Genotype F with 4 subtypes (F1–F4) is prominently prevalent in Central and South America. Genotype G has been predominantly reported in Europe and the United States. The eighth genotype, H, is found in Central America (McMahon et al., 2009; Kurbanov et al., 2010; Cao et al., 2009; Kao et al., 2006; Datta et al., 2008). At present, a novel

genotype I, associated with genotypes A, C, and G is detected in Vietnam and Laos (Tran et al., 2008; Thuy et al., 2010; Olinger et al., 2008). The newest genotype J of HBV is found in the Ryukyu islands in Japan, which has a close correlation with gibbon/orangutan genotypes and human genotype C (Tatematsu et al., 2009).

Most retrospective or case-control studies illustrate that HBV genotype C can cause the more severe liver disease such as cirrhosis and HCC, compared with HBV genotype B (Chan et al., 2004; Kao et al., 2003; Yuen et al., 2004; Kao et al., 2000). In addition, earlier studies revealed that genotype C had higher frequency mutation rate than genotype B, for example, the basal core promoter (BCP) A1762T/G1764A mutation (Kao et al., 2000). This contributes to a higher risk of HCC in HBV genotype C compared to genotype B. Furthermore, patients with HBV subgenotype C2/Ce infection also had significantly higher risk of developing HCC than those with HBV subgenotype C1/Cs (Chan et al., 2008). However, the mechanism of hepato-carcinogenesis by genotype-specific HBV is still unknown.

1.2.3 Morphology and Genome of Hepatitis B Virus

HBV is a small, enveloped DNA virus, which belongs to the family called Hepadnaviridae. The infectious virion has a narrow host range, preferential directivity to hepatocytes, and induces acute and chronic liver diseases. HBV particles were found at least three different forms in blood of patients with HBV infection by cryoelectron microscopy (Hollinger et al., 1987). Most of these particles are defective envelope subvirus with the size ranging between 15 and 20 nm. The mature virion, also called Dane particles, is a 42 nm in diameter of spherical particle with a lipid viral envelope coating the inner core. This inner core consists of a circular, partially double-stranded viral DNA genome, polymerase protein, and core protein. The genomic DNA is 3.2kb in length, and consists of two linear strands of different length. The long strand codes negative strand (-), while the short strand is the complementary strand (+), and variable length with the range from 50 to 100% of the negative strand. The HBV genomic DNA encompasses four partially overlapping open reading frames (ORFs), named S, C, P and X (Colgrove et al., 1989) (Fig.1.1). The S-ORF consists of preS1, preS2 and S regions. These regions encode the viral surface proteins (HBsAg) or surface antigenic determinants, which represent for respectively large (preS1+ preS2+S), middle (preS2+S), and small (S) proteins. The C-ORF contains preC and C regions which encodes the corresponding preC and C ptoteins (HBc Ag), making up the core proteins. The core proteins act as nucleocapsids covering the pregenomic viral RNA and the polymerase protein are responsible for viral genome replication.

The preC region generates a signal peptide which secrets the protein called HBeAg. Due to emerging at the highly replicative phase of HBV infection, HBeAg is regarded as a serum marker to identify highly infectious patients and the surveillance indication of curative effect for active antiviral therapy. The P-ORF codes for the multi-functional protein including the virus-associated DNA polymerase and the terminal protein (TP). The viral polymerase has DNA polymerase, reverse transcriptase (RT) and RNaseH activities; while the terminal protein binds to the viral RNA packaging signal and directs the synthesis of HBV genomic DNA. Finally, the X-ORF encodes a 154 amino acid polypeptide called HBx protein or X protein, which has been implicated to play a major role in viral infection and the development of liver disease, but its specific functions remain partially understood (Fig.1.2).

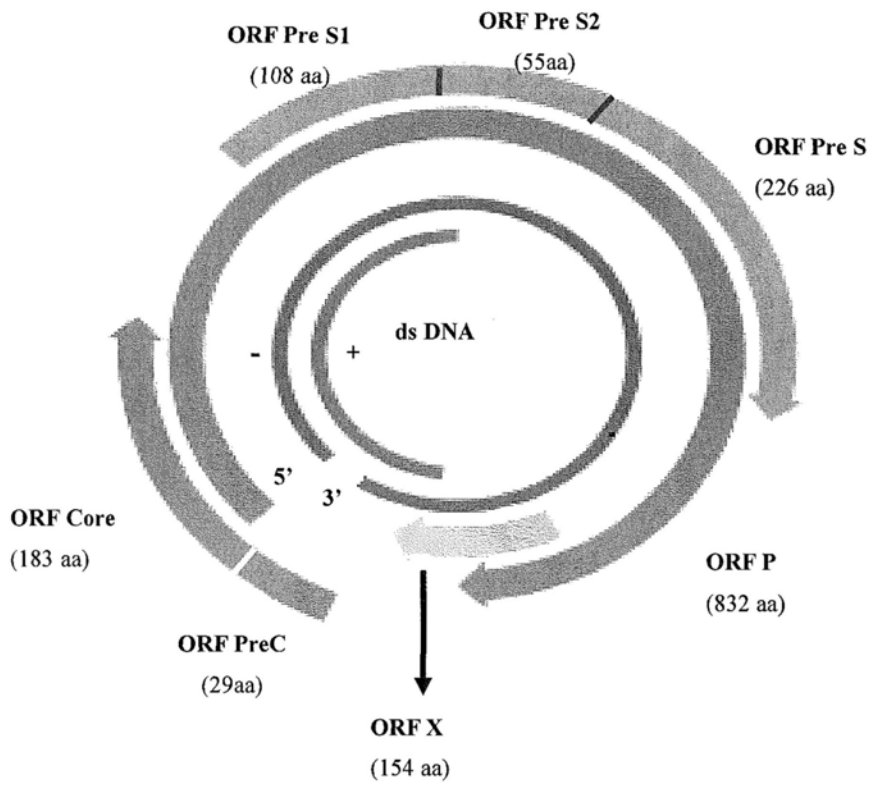

Fig. 1.1 Genomic structure of HBV. HBV is a partially double-stranded viral DNA genome including four partially overlapping open reading frames(ORFs), called preS1/preS2/S gene, preC/C gene, P gene and X gene.

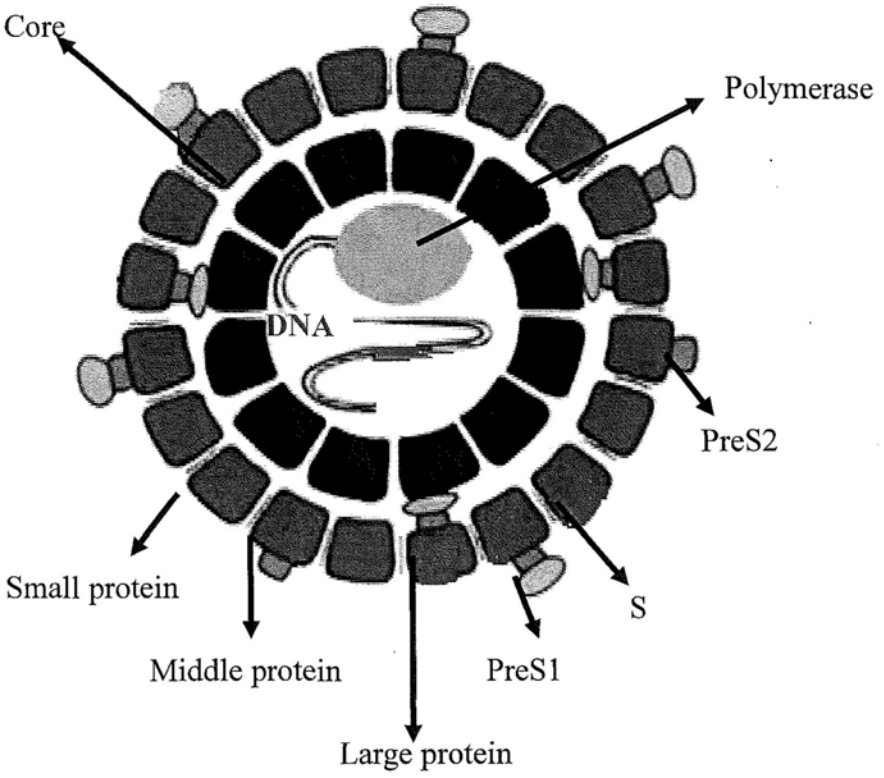

Fig. 1.2 Schematic structure of hepatitis B virus. HBV is a spherical particle with a lipid viral envelope coating the inner core, which is called Dane particles. The outer envelope consists of large, middle and small surface protein, while the inner core contains the viral genome, polymerase and core protein.

1.3 Hepatitis B Virus X Protein

1.3.1 Structure of HBx protein

HBx is a multifunctional regulator that modulates cellular signal transduction parthways, transcription, cell proliferation and apoptosis, protein degradation, and genetic stability by direct and indirect interaction with host factors. HBx codes for a 154 amino-acid polypeptide with a molecular mass of 17.5 kDa which is the most frequently found in HCC and has been strongly linked to the development of HCC. HBx contains three important regions: regulatory domain, damage-specific DNA binding protein (DDB1) binding domain, p53 binding domain (Diao et al., 2001).Owing to multifunction domains (such as p53 binding domains) in the distal COOH terminal region, the C terminus of HBx was thought to play a critical role in controlling cell proliferation and apoptosis (Fig.1.3).

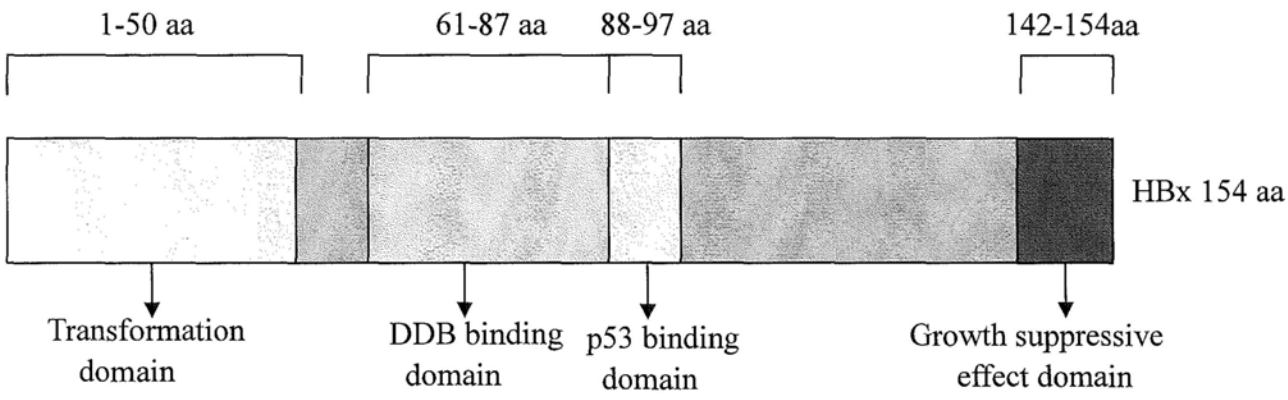

Fig.1.3 Domains of HBX protein (154 amino acid) containing important regions in Transformation domain, DDB binding domain, p53 binding domain, and Growth suppressive effect domain.

1.3.2 HBx activates various signal transduction pathways

HBx is a promiscuous transactivator, which not only activates mitogenic signaling cascades in the cytoplasmic but also physically interacts with DNA-bound transcription factors to directly regulate gene transcription in the nucleus. These multifunctional characteristics of HBx depend on its differential intracellular localization. When the expression levels of HBx is low, HBx is mainly localized in the nucleus; while the expression levels of HBx is abundant, HBx spread to the cytoplasm in addition to the nucleus (Henkler et al., 2001; Cha et al., 2009).

Ⅰ) Signal transduction pathways of HBx in the cytoplasm

In view of cytoplasmic localization of HBx, HBx has been identified to regulate the activation of different signaling transduction pathways (Fig.1.3). Activation of these signaling pathways may affect various cellular fates such as transformation, differentiation, survival, and apoptosis. For example, the Ras-Raf-mitogen-activated protein kinase (MAPK) activated by HBx is essential for the transformation of differentiated hepatocytes (Sto¨ckl et al., 2003; Tarn et al., 2001), and is able to abrogate the pro-apoptotic effects of HBx and deregulate cell cycle checkpoint controls and stimulate cell cycling (Benn et al., 1995), leading to hepatocarcino-genesis in HBV-infected cells (Noh et al., 2004). Protein kinase C (PKC) is a large family of phospholipid-dependent kinases involved in cell growth, differentiation, and carcinogenesis. The transactivation of the PKC signaling pathway can result in the

disordered cell growth and transformation. The up-regulated activity of stress-activated protein kinase/NH2-terminal-Jun kinase (SAPK/JNK) is shown to be a survival pathway for cells undergoing Fas-mediated apoptosis. Furthermore, HBx can improve the cell proliferation through the suppression of the apoptosis signaling pathway. HBx up-regulates the activity of Survivin-HBXIP complexes, which selectively inhibits the initiation of apoptosis. HBx can interfere competitively with the transactivation of tumor suppressor gene p53, which can block the cellular apoptosis. HBx activates the expression of MAT2A via nuclear factor-κB (NF-κB) and cAMP-response-element- binding protein (CREB) signaling pathways, resulting in the inhibition of hepatoma cell apoptosis (Liu et al., 2011). On the other hand, HBx interacts with various cellular signaling factors to induce apoptosis or enhance the susceptibility of apoptosis (Sirma et al., 1999; Bergametti et al., 1999; Terradillos et al., 1998; Kim et al., 1998; Chirillo et al., 1997; Takada et al., 1999; Koike, et al., 1998; Schuster et al., 2000; Kim et al., 2001). HBx causes apoptosis by interacting with cellular signaling proteins such as c-FLIP and Hsp60 (Kim et al., 2003; Satoh et al.,1997) and inducting five genes: apoptotic cysteine protease (MCH4), Fas ligand associated genes, Fas- activated serine/threonine kinase, Bak, and glutathione S-transferase (Han et al., 2000). HBx can also interact with Bax to reduce mitochondrial membrane potential, which can activate the death programme of cell. Moreover, the enhanced sensitization of tumor necrosis factor-α-induced apoptosis by HBx may modulate the activation of mitogen-activated-protein kinase kinase 1 and Myc protein (Su et al., 2001; Su et al., 1997).

II) Signal transduction pathways of HBx in the nucleus

According to the data of co-precipitation and confocal immunofluorescence microscopy experiments, HBx is also proven to be localized in the nuclear. Since HBx does not bind directly to DNA, it can affect transcriptional activity of gene through interaction with transcriptional transactivators (Unger et al., 1990; Qadri et al., 1996, Haviv et al., 1996). HBx targeted to the nucleus can regulate the transcription of host genes indirectly through interacting with nuclear transcription factors including NF-κB, CREB, AP-1 and DDB1. NF-κB binding to its inhibitory proteins IκBa and IκBb is normally localized in the cytoplasm. Free NF-κB activated by HBx is translocated into the nuclear and enhances transcriptional activation of host genes such as Bcl-2 and IAP (De Luca et al., 1999) which can suppress the apoptosis and improve infected cell survival. HBx also interacts directly with CBP/p300 protein, and regulated the transcriptional activation of host endogenous cellular genes such as interleukin 8(*IL-8*) and proliferating cell nuclear antigen (*PCNA*) by physically occupying the CREB-binding site in the promoters of these genes. These two genes are very closely linked to the HBV-associated cancer development (Fig.1.4).

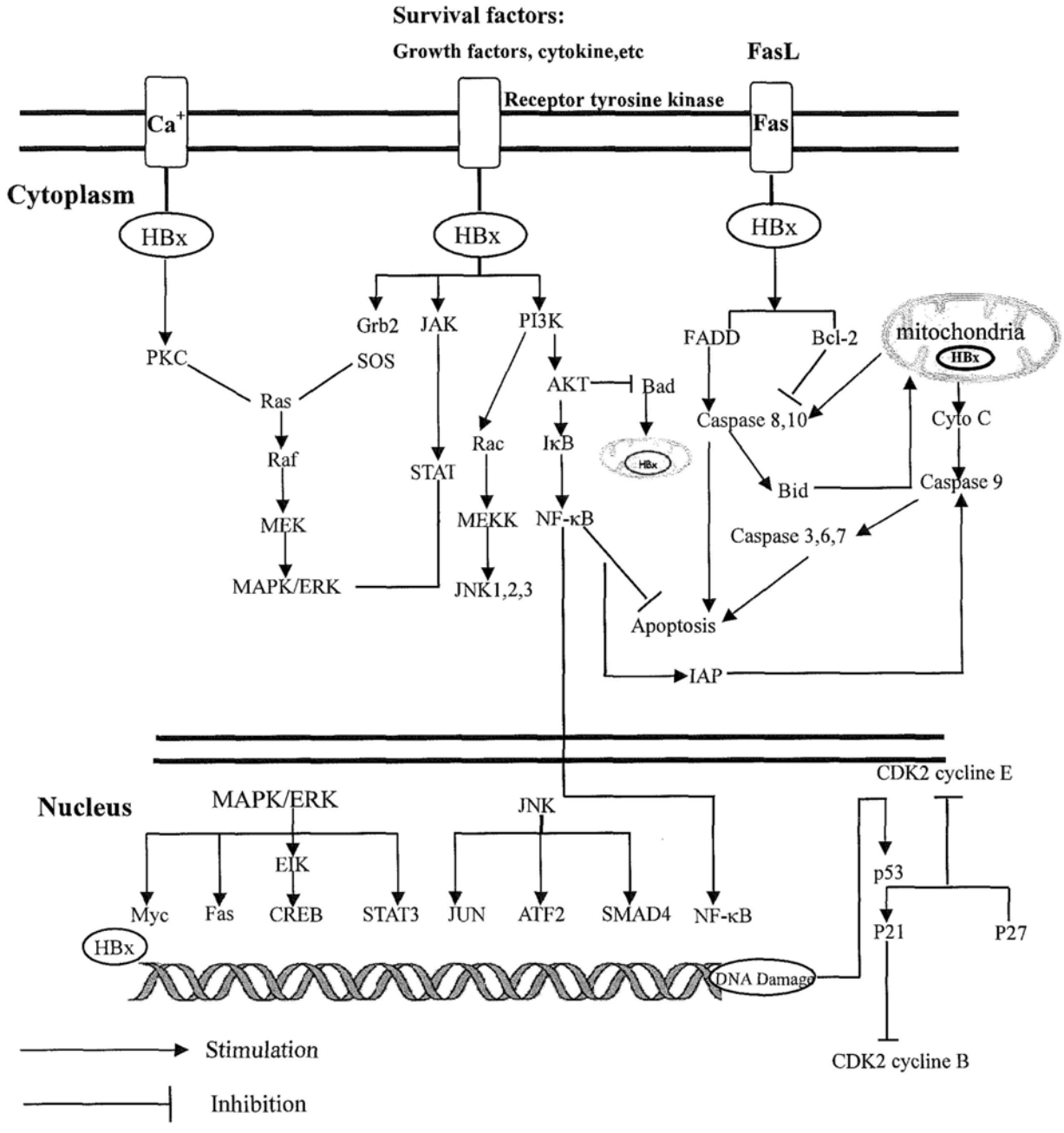

Fig. 1.4 Transduction signal pathways affected by HBx

1.3.3 Significance of COOH-terminal Truncated HBx in Liver Tumors

Recent studies have sequentially reported that carboxyl (COOH)-terminal truncated HBx was detected frequently in HBV-related HCC tumor tissues. (Tu et al., 2001; Wang et al., 2004; Iavarone et al., 2003; Ma et al., 2008). Increasing evidence has shown that COOH-terminal truncation of HBx may play a pivotal role in regulating its transcriptional activity and controlling cell proliferation and viability. In order to define the specific function of different region in distal COOH terminal region, Tu and colleagues examined the functions of different HBx mutants derived from patient sera and tumor tissue samples. The studies showed that the last 14 aa at the COOH terminus of HBx possesses the transactivation activity (Arii et al., 1992; Kumar et al., 1996). Deletions of more than 16 aa in length at the COOH terminus of HBx missed the function of transactivation activity (Quade et al., 1992; Wang et al., 2001; Tu et al., 2001).In addition, COOH-terminal truncation has been demonstrated to abrogate the HBx-related proapoptosis. The deletion of 14 aa was enough to abrogate the growth suppressive effects of HBx. Furthermore, COOH terminus may also facilitate the cell transformation. While the first 50 aa at the NH2 terminus of HBx was defined to be the transformation domain, a deletion at the COOH-terminal end may lose the inhibitory effect on transformation (Gottlob et al., 1998). Taken together, COOH-terminal truncation may interrupt the balance of wild-type HBx functional domains in modulating cell proliferation, viability, and transformation. It is also worth mentioning that the amino acid sequences of HBx truncation derived from HCC

tissues frequently showed a deletion longer than 16 aa at their COOH-terminal ends (Elmore et al., 1997). Some studies have found that most carboxyl-terminal truncated HBx proteins in HCC tumor tissues missed the last 35 amino acid. For example, most G-to-A mutations occurred at positions 359 and 360 (TGG to TAA) in 3' end of HBx gene, which can generate a premature stop codon at position 120aa, resulting in the last 35 amino acid lost (Ma et al., 2008; Xu et al., 2007). However, the molecular mechanism underlying carboxyl-terminal truncated HBxΔ35-induced hepatocarcino-genesis is not fully clear.

1.4 Growth arrest-specific gene 2 (GAS2)

1.4.1 Definition and function of GAS2

Growth arrest-specific (*GAS2*) genes encode proteins implicated directly in reversible growth arrest. They are upregulated collectively in the murine 3T3 cell line through serum starvation and contact inhibition (Schneider et al., 1988).This family contains six genes (GAS1–GAS6), which encode proteins exhibiting distinct biochemical properties (Nuoffer et al., 1991; Snipes et al., 1992; Manfioletti et al., 1993). Among these genes, the protein encoded by *GAS2* gene is a cell death substrate of caspase-3 that plays a role in modulating microfilament and cellular morphological changes during apoptosis (Sgorbissa et al., 1999; Brancolini et al., 1995). The *GAS2* gene maps to the human chromosome 11p15.2-p14.3, coding for a protein of 314 amino acids with molecular weight 36kDa approximately. GAS2 protein is highly expressed in 3T3 fibroblasts and is phosphorylated by cysteine proteases during growth arrest (Schneider et al., 1988; Brancolini et al., 1992). Its hyperphosphorylation is specifically relocalized to the appearance of membrane ruffles formed at the edges of the cells during G0–G1 transition (Brancolini et al., 1994). Therefore, through microfilament alterations regulated by GAS2, the actin cytoskeleton and cell shape are rapidly rearranged in response to the growth arrest induced by environmental stimuli such as apoptosis, different proliferative stimuli with various growth factors. In the course of apoptosis, the carboxyl-terminal domain of GAS2 polypeptide is phosphorylated by caspase enzymes. This proteolytical process is triggered by

caspase-3 but not by caspase-2 (Brancolini et al., 1997a). These aspartic-specific cysteine proteases are the fundamental effectors of the apoptotic program, resulting in the apoptosis by cleaving specific cellular targets or death substrates (Martin and Green, 1995; Jacobson et al., 1997). Removal of the carboxyl terminal domain of GAS2 dramatically performs the potential cell shape changes of the affected cells through reorganizing the microfilaments system (Brancolini et al., 1995). Moreover, some studies have found that caspases manipulate morphogenetic changes during apoptosis by processing distinct regulators of the actin cytoskeleton such as Fodrin, RhoGDI, beta-catenin and so on (Cryns et al., 1996; Martin et al., 1996). Fodrin (non-erythroid spectrin) which is distributed widely in cytoskeletal proteins involved in actin crosslinking, is proteolyzed during apoptosis. Likewise, D4-GDI, a substrate of caspase-3, is also proteolyzed during Fas-induced apoptosis (Leto et al., 1988; Na et al., 1996). The abrogation of cell-cell contacts during apoptosis involves proteolytic cleavage of beta-catenin via a caspase-dependent pathway (Brancolini et al., 1997a). As a consequence, the processing of GAS2 throughout apoptosis by caspase enzymes could exert some critical effects on regulating the complicated morphological changes that characterize cell death.

1.4.2 GAS2 and p53-dependent apoptosis

Since GAS2 is a promising death substrate, its expression is also involved in the susceptibility to apoptosis (Brancolini et al., 1997b). The tumor suppressor protein p53 is a capital regulator of apoptotic susceptibility, which can be regulated by some enviromental stress stimuli including UV irradiation, DNA damage, hypoxia, changes of the redox potential, and expression of some oncogenes (Levine et al., 1997; Giaccia and Kastan, 1998). Accordingly, the apoptotic mechanism of p53 has been explored intensively and the multiple pathways involved have been clarified (Giaccia and Kastan, 1998). An initial capital step in the p53 apoptotic response is the stabilization and accumulation of the p53 protein. The ectopic expression of GAS2 up-regulates p53 level and transcriptional activity following the exposure to UV irradiation or treatments with DNA-damaging agents such as etoposide or methyl methanesulfonate (MMS) that is dependent on p53 status (Benetti et al., 2001).p53 is proteolytically cleaved in vitro by calpains, a family of calcium-activated non-lysosomal neutral cysteine proteases involved in numerous physiological and pathological processes including apoptosis (Sorimachi et al., 1997; Carafoli and Molinari, 1998; Ono et al., 1998). p53 is the substrate of calpains both in vitro and in vivo (Gonen et al., 1997; Pariat et al., 1997). The role of calpain in degradation of wild-type p53 and p53-dependent apoptosis has been investigated (Kubbutat and Vousden, 1997; Pariat et al., 1997). Among diverse calpains, calpastatin is the specific inhibitor (Maki et al., 1991; Carafoli and Molinari, 1998; Suzuki and Sorimachi, 1998). Ectopic expression

of calpastatin can elevate persistently transcriptional activation of p53 (Pariat et al., 1997) and enhance susceptibility to apoptosis (Atencio et al., 2000; Hiwasa et al., 2000). Furthermore, it is reported that the activation of calpain or its inhibitor, calpastatin, can mediate the activity of p53 protein (Pariat et al., 1997). During apoptosis, GAS2 regulates the level of p53 by suppressing the activity of m-calpain. Cleavage of GAS2 can initiate the foremost step for overall activation of m-calpain, involving a complicated interaction with members of these two cysteine proteases families (Meredith et al., 1998; Porn-Ares et al., 1998). Overexpression of either GAS2 or calpastatin can render a rapid accumulation of transcriptionally active p53 by inhibiting the activity of m-calpain. GAS2 seems to act like calpastatin, because both bind to the regulatory domain of m-calpain and are both cleaved by caspase-3 (Brancolini et al., 1992; Porn-Ares et al., 1998) (Fig.1.5). However, a growing body of evidence has indicated that a C-terminal deletion of GAS2 (Δ171–314) does not inhibit the activity of m-calpain, although it binds to m-calpain. This implies a truncation of GAS2 abolishes the function of wide-type GAS2 with regard to the inhibition of m-calpain activity, p53 stabilization, and susceptibility to apoptosis (Benetti et al., 2001).

The ultimate effect of the p53 apoptotic pathway is the activation of caspases cascade, which is pivotal procedure on the apoptotic program from nematodes to humans (Cohen et al., 1997; Yuan et al., 1997). Caspases can affect the morphological changes by regulating specific cellular proteins involved in the apoptotic phenotype.

Moreover, they can also mediate susceptibility to apoptosis by cleaving the corresponding substrates so as to control cell survival or death (Tan and Wang, 1998; Porter and Janicke, 1999). Hence, increased susceptibility to p53-dependent apoptosis has been regarded as an important mechanism whereby the transformation of cell and tumor growth are inhibited, whereas decreased apoptotic susceptibility contributes to the pathogenesis of several diseases including tumor.

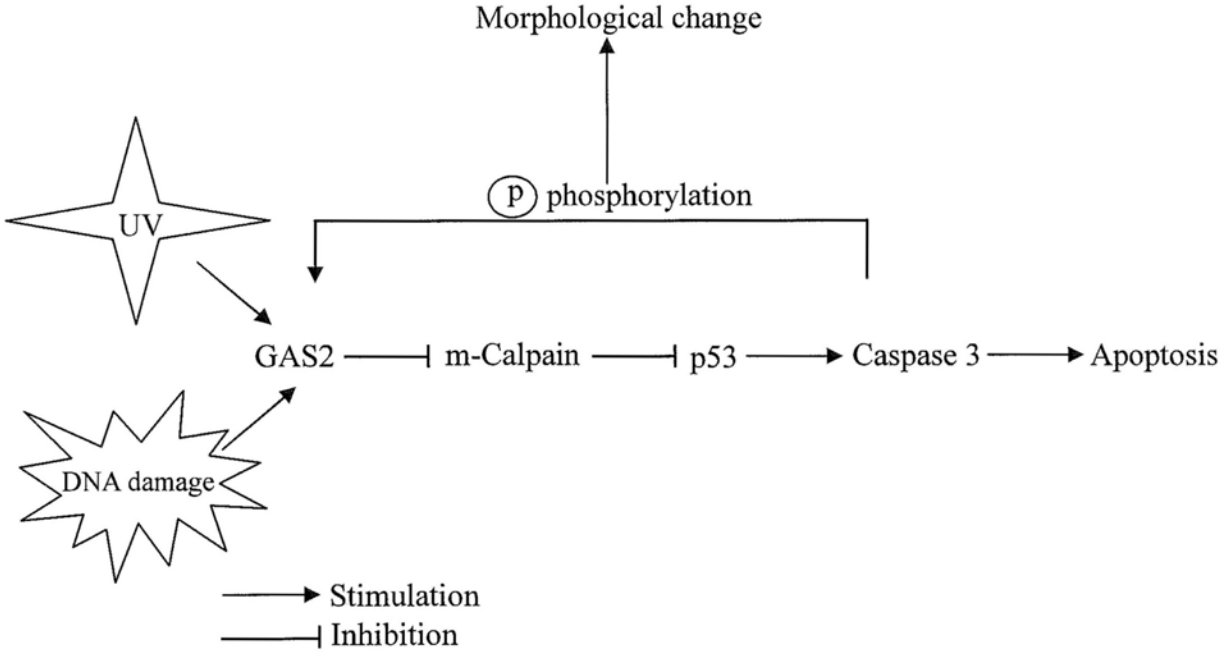

Fig.1.5 A working model for the regulatory network of p53-dependent apoptosis induced by GAS2

1.4.3 GAS2 and cancer

To date, the role of GAS2 in cancer has been still full undefined. GAS2 expression is silenced in several cancer cell lines such as prostate cancer cells (PC3) and breast cancer cells (MCF7, HCC1954). After treatment with etoposide, GAS2-transfected MCF7 cells with wild-type p53 can enhance drug-induced apoptosis, while GAS2 overexpression in PC3 without p53 can not increase susceptibility to apoptosis, consistant with the option that p53 is critical in the apoptosis induced by GAS2 (Kondo et al., 2008; Allegrucci et al., 2011). In the course of tumorigenesis, abnormal translational control is one of common features in cancer (Schneider and Sonenberg, 2007).The translation initiation factor, eIF4E, an important oncogene overexpressed in numerous cancers, is implicated in mechanisms underlying senescence. eIF4E, like other oncogenes (e.g., Akt or Ras) can induce senescence, which functions as an intrinsic barrier to cancer (Campisi and d'Adda di Fagagna, 2007; Collado et al., 2007; Lowe et al., 2004). The eIF4E-binding proteins (4E-BPs) negatively regulated the activity of eIF4E. However, cells lacking 4E-BPs, but with p53 protein, still exhibit premature senescence and resist oncogene-driven transformation, potentially due to GAS2 protein suppression by 4E-BPs at the posttranscriptional level. On the other hand, up-regulated expression of GAS2 was detected in blast crisis in chronic myeloid leukemia. Since p53 mutations were found mainly in myeloid blast crisis,over-expression of GAS2 may substitute p53 aberration (Janssen et al., 2005). Further studies show that without p53, GAS2 can up-regulate the β-catenin expression and

activation by the inhibition of m-calpain activity. Accumulated β-catenin is transcriptionally active and increases the expression of genes modulating cell proliferation and survival (Benetti et al., 2005).

1.5 Hypothesis and objectives of the Study

Based on the previous findings on the oncogenic ability of carboxyl-terminal truncated HBx in HCC, we hypothesize that carboxyl-terminal truncated HBx directly regulates specific target genes to promote HCC development. A set of studies aim to elucidate the signaling network regulated by carboxyl-terminal truncated HBx in hepatocarcinogenesis. Firstly, the target genes of C-truncated HBx are identified in human normal hepatocytes cell lines through a genome-wide approach called chromatin immunoprecipitation microarray (ChIP-chip). Then the biological functions of the identified target gene, *GAS2* are investigated. Finally, the significance of *GAS2* in clinical HCC specimens is evaluated.

The workflow of our study is:

1. Confirmation of oncogenic ability of C-terminal truncated HBx in human normal hepatocytes cell lines
2. Identification of target genes of C-terminal truncated HBx in human normal hepatocytes cell lines by ChIP-chip
3. Validation of target genes of C-terminal truncated HBx in human normal hepatocytes cell lines by ChIP-PCR and RT-PCR
4. Characterization of biological functions of the identified target gene, *GAS2*
5. Expression analysis of GAS2, in clinical HCC specimens in relationship to HBx truncation

CHAPTER TWO- METHODOLOGY

2.1 Cell cultures

MIHA and LO2 are human immortalized non-tumorigenic liver cell lines. HepG2 is human hepatoblastoma cell line. Huh7 is human well differentiated HCC cell line. PLC5 and Hep3B are derived from human HCC with HBsAg antigen. SK-Hep1 is human adenocarcinoma cell line. They were stored at liquid nitrogen condition in our laboratory. The Huh7, PLC5, SK-hep1, Hep3B, HepG2 and MIHA cell lines were maintained in high glucose Dulbecco' s Modified Eagle's medium (DMEM; Gibco) supplemented with 10% Fetal Bovine Serum (FBS; Thermo Scientific HyClone). LO2 was cultured in high-glucose DMEM supplemented with 10% FBS and 1%MEM Non-Essential Amino Acids (Gibco). The cells were incubated at 37°C in a humidified incubator containing 5% CO_2. The cultures were passed at pre-confluent densities using a solution of 0.25% trypsin and 1mM EDTA-Na (Invitrogen).

2.2 Patients and clinical specimens

Liver specimens were obtained from 54 HBV-related patients who underwent curative hepatic resection for HCC at the Prince of Wales Hospital. The vast majority of patients were HBV-positive. HCC liver tissue samples from all patients were taken from the most viable areas of tumor immediately after surgical resection excluding the necrotic and hemorrhagic area of tissues. The matched adjacent nontumor tissues were selected at a clear distance from the tumor edge (>5 cm) if there was no evidence of tumor invasion. Tissues were snap-frozen immediately after resection and stored at -80℃ until use. The availability of tissue DNA and RNA for study were indicated in Table 2.1.

Table 2.1 Demographic information of 54 patients diagnosed with HCC. The availability of clinical samples, including tissue DNA and RNA was marked as "+"present and "-" absent, NA means not available.

Case no.	Sex	Age	HBsAg (+ / - / NA)	Diagnosis	Availability of Tissue RNA	Availability of Tissue DNA
475	M	38	+	HCC	+	+
480	M	44	+	HCC	+	+
485	M	43	+	HCC	+	+
488	M	59	+	HCC	+	+
493	M	50	+	HCC	+	+
495	F	60	+	HCC	+	+
498	M	47	+	HCC	+	+
502	M	72	+	HCC	+	+
510	M	66	-	HCC	+	+
511	M	54	+	HCC	+	+
522	F	42	+	HCC	+	+
523	M	47	+	HCC	+	+
524	M	39	+	HCC	+	+
529	M	59	+	HCC	+	+
531	M	68	+	HCC	+	+
532	M	71	+	HCC	+	+
545	M	55	+	HCC	+	+
568	M	54	+	HCC	+	+
581	M	50	+	HCC	+	+
588	M	77	+	HCC	+	+
591	M	61	+	HCC	+	+
593	M	50	NA	HCC	+	+
594	M	62	NA	HCC	+	+
603	M	36	+	HCC	+	+
610	M	44	+	HCC	+	+
615	M	55	+	HCC	+	+
617	M	62	+	HCC	+	+
620	M	58	+	HCC	+	+
628	M	44	+	HCC	+	+
644	M	53	+	HCC	+	+
646	M	54	+	HCC	+	+
653	F	54	+	HCC	+	+
654	M	81	+	HCC	+	+
655	M	66	+	HCC	+	+
656	M	51	+	HCC	+	+
659	M	54	+	HCC	+	+
661	F	72	+	HCC	+	+

663	M	63	+	HCC	+	+
665	M	44	+	HCC	+	+
666	F	59	−	HCC	+	+
668	M	52	+	HCC	+	+
669	M	56	+	HCC	+	+
670	M	80	+	HCC	+	+
672	M	63	+	HCC	+	+
673	M	53	+	HCC	+	+
675	M	63	+	HCC	+	+
676	M	61	+	HCC	+	+
677	M	55	+	HCC	+	+
679	M	58	+	HCC	+	+
680	M	54	+	HCC	+	+
688	F	63	+	HCC	+	+
690	M	76	+	HCC	+	+
692	M	43	+	HCC	+	+
721	F	74	−	HCC	+	+

2.3 Vector construction and lentivirus production

DNA fragment of COOH-terminal truncated HBx derived from the serum of an HCC patient, CH230, was amplified by polymerase chain reaction (PCR), and the cloning of PCR products was performed using the TOPO TA Cloning Kit (Invitrogen). TOPO3.1 empty vector, TOPO3.1-XΔ35 was generated. HBx was sub-cloned to the *EcoR*I and *Sal*I restriction sites of a lentiviral vector, pRRL-cPPT-CMV-X-IRES-EGFP-PRE-SIN (a generous gift from Prof. Y. Chen) (Figure 2. 1). The cloning experiment had been performed by other fellow, YIP Wing Kit, in our laboratory.

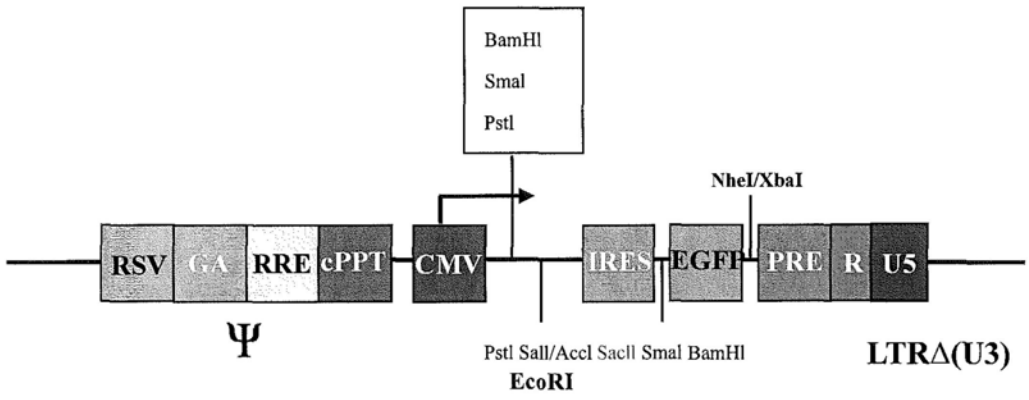

Fig. 2.1 A schematic diagram of a lentivirus Vector, pRRL-cPPT-CMV-X-IRES-EGFP-PRE-SIN.

Abbreviations: RSV, Rous sarcoma virus and HIV chimeric long terminal repeat; RRE, HIV Rev response element; cPPT, HIV-1 central polypurine tract; CMV, human cytomegalovirus; IRES, the internal ribosome entry site of the encephalomyocarditis virus; EGFP, enhanced green fluorescent protein; PRE, human hepatitis virus posttranscriptional regulatory element, LTR (ΔU3), deletion in the HIV-1 LTR U3 sequence (Barry et al., 2001; Chen et al., 2007).

2.4 Generation of Lentivirus

Package of lentivirus was performed by transient transfection of 293T human embryonic kidney cells with the lentivirus transfer vectors and three packaging vectors, pMDL/pRRE, pRSV-REV and pCMV-VSVG by calcium phosphate method as previously described (Chen Y et al., 2007). The lentivirus products were stored at -80°C.

2.5 Lentivirus Infection

One day before infection, 2 x 104 of cells per well were seeded in 24-well plate and cultured in a humidified incubator containing 5% CO2 at 37°C. On the day of infection, the medium was removed and replaced with the mixture containing polybrene 4μl (Sigma-Aldrich, Inc.) and 15μl of lentivirus in fresh DMEM medium supplemented with 10% FBS (381μl). After 48 hours, the medium containing virus was discarded, and washed twice with PBS to remove any residual virus. The transduction efficiency was monitored by a fluorescent microscope. The infected EGFP-positive cells emitted green fluorescence. The intensity and scope of green fluorescence infected cells were measured as the criteria of transduction efficiency.

2.6 Plasmids and transfection

TOPO3.1 empty vector and TOPO3.1-X Δ35 were produced as mentioned above. pDEST40-CTRL and pDEST40-GAS2 were given generously by Dr. Yutaka Kondo, Nagoya, Japan.

1–3 x 10^5 cells per well were seeded in six-well plate overnight to achieve the desired density of 50–80% confluence. Plasmids were transfected into cells using FuGene 6 reagent (Roche) according to the manufacturer's instructions. Plasmid (1 μg) was mixed with FuGene 6 reagent (3 μl) in serum-free medium (97 μl) for 20 minutes at room temperature, and evenly added into the cells in a drop-wise manner. The transfected cells were cultured in the incubator until gene expression analysis was performed.

In knock down experiments, siRNA against GAS2 or P53 (siGAS2 50μM, or siP53 100μM, ON-TARGET plus SMART pool, Thermo Fisher Scientific Limited) was mixed with 12μl of HiperFect Transfection Reagent in 100μl of culture medium without serum. The samples were then incubated for 5-10 minutes at room temperature to allow the formation of transfection complexes. The complexes were added evenly to the cells in a drop-wise manner. The plate was swirled gently and cultured in a humidified incubator containing 5% CO_2 at 37°C.

2.7 Western Blot Analysis

The colleted cells were lysed in lysis buffer (50mM Tris-HCl, PH 7.5, 150 mM NaCl, 1% NP-40, 0.5% Na-deoxycholate) supplemented with protease inhibitor cocktail (Roche) on ice. Tissues were homogenized thoroughly with pestles in the T-PER Tissue Protein Extraction Reagent (Thermo Scientific) supplemented with protease inhibitor cocktail on ice. The lysates were centrifuged at 12,000×g for 10 minutes at 4°C and soluble supernatants from each sample were collected into new tubes and stored at -20°C before use.

Protein concentrations were measured using the method of Bradford (Bio-Rad Laboratories). The concentration of BSA is prepared to be 0.25, 5, 1, 2 and 4 mg/ml which were used for standard curve construction. 5μl standards and samples were pipetted into a 96-well microtiter plate with the addition of 25μl of mixture (reagent A and S). 200μl of reagent B was then added into each well and incubated for 15 minutes at room temperature. The reaction products were measured at the wavelength of 750 nm in ELISA reader.

Fifty micrograms of protein were loaded on a 15% sodium dodecyl sulfate polyacryl-amide gel electrophoresis (SDS-PAGE, Bio-Rad). A Nitrocellulose Membrane (Bio-Rad Laboratories), 2 filter papers and the SDS-PAGE were equilibrated in a transfer buffer (39 mM glycine, 48 mM Tris-HCl, 0.037% SDS, 20% methanol, pH 8.3)

before assembly in the Trans-Blot Semi-Dry Electrophoretic Transfer Cell (Bio-Rad Laboratories, Inc.).

After blotting, the membrane was blocked in 5 ml of blocking buffer [Tris-buffered saline-Tween 20 (TBST) with 5% (w/v) non-fat dried milk powder] at room temperature for 1 hour. The membrane was incubated with primary antibodies at 4°C overnight. After 3 washes with TBST, the membrane was probed with a horseradish peroxides-conjugated secondary antibody (1:5000, Sigma) for 2 hours at room temperature. The membrane was then washed for 3 times by 5 ml of TBST.

The antigen-antibody complexes were detected with Western Lightning Chemi-luminescence Reagent Plus (*Amersham Biosciences*) by exposing to the FUJI Medical X-Ray Film (FUJI) in a dark room (Table 2.2).

Table 2.2 Antibodies used in Western Blot

Immunogen	Source	Dilution Ratio	Brand	Application
HBx	mouse	1:500	Abcam	Primary antibody
GAS2	mouse	1:500	Santa Cruz	Primary antibody
P53	mouse	1:1000	Santa Cruz	Primary antibody
b-actin	mouse	1:5000	Santa Cruz	Primary antibody
PARP	rabbit	1:1000	Cell Signaling	Primary antibody
Caspase 3	rabbit	1:1000	Cell Signaling	Primary antibody
Anti-mouse	goat	1:5000	Santa Cruz	Secondary antibody
Anti-rabbit	goat	1:5000	Santa Cruz	Secondary antibody

2.8 Counting Cell

Cells were plated on a 6-well plate at $1x10^4$ cells per well. The cells were maintained in DMEM with 10% FBS medium. Cell numbers were determined in a counting chamber by trypan blue exclusion every 24 hours for 5 consecutive days. All experiments were performed in triplicate and in 3 independent experiments.

2.9 Proliferation Assay

Cell viability was determined by [3-(4,5-dimethythiazol-2-yl)-5-(3-carboxymethoxy -phenyl)-2-(4-sulfophenyl)-2H-tetrazolium(MTS) assay which is a colorimetric method using CellTiter 96® AQ_{ueous} One Solution Cell Proliferation Assay (Promega Biotech Co., Ltd) for 5 consecutive days. Briefly, infected cells ($3x10^3$/well) were seeded in 96-well plates and maintained in 100 µl of culture medium (DMEM supplemented with 10% FBS) in 6 replicates. The plate was kept in a 37°C humidified incubator before MTS assay. Culture medium was discarded, and replaced with a 120 µl of MTS mixture including 100 µl of fresh culture medium (DMEM with 10% FBS) and 20 µl of MTS solution. The plates were kept in a 37°C humidified incubator for 1 hour in the dark. The absorbance of the colorimetric products formed was measured at 490 nm by Quant Microplate Spectrophotometer (BioTek Instruments, Inc.). The background absorbance was subtracted. All experiments were performed in triplicate and in 3 independent experiments.

2.10 Colony Formation Assay

Cells ($1x10^5$/well) in 12-well plates with 70~80% confluence were transiently transfected with indicated vector using FuGene 6 reagent according to the manufacture's instructions. After 2 days, the cells were subcultured in 6-well plates and cultured for 2 weeks in antibiotic-containing selection medium. The drug-resistant colonies were washed with PBS twice and stained with 0.2% crystal violet for 10 minutes at room temperature. Cell numbers were counted under the microscope and data were obtained from 3 independent experiments.

To assess the growth ability of C-terminally truncated HBx, LO2 cells were transfected with pcDNA3.1 and truncated HBxΔ35 using FuGene 6 reagent with the ratio of 1μg (plasmids):3μl (FuGene 6) in 97μl of serum-free medium (DMEM) per well. Geneticin G418 (Invitrogen) (1000 μg/ml) were added to select transfected cells 48 hours after transfection. To examine the proliferative capacity of GAS2, SK-hep1 ($5x10^4$/well) cells were seeded in the 12-well plate. By selecting with G418 (500 μg/ml) for 14 days, the number of colonies was counted.

2.11 Chromatin Immunoprecipitation Microarry (ChIP-chip)

2.11.1 Chromatin Immunoprecipitation (ChIP)

The ChIP assays were performed according to the standard protocol of the Transcription Factor Chromatin Immunoprecipitation Kit (Red ChIP Kit ™, Diagenode, Catalog #: kch-redTBP-012). MIHA and LO2 cells infected by LV and X35 were seeded at the concentration of $1x10^6$ /well in the 100 mm dishes. The cells in 80% confluence were crosslinked with the cross-linking buffer (37% formaldehyde 90ul, Buffer A 210ul, PBS 3ml), mixed immediately and incubated for 10 minutes at room temperature. 1.25 M Glycine (330ul) was then added to the cells for 5 minutes at room temperature to stop the cross-linking reaction, followed by washing by ice-cold PBS. The cells were scraped after adding 500 ul of Buffer B, centrifuged for 5 minutes at 500 g (1,600 rpm) at 4°C and supernatant was discarded. The pellets were then washed by 15 ml of ice-cold Buffer C, with incubation for 10 minutes at 4°C with gentle mixing. The pellets were centrifuged again for 5 minutes at 500 *g* (1,600 rpm) at 4°C, and the supernatant was discarded. Subsequently, the centrifuged pellets were resuspended by 90 ul of freshly prepared [P.I.-buffer D] cocktail (4 µl of P.I. 100 µl of Buffer D.).

The chromatin containing sample (300ul) was transferred into the 1.5ml tubes and sonicated for 15 cycles [30 seconds "ON" / 30 seconds "OFF"]. After shearing, the samples were centrifuged for 5 minutes at 14,000 *g* (13,000 rpm) at 4°C to remove

debris. The supernatants were kept which contained the sheared chromatin sample. An aliquot of 10 µl of sheared chromatin was placed in the 1.5 ml tube for preparation of input sample and stored at -20°C until processing. At the meantime, the beads were prepared. The pre-blocked protein A/G bead suspension was centrifuged for 2 minutes at 500 *g* (3,000 rpm) to pellet the beads. 1 ml of freshly prepared [P.I.-ChIP buffer 1x] mixture (1520 µl of water, 400 µl of Buffer E and 80 µl of P.I.) was added to the beads for washing and centrifuged for 2 minutes at 500 *g* (3,000 rpm). 415 µl of [P.I.-ChIP buffer 1x] was then added to the pelleted beads to obtain a 1:3 bead suspension for immunoprecipitation

Buffer E (60 µl), beads for IP (30 µl), anti-HBx (1 mg/ml, 5µl), or IgG (2.5 µg /µl, 0.8µl) were added to the sheared chromatin. Then, the IP-incubation mix (5% BSA with proteinase inhibitor) was mixed by inverting several times and incubated over-night at 4℃ on a rotating wheel. After incubation, pellet beads were centrifuged for 2 minutes at 500 *g* (3,000 rpm) at 4°C and supernatant was removed gently. 350 µl of ice-cold wash buffer was added per IP tube and incubated for 5 minutes with rotation. The beads were pelleted by centrifugation for 2 minutes at 500 *g* (4,000 rpm) at 4°C and supernatant was removed, followed by washing with the following: wash buffer-1, twice; wash buffer-2, once; wash buffer-3, once; wash buffer-4, twice). The [DNA-protein-antibody] complex bound to the beads was eluted by adding 400 µl of Buffer F followed by incubating for 20 minutes at room temperature with rotation. The beadswere precipitated by centrifuging for 2 minutes at 500 g (3,000 rpm) at

room temperature and the supernatant was transferred to new 1.5 ml tubes. 390 µl of Buffer F was then added to 10 µl sheared chromatin sample to bring the final volume to 400 µl which corresponds to the input sample(s). After adding 16 µl of 5 M NaCl, the samples were mixed and incubated in a thermoshaker for 4 hours at 65 ^{o}C to reverse cross-linking followed by cooling down to room temperature. 400 µl of phenol/chloroform/isoamyl alcohol (25:24:1) was added to the samples, then vigorously vortexed for 5 seconds. After centrifugation for 5 minutes at 15,000 *g* at room temperature, the top aqueous phase was transferred into a new 1.5 ml tube. 400 µl of chloroform/isoamyl alcohol (24:1) was added into the samples followed by vortexing vigorously for 5 seconds. The top aqueous phase was transferred into new 1.5 ml tube after centrifugation. 5 µl of the provided DNA co-precipitant, 40 µl of the DNA precipitant and 1 ml of ice-cold 100% ethanol were then added. After mixing, the samples were left at -20 ^{o}C for 30 minutes. Then, the samples were centrifuged for 25 minutes again at 14,000 *g* (13,000 rpm) at 4°C. 500 µl of ice-cold 70% ethanol was added to the pellet after removing the supernatant. The samples were centrifuged again for 10 minutes at 14,000 *g* (13,000 rpm) at 4°C. After removing the supernatant, the tubes were air-dried for 30 minutes at room temperature to evaporate the remaining ethanol. The pellets are: 1) DNA that was purified from the sheared chromatin (input sample), and 2) DNA that was isolated by ChIP (ChIP samples). The ChIP samples were added 200 µl of water, and the input samples were added 100 µl of water. The tubes were placed into the tubes in shaker for 30 minutes at 12,000 rpm at room temperature to dissolve the pellets.

2.11.2 Microarray hybridization

Before DNA microarray, CHIP (X35 with HBx antibody) DNA was labeled with distinct fluorescent dye Cy5 and LV control was labeled with distinct fluorescent dye Cy3. Reciprocal experiments were performed to avoid labeling bias. And the samples were cohybridized to human DNA microarray, which contains 17,000 defined human transcripts. The data were analyzed by feature extraction (Agilent).

2.11.3 Data Analysis and Identification of In vivo DNA Binding Sites

Statistical analysis was performed with ChIP Analytics v.1.3, which utilizes user-configurable heuristics for binding event identification based on *P* values and adjacent probes, as well as data normalization and Whitehead Error Model v.1.0. The Default settings were used with blank subtraction and Lowess normalization. A gene promoter was considered as positive for HBx binding if the probes have *P* (Xbar)$<10^{-3}$

2.12 RNA Extraction

$1x10^6$ MIHA and LO2 cells infected LV and X35 were collected for RNA extraction. Total RNA containing small RNA molecules was extracted by TRIzol reagent (Invitrogen). The collected cells or tissues were homogenized in 1ml TRIzol for 5 minutes at room temperature to permit the complete dissociation of nucleoprotein complex. The homogenate was then centrifuged for 15 min at 12000 × *g* at 4°C to discard the precipitation. 200μl of chloroform was added, followed by vigorously shaking for 15 seconds. After incubation for 2-3 minutes at room temperature, the samples were centrifuged at 12000 × g at 4°C for 15 min. The colorless upper aqueous phase was transferred into a new tube. Total RNA was precipitated by mixing with 500μl of isopropyl alcohol for 10 minutes and pelleted by centrifugation at 12000 × g for 10 minutes at 4°C. The pellet was subsequently washed with 1ml of 75% alcohol and centrifuged at 7500 × g at 4°C for 5 min. The RNA pellet was dried by air and dissolved in DNase/RNase-free water.

2.13 Reverse transcription (RT)

1μg of total RNA sample was mixed with DNase I (1μl, 1U/μl, Invitrogen) in DNase I reaction buffer (10X, 1μl, Invitrogen) and incubated for 15min at room temperature in order to remove DNA contamination. 1 μl of EDTA solution (25 mM) was added into the reaction mixture to inactive the DNase I. The cocktail was then heated for 10 min at 65°C.

The RNA solution was mixed with 2X RT Master (Invitrogen): 2 μl 10x RT Buffer , 0.8 μl 25x dNTP Mix (100 mM) , 2 μl 10x RT Random Primers , 1 μl MultiScribe™ Reverse Transcriptase , 1 μl RNase Inhibitor and 3.2 μl Nuclease-free H_2O. 10 μl of RNA samples were added to the 2X RT Master mixtures and incubated at thermal cycling conditions: 25°C, 10 minutes; 37°C, 120minutes; 85°C, 5 seconds.

2.14 Quantitative RT-polymerase chain reaction (Real-time PCR)

Real-time PCR was performed with 7500 FAST REAL TIME PCR System (Applied Biosystems) using a Power SYBR Green PCR Master Mix (Applied Biosystems) [2X Sybrgreen 10 µl, 0.5 µl of 10 µM Forward primer, 0.5 µl of 10 µM Reverse primer, nuclease-free water 7 µl and cDNA template (1:5) 2 µl]. Real-time PCR profile to detect gene transcripts in cDNA templates was initiated by a denaturation step of 10 minutes at 95°C, and the cycling parameters were 95°C for 15 seconds and 58°C for 1 minute for 40 cycles, followed by a melting curve analysis. Human *PNN* was used as an internal control because it was reported that it has a very low variation coefficient in human liver tissues (Cougot et al. 2007). All reactions were carried out in triplicate and data were analyzed using 7500 FAST System SDS software.

Table 2.3 Sequence of Primers used in Real-time PCR& semi quantitative-PCR

Primer Name	Primer Sequence
ADAL-F	5'-GGATGACCGTAGTGACAGATAAAGC-3'
ADAL-R	5'-GGACAATCATAAAGAGGGCAAAA-3'
ASPH-F	5'-TCCTGTTCTTTTGTTTTGCTGGTA-3'
ASPH-R	5'-TCCTCCCATGCCTCTTCATC-3'
B3GALT1-F	5'-CCTCATCAGCACCACTCACAA-3'
B3GALT1-R	5'-CCCCCCACGTCTCTCTGATT-3'
CD36-F	5'-TTCCTGCAGCCCAATGGT-3'
CD36-R	5'-GTCAGCCTCTGTTCCAACTGATAG-3'
CDKN2B-F	5'-CCCCCCCCAACACACCTA-3'
CDKN2B-R	5'-TCCCTGTGCTTCAGTTTGAAAA-3'
CRIPT-F	5'-TCCATCTGCTGGGCTCAAG-3'
CRIPT-R	5'-CGCCTGTAGTCCCCAGCTACT-3'
DDX26B-F	5'-TGAAGCCTCCTGGAATGTTTG-3'
DDX26B-R	5'-CCCCACTGCTGCTGCTTCTTAGC-3'
DMD-F	5'-TCCTCTACCACCACACCAAATG-3'
DMD-R	5'-GCCCCACTCAGCTGACAGTT-3'
DTNA-F	5'-GCCAGAGAAGGCACAGCAA-3'
DTNA-R	5'-TGTCTGAGGAGCCGGAGTTC-3'

Primer Name	Primer Sequence
ELAVL2-F	5'-CACGGAGCCAATCACTGTAAAG-3'
ELAVL2-R	5'-AAGGATGGCCTGATTGGTTTT-3'
EPHA7-F	5'-GAATGTTGGTGAAGGCAAGTCTCT-3'
EPHA7-R	5'-TGTCACGAGAATGAAAAAATCTTGA-3'
FBXO30-F	5'-CGAGAAACGGGAGGAAGCA-3'
FBXO30-R	5'-TCCTTCTTTAGTGAGTTCTCGTGTCA-3'
FBXW7-F	5'-CAGTGGTCATTGGGCAGTGT-3'
FBXW7-R	5'-TGGTAAAAGAACAGGCTAGCAGAA-3'
GAS2-F	5'-TGCAAATGCCCAAACAAGTTC-3'
GAS2-R	5'-TTCTCCCACTCGGTATCTTCCTT-3'
GOLPH4-F	5'-GAAATGTAGCGGCACCCAAT-3'
GOLPH4-R	5'-GGCAGATTTATGTTTGAGCAGCTT-3'
INTS12-F	5'-TGACAGACAAGGAAGCGAATGA-3'
INTS12-R	5'-GTCTGGTACATCGGGCACAA-3'
KIAA1468-F	5'-TCAGAGAAAGAAGTAGAAGCAGGAAA-3'
KIAA1468-R	5'-TCGGCTTGAGGTCCATCTTAG-3'
KRR1-F	5'-CCTTGCTCATTTTGCAGATTTAGA-3'
KRR1-R	5'-AGGTTGCCACAGGTGGACTTT-3'
LIMCH1-F	5'-TTATGCCCTGCCCACTTCA-3'
LIMCH1-R	5'-TGATAGCAAAAAAAGTGATGGAGAA-3'

Primer Name	Primer Sequence
MBNL1-F	5'-TTTCTCCCACCAGGCTCAAT-3'
MBNL1-R	5'-TGCACCATGGGAACAACACT-3'
MUM1L1-F	5'-GGGAACCGATGGCTGGCTGTAACTT-3'
MUM1L1-R	5'-CGGTCAGGGAGAATTTTTTGG-3'
NEDD4-F	5'-TCAAAAGTAGGCGTAAGCAGAATAAG-3'
NEDD4-R	5'-TATCTTTGCAGGTGTGCTGGAA-3'
OTOR-F	5'-TGAATTTCCTCTTCCTGTGCAA-3'
OTOR-R	5'-ACCTGCATCCTCCTCAGATTTC-3'
PDE1A-F	5'-GGATTGACAGAGCCAAAACCA-3'
PDE1A-R	5'-TGGCTGGGTGGCTGATGT-3'
PHIP-F	5'-TCCAAAGCATATACACCAAGCAA-3'
PHIP-R	5'-GAAAGCAGACAGGCGCAAA-3'
POSTN-F	5'-TGGAAAACAGCAAACCACCTT-3'
POSTN-R	5'-CAGAGCAGATGCCAAGCCTAA-3'
PPARG-F	5'-TCAGGGCTGCCAGTTTCG-3'
PPARG-R	5'-GCTTTTGGCATACTCTGTGATCTC-3'
PTPRH-F	5'-CCCCAGCCGAGAAGGAA-3'
PTPRH-R	5'-GGATGGCGGCCACGTT-3'
PTPRK-F	5'-GCAGGAGGAATGCGAGGAA-3'
PTPRK-R	5'-GCCCGCCACCATTTAGG-3'

Primer Name	Primer Sequence
RRH-F	5'-ACCATCTGCCTTCCTGACGTA-3'
RRH-R	5'-TCCCAGAATCAAGCCGATGT-3'
SLITRK6-F	5'-GCCATAAAACCACTCATCATCACACTACT-3'
SLITRK6-R	5'-GGGCTCACCATGTGCTGTT-3'
SPOCK3-F	5'-CAAAATGGCAAGTATGGAAAACC-3'
SPOCK3-R	5'-ATGAGACTGCCATCCAAATTAAAAT-3'
SPP1-F	5'-TGAGCATTCCGATGTGATTGA-3'
SPP1-R	5'-TGTGGAATTCACGGCTGACTT-3'
ST6GAL2-F	5'-CGCTGCTGATTGACTCTTCTGA-3'
ST6GAL2-R	5'-ACCCAAACGGGACCTACCTAA-3'
TANK-F	5'-GACCCATCTGATGCACCTTTTC-3'
TANK-R	5'-GGTCCTCGGATTGCTTTTCC-3'
TCERG1L-F	5'-ACCCGCCCCACAAACG-3'
TCERG1L-R	5'-TGGACCCATCGCTGTTGTC-3'
TMEM90B-F	5'-ACCTGCCCCTCTTTCTTTCC-3'
TMEM90B-R	5'-CCGGAGGTGGCTTGACAT-3'
TRIM9-F	5'-TGAACAACAAGGTCCCATAGCA-3'
TRIM9-R	5'-GCTGACCGCAGGGAAGAAG-3'
WWC3-F	5'-GCCTGTGTCCGCTTTTGC-3'
WWC3-R	5'-GGCCTTCCTTTGTCTTTTCTTTC-3'

Primer Name	Primer Sequence
XKR4-F	5'-AAGCCCCAAACAACTGAGAATG-3'
XKR4-R	5'-TCGTTCTCTCGCCTGCTTTTA-3'
ZBTB33-F	5'-TCCAAGCGAACAGCAACCT-3'
ZBTB33-R	5'-AGAGACTTGTCTGCATGGCTATTTT-3'
ZNF556-F	5'-TCAGGAACGGACAGGACATG-3'
ZNF556-R	5'-CAGCGTGAAATCCACAACCA-3'
PNN-F	5'-CCTTTCTGGTCCTGGTGGAG-3'
PNN-R	5'-TGATTCTCTTCTGGTCCGACG-3'

2.15 Semi-quantitative polymerase chain reaction (PCR)

2.15.1 RT-PCR

PCR products were synthesized according to the standard protocol of Promega GoTaq Fexi DNA polymerase [5 µl of 5X GoTaq Green Buffer, 2 µl of 25 mM $MgCl_2$, 0.5 µl of 10 mM dNTP (Fermentas), 0.5 µl of 10 µM Forward primer, 0.5 µl of 10 µM Reverse primer, 0.125 µl of GoTaq DNA Polymerase (5U/µl), nuclease-free water 14.375 µl and cDNA template (1:5) 2 µl, or 100 ng of DNA template] in a total volume of 25 µl reaction mixture.

PCR was carried out in the GeneAmp® PCR System 2700 Thermal Cycler (Applied Biosystems) at 95°C for 5 min, 35 cycles of 95°C for 30 sec, 60°C for 30 sec and 72°C for 30 sec, and 72°C for 10 min. 95°C for 5 min, 33 cycles of 95°C for 30 sec, 58°C for 30 sec and 72°C for 30 sec, and 72°C for 10 min for the amplification of PNN gene. PCR of human PNN gene was used as a loading control. The primers of the selected target genes were listed in Table 2.3.

100 ng of DNA from HCC tissues was used as template. The condition of PCR product generated: 95°C for 2 min, 36 cycles of 95°C for 1 min, 62°C for 1 min and 72°C for 1 min, and 72°C for 10 min for the amplification of full-length and truncated HBx genes, while 95°C for 2 min, 28 cycles of 95°C for 30 s, 58°C for 30 s and 72°C for 30 s, and 72°C for 7 min for the amplification of β-actin gene (Table 2.4). β-actin

gene was used as a internal control. The PCR products were then analyzed by electrophoresis on a 1.5% agarose gel stained with GelRed Nucleic Acid Stain (Biotium) and visualized by GelDoc XR (Bio-Rad Laboratories, Inc.).

Table 2.4 Sequence of Primers for RT-PCR

Primer Name	Primer Sequence
XF (nt1286-1305)	5'-CAGCTTGTTTTGCTCGCAGC-3'
XR1 (nt1551-1570)	5'-GCAGATGAGAAGGCACAGAC-3'
XR5 (nt1816-1835)	5'-GGCAGAGGTGAAAAAGTTGC-3'
β-actin F	5'-CTTCAACACCCCAGCCATGTACG-3'
β-actin R	5'-CATGAGGTAGTCAGTCAGGTCCCGG-3'

2.15.2 Real-time ChIP-PCR

ChIP real-time PCR was performed with the same system as mentioned above with 2X Sybrgreen 10 µl, 0.5 µl of 10 µM Forward primer, 0.5 µl of 10 µM Reverse primer, nuclease-free water 7 µl and template DNA (derived from CHIP assay) 20ng. The DNA templates were derived from MIHA-LV-HBx, MIHA-X35-HBx, MIHA-X35-IgG, MIHA-input; LO2-LV-HBx, LO2-X35-HBx, LO2-X35-IgG, LO2-input, Input was used as the standard control, and IgG was used as negative control for CHIP assay. The condition of real-time PCR was 95°C for 10 min, 40 cycles of 95°C for 15 sec, 60°C for 1 min followed by the dissociation stage 95°C 15sec, 60°C 1min, 95°C 15sec. Input and IP samples were directly detected for HBx binding sites on putative target genes by quantitative PCR amplification.

2.15.3 Conventional ChIP-PCR

20 ng of DNA (MIHA-LV-HBx, MIHA-X35-HBx, MIHA-X35-IgG, MIHA-input; LO2-LV-HBx, LO2-X35-HBx, LO2-X35-IgG, LO2-input) was used as template. Input was regarded as the positive control while IgG was used as internal negative control for ChIP assay. The condition of PCR was 95°C for 2 min, 40 cycles of 95°C for 1 min, 60°C for 1 min and 72°C for 1 min, and 72°C for 10 min for the selected target genes (Table 2.5).

Table 2.5 Sequence of Primers for real-time and conventional ChIP-PCR

Primer Name	Primer Sequence	Primer location
GAS2-L-F	CAGCCAAACCGTTGAGTCATT	chr11:22647319-22647378
GAS2-L-R	CAATTTCTCATGATCCTTTTTTTCAC	
GAS2-M-F	TGATCATGCTAGCTGAATCCATTT	chr11:22649885-22649944
GAS2-M-R	CTGCAGGTCTTGGATTTAGATTTG	
FBXO30-L-F	AAAACACCATGTTATCCCCAATTAA	chr6:146175850-146175909
FBXO30-L-R	TCCGCTGAATCACTCTTCTTCA	
INTS12-M-F	CCGGCAAATATCCATATAGTGAAA	chr4:106843733-106843792
INTS12-M-R	TTACACCAAGTTGCTGACCTCTTT	
INTS12-L-F	TGCCATTGGCTGCTTTGTTA	chr4:106840087-106840146
INTS12-L-R	GGAGGTATGGATGAACTCTGAGAAC	
PDE1A-L-F	CCCTCATTTCTCATAGTTTCCATTTAT	chr2:183097560-183097619
PDE1A-L-R	GGTAAACAGGAATGAAGGAACTACTTG	
PTPRH-L-F	ATCTAAGAGCCCAGGTGTAAGACTCT	chr19:60412670-60412720
PTPRH-L-R	GCTGAAGATCCCCTGGAGAAG	

2.16 Flow cytometry

Flow cytometry was applied to not only measure the relative cellular DNA content but also the cell distribution during the various phases of the cell cycle.

To assess the ability of GAS2 in P53-induced apoptosis, we introduced an antitumor drug, etoposide whose function was dependent on a functional P53. 1 x 10^5 of cells were seeded in the 6-well plate. After transfection of CTRL and GAS2-expressing plasmids for 24 hours, 100μM of etoposide was added to the transfected cells for 24 hours. The cells were then harvested and washed twice with cold PBS. Cell pellets was fixed with ice-cold 70% ethanol overnight at 4°C. On next day, the fixed cells was collected and washed again with PBS once. The samples were stained with 500μl propidium iodide solution (PI, 50μg/ml) containing 3.8mM sodium citrate and 100μg/ml RNase A (Invitrogen), and incubated for 30 minutes at 4°C in the dark. Cellular DNA content was determined by a Fluorescence-activated cell sorting (FACS) caliber flow cytometer (BD Biosciences). The different phases of cell cycle were analyzed using WinMDI2.9 software in 3 independent experiments.

2.17 Annexin V Apoptosis Assay

Cell apoptosis was also assessed by flow cytometry using an APC Annexin V Apoptosis Detection Kit I (BD Pharmingen). The detection Kit I adopted two fluorescent dyes, 7-Amino-actinomycin D (7-AAD) and APC-conjugated Annexin V, to differentiate viable cells from cells that underwent apoptotic or necrotic cell death. The early apoptotic cells showed 7-AAD negative and APC Annexin V positive, while the viable cells showed both APC Annexin V and 7-AAD negative. The late apoptosis or dead cells were both APC Annexin V and 7-AAD positive.

1×10^5 of cells were seeded in the 6-well plate. After treatment, the cells were collected and washed twice with cold PBS. The samples were then resuspended in 1X Binding Buffer at a concentration of 1×10^6 cells/ml and 100 µl (1×10^5 cells) was transferred to a 5 ml culture tube. The cells were mixed with 5 µl of APC Annexin V and 5 µl of 7-AAD and then incubated for 15 min at room temperature. Finally, 400 µl of 1X Binding Buffer was added to each tube and analyzed by flow cytometry within 1 hour. The data was analyzed using WinMDI2.9 software.

2.18 Statistical analysis

Statistical analysis was performed by GraphPad Prism (GraphPad Software). Fisher's exact test was used to determine truncated HBx integration in HCC tissues. Student's t test was used to analyse colony formation assay, cell proliferation and cell cycle analysis. P value less than 0.05 was considered as statistically significant.

CHAPTER THREE- RESULTS

3.1 Oncogenic ability of carboxyl-terminal truncated HBx

Naturally occurring COOH-terminal truncated mutants of HBx derived from HCCs have been shown to improve the proliferation ability of HCC cell lines and thereby contribute to hepatocarcinogenesis (Tu et al., 2001; Xu et al., 2007). We therefore examined the effects of 3'- deleted Δ35aa of HBx gene (HBxΔ35) in human normal hepatocytes. Human immortalized non-tumorigenic liver cell lines MIHA and LO2 were infected with lentivirus expressing HBxΔ35 (lenti-HBxΔ35) or empty vector control (lenti-CTRL). The extent of green fluorescence in infected cells was used to indicate the transduction efficiency. Extensive transduction (>80%) was achieved at 72 hours in the MIHA and LO2 cell lines (Fig.3.1). The protein expression of C-terminal deleted HBx mutants in the infected cells was further confirmed by Western blot analysis (Fig.3.2).

The effect of HBxΔ35 overexpression on MIHA and LO2 cell growth was then analyzed by cell counting assay. Lenti-HBxΔ35 infection increased cell growth rate when compared with lenti-CTRL in both MIHA and LO2 cells (Fig.3.3A). Cell viability assay (MTS assay) verified the increased cell growth rates in MIHA-HBxΔ35 & LO2-HBxΔ35 compared with MIHA-CTRL & LO2-CTRL cells (Fig. 3.3B). In addition, colony formation assay also demonstrated that the expression of

HBxΔ35 in LO2 caused a substantial increase in the number of colonies when compared with the control cells (Fig. 3.4).

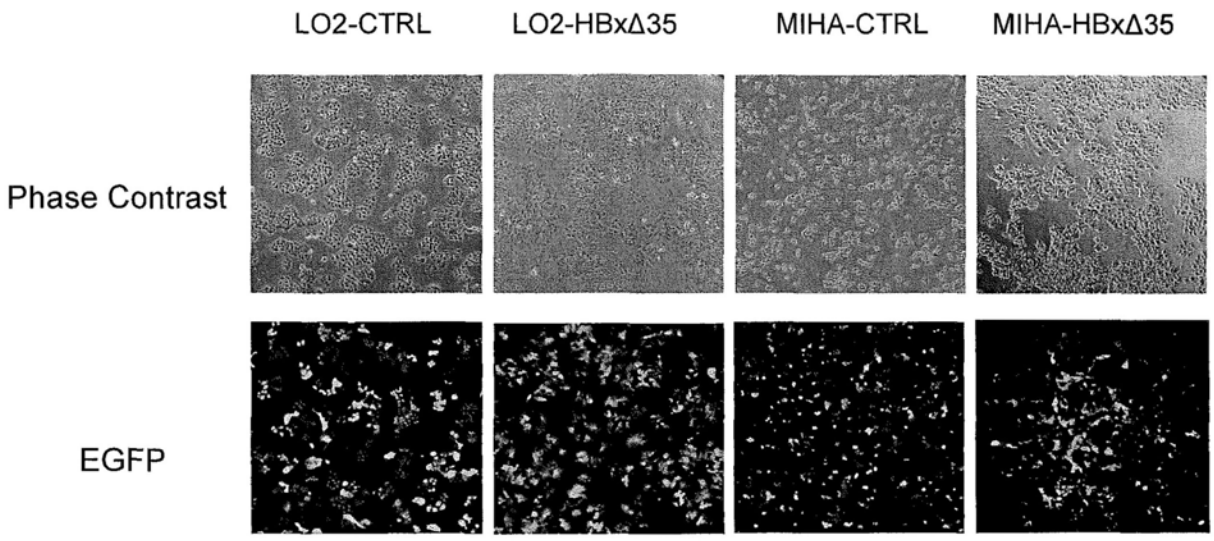

Fig. 3.1 Expression of HBxΔ35 protein in lentivirus-infected LO2 and MIHA cells. Phase contrast and fluorescent microscopic examination of LO2 and MIHA hepatocytes infected by lentivirus containing HBxΔ35 or EGFP alone. The transduction efficiency was estimated by the intensity and percentage of green fluorescence emitted by EGFP-positive cells under a fluorescent microscope. Photographs were taken at day 3 post-infection.

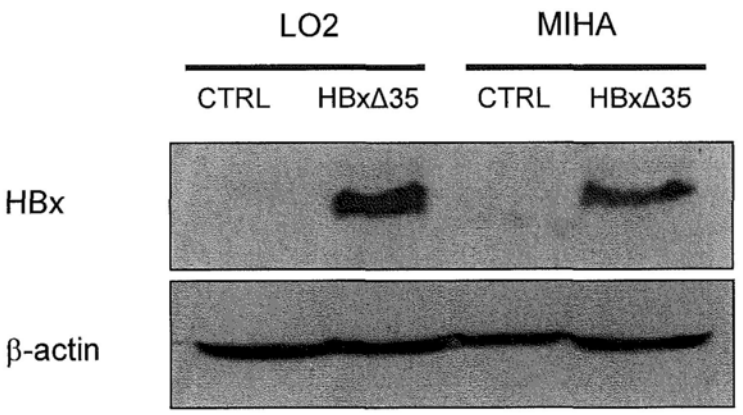

Fig. 3.2 Western blot analysis of HBxΔ35 protein expression in LO2 and MIHA cells infected with lenti-HBxΔ35 or lenti-CTRL. β-actin was used as loading control.

A

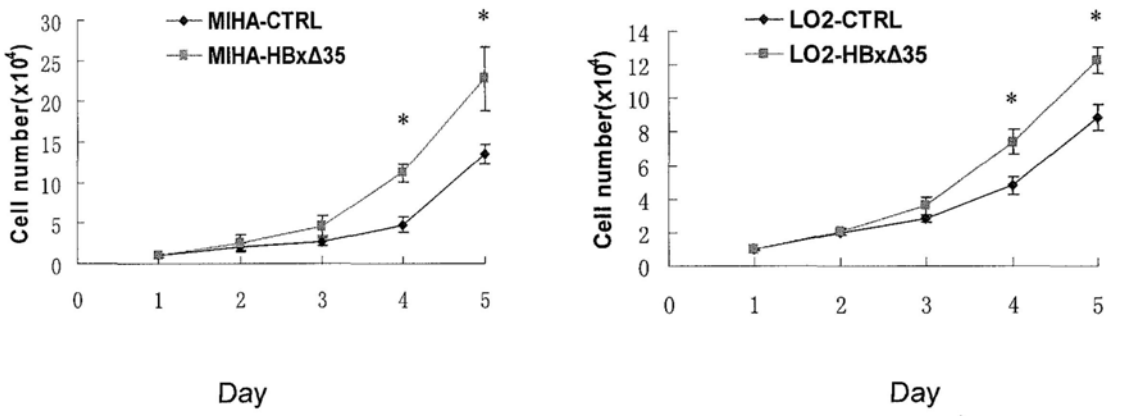

B

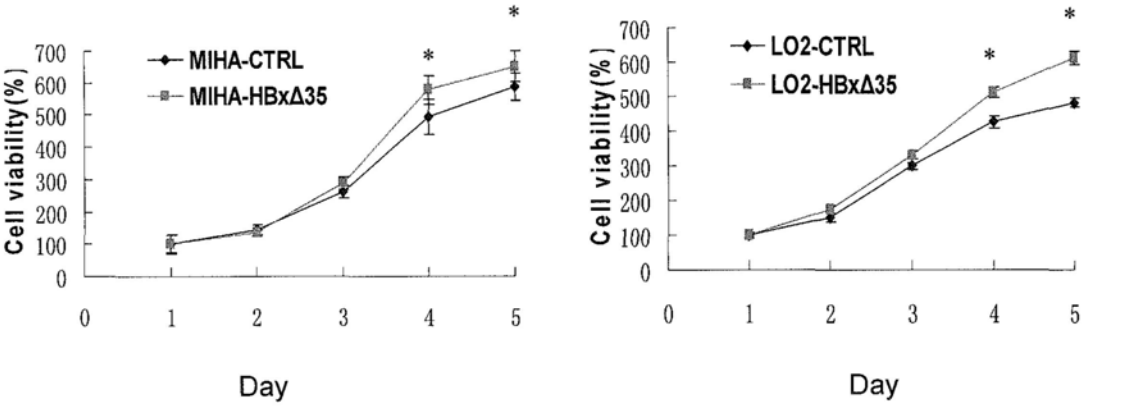

Fig.3.3 COOH-terminal truncated HBx (HBxΔ35) increased the growth rate of non-tumorigenic liver cell lines. (A) Cell growth rate of lenti-HBxΔ35 or lenti-CTRL-infected MIHA and LO2 cells assessed by cell counting assay. **P*<0.05. (B) Cell viability assays of lenti-HBxΔ35 or lenti-CTRL-infected MIHA and LO2 cells. **P*<0.05.

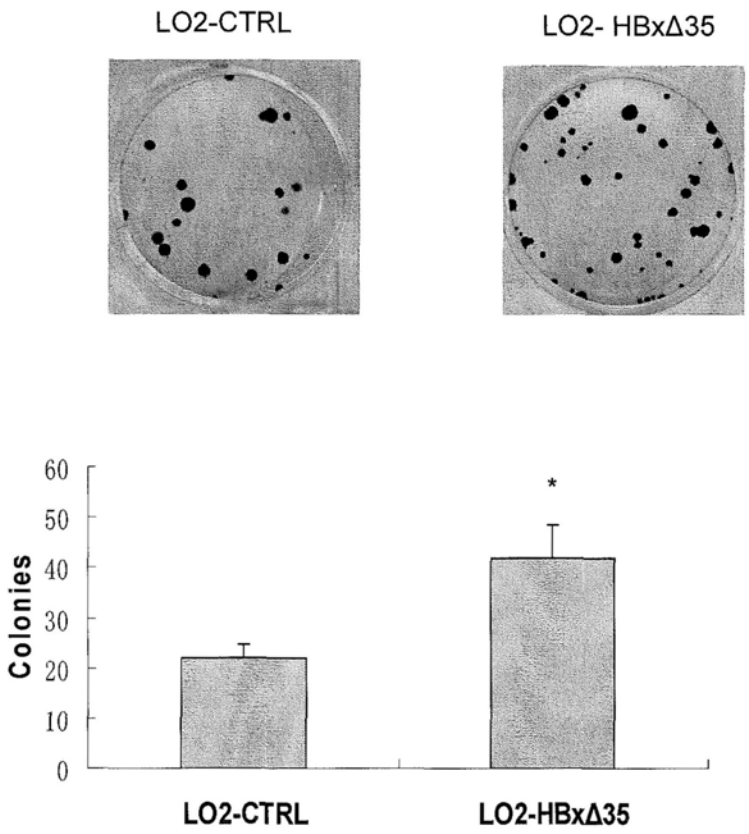

Fig. 3.4 Effect of HBxΔ35 on colony formation. LO2 cells were transfected with HBxΔ35-expressing or control plasmid. After G418 selection for 2 weeks, the number of colonies was scored. *P<0.05

3.2 Identification of direct target genes of HBxΔ35 in human hepatocytes

3.2.1 Genome-wide location analysis of HBxΔ35 binding sites

To identify the direct targets of HBxΔ35 that confer oncogenic properties, we performed HBx ChIP coupled with promoter microarrays covering～17,000 best-defined human transcripts in MIHA and LO2 hepatocytes infected with lenti-HBxΔ35 or lenti-CTRL. We found that 485 and 347 promoters (2-3%) were significantly bound by HBx with high-confidence (p<0.001) in LO2 and MIHA cells, respectively, of which 42 targets were common in both cell lines (Fig.3.5). The specificity of HBx ChIP was further confirmed by amplification of 2 previously reported HBx targets, *IL-8* and *PCNA* (Sung et al., 2009). These positive control loci showed strong enrichment for HBx antibody but not IgG control (Fig.3.6). Notably, gene ontology analysis of these target genes revealed a significant enrichment of negative regulators of cell proliferation compared with the proportion in human genome ($p < 0.005$).

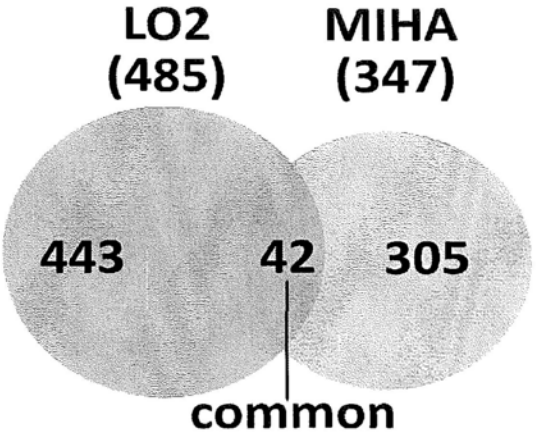

Fig. 3.5 Identification of common direct targets of HBxΔ35 in LO2 and MIHA hepatocytes. Venn diagram illustrates that 42 target genes were commonly bound by HBxΔ35 in both cell lines.

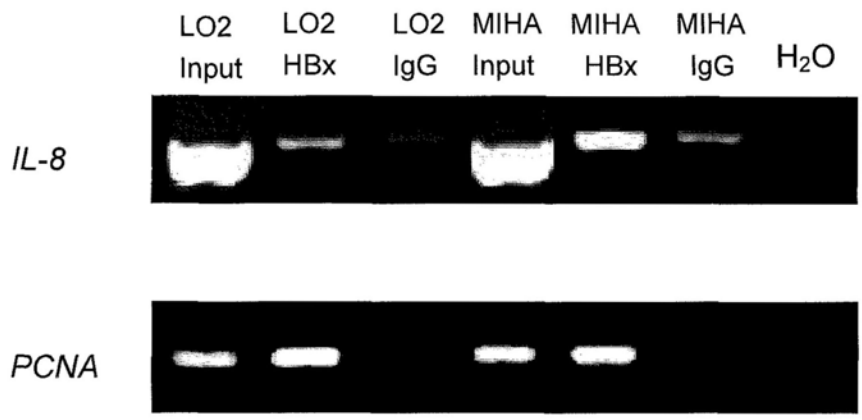

Fig. 3.6 Confirmation of authenticity of ChIP assay. The authenticity of HBx ChIP was confirmed by ChIP-PCR amplification of 2 known HBx direct target genes, *IL-8* and *PCNA*, using DNA pulled down by HBx antibody in both LO2 and MIHA cells. Input (2%) represents genomic DNA as positive control. Non-specific IgG antibody was used as negative control.

3.2.2 Validation of HBxΔ35 target genes in hepatocyte cell lines

To examine whether the common target genes were transcriptionally regulated by HBxΔ35, we compared the mRNA expression of the 42 target genes in the 2 hepatocyte cell lines infected with lenti-HBxΔ35 and lenti-CTRL by quantitative RT-PCR. *PNN* was used as an internal control because this gene was reported to have a very low variation coefficient in human liver cell lines (Cougot et al., 2007). Quantitative RT-PCR analysis showed that 8 and 16 target genes were differentially expressed by at least 1.5-fold in MIHA and LO2 cells, respectively (Fig.3.7). Interestingly, most of the target genes were repressed by HBxΔ35 in the hepatocyte cell lines (6/8 in MIHA and 13/16 in LO2 cells). We further found that one of these targets, *GAS2*, was commonly repressed in both cell lines (Fig.3.7).

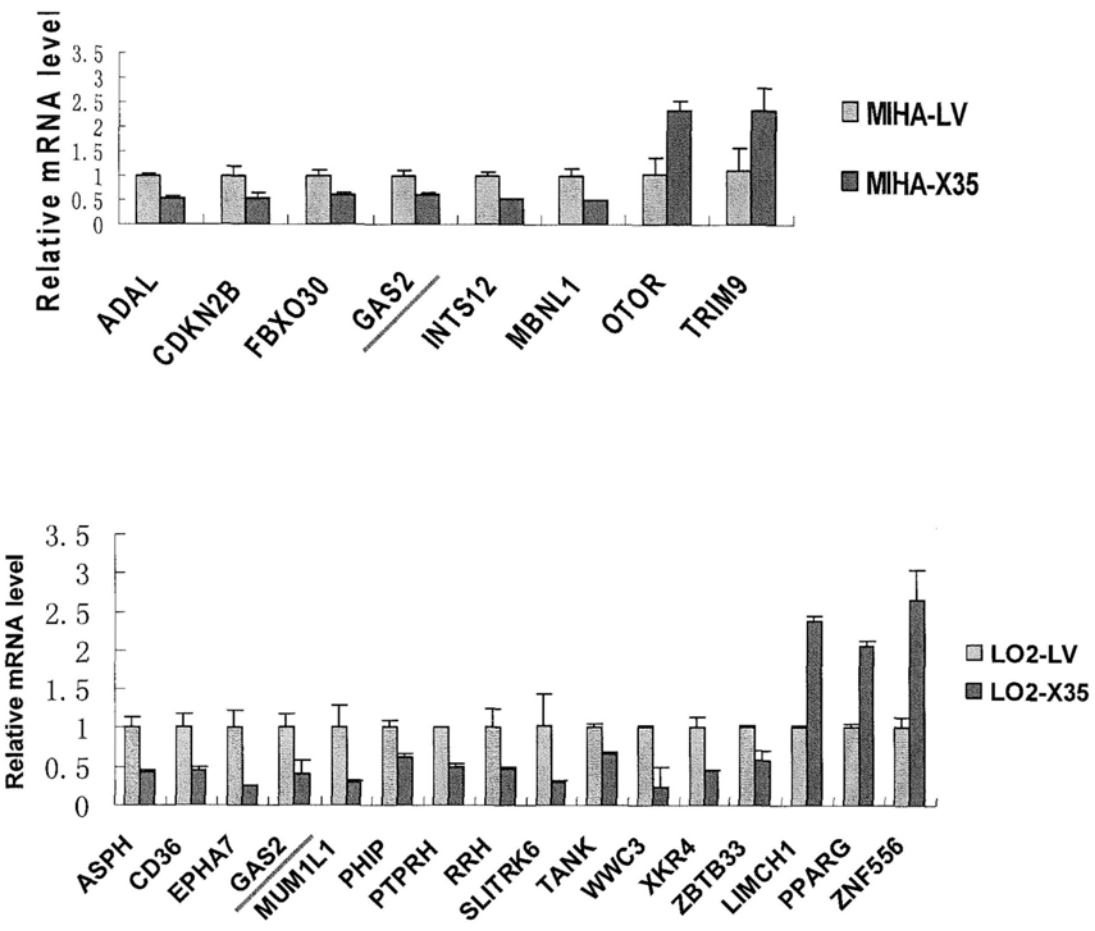

Fig. 3.7 Quantitative RT-PCR analysis of HBxΔ35 target genes in MIHA and LO2 cells. *GAS2* (underlined) was found to be repressed by HBxΔ35 in hepatocyte cell lines.

3.3 Confirmation of GAS2 as a direct transcriptional target of HBxΔ35

3.3.1 Binding of HBxΔ35 in GAS2 gene promoter

Because *GAS2* was a common HBxΔ35-repressed target gene in both MIHA and LO2 cell lines, its transcriptional regulation and function were further characterized in this study. By ChIP-chip analysis, the HBxΔ35 binding site in *GAS2* promoter was mapped at 2.5-3 kilo-base (kb) upstream of the transcription start site (TSS) in MIHA cells and at both 1.5 and 2.5 kb upstream of TSS in LO2 cells (Fig. 3.8). Quantitative and conventional ChIP-PCR assays were performed to validate the occupancy of HBxΔ35 in the common putative *GAS2* binding region (i.e. 2.5 kb upstream of TSS) in both MIHA & LO2 cells. ChIP-PCR analysis illustrated that the *GAS2* loci showed strong enrichment for HBx antibody but not IgG control in both cell lines (Fig.3.9). However, weak non-specific signal was also found in the lenti-CTRL-infected LO2 cells. On the other hand, high specificity of HBx binding (in lenti-HBxΔ35 but not lenti-CTRL) was demonstrated in the MIHA cells (Fig. 3.9).

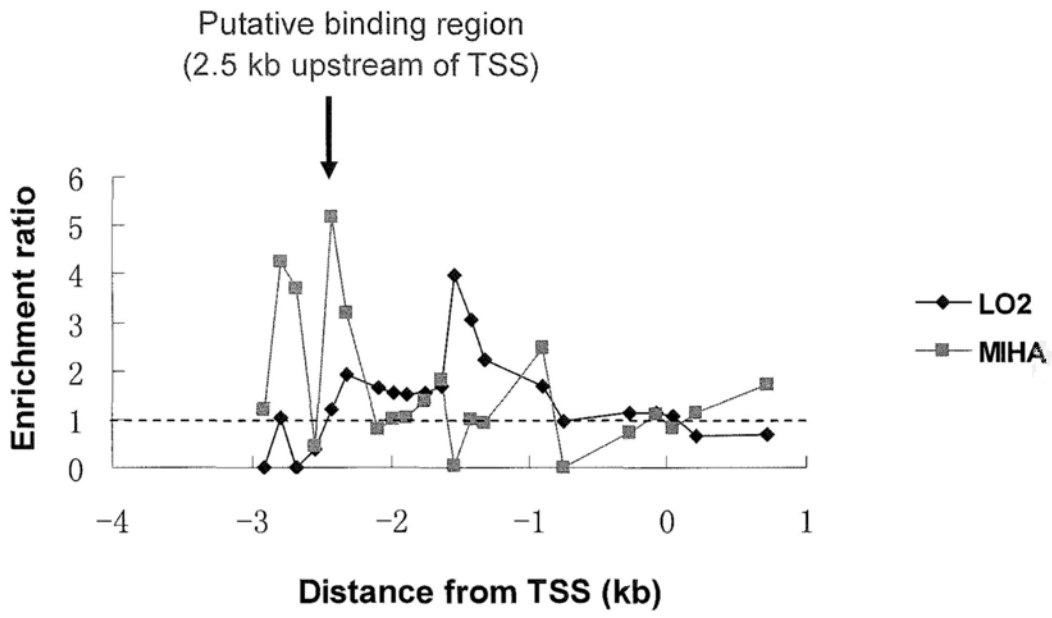

Fig.3.8 Enrichment map demonstrating the HBxΔ35 binding region in the *GAS2* proximal promoter of the LO2 and MIHA cells. Dotted line indicative of no enrichment (lenti-HBxΔ35 over lenti-CTRL) is shown as reference.

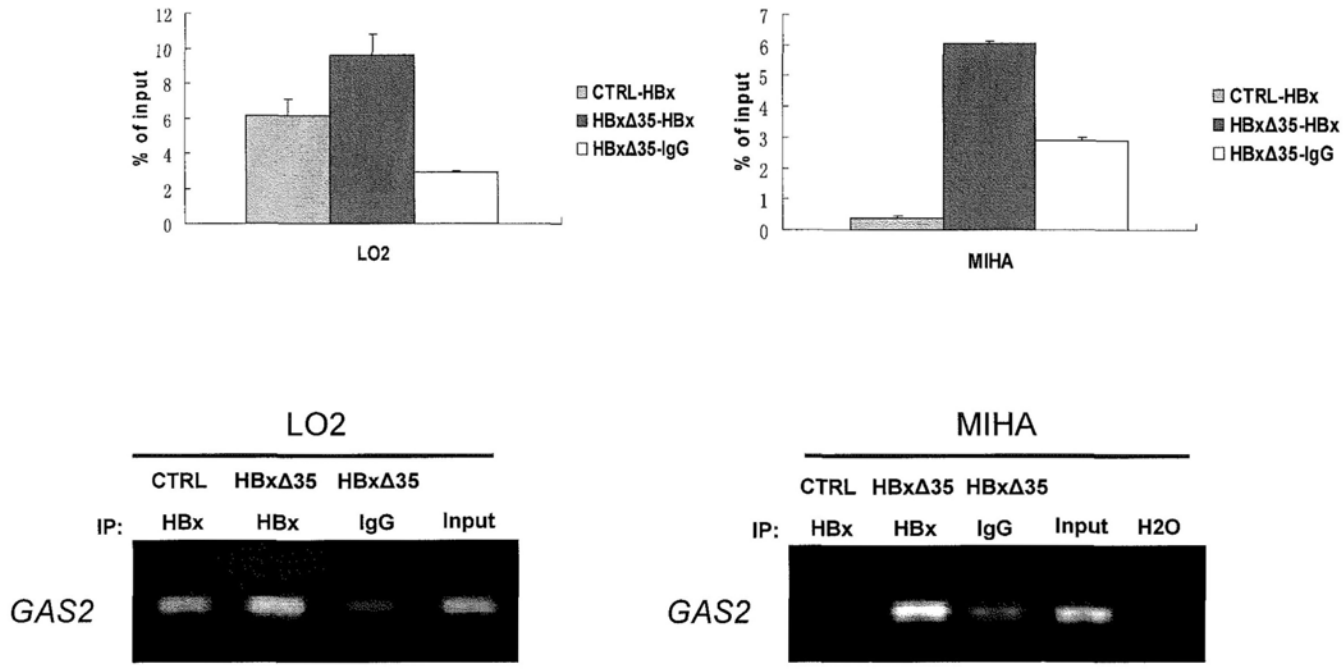

Fig.3.9 Confirmation of *GAS2* as HBxΔ35 target gene by quantitative and conventional ChIP-PCR assays in LO2 and MIHA cells. Using specific primers encompassing the putative HBxΔ35 binding region (2.5 kb upstream of TSS), strong enrichment was found in the anti-HBx immunoprecipitated DNA compared with IgG control in lenti-HBxΔ35-infected cells.

3.3.2 HBxΔ35 down-regulates GAS2 mRNA and protein levels

To investigate whether direct HBxΔ35 binding affects GAS2 expression, the *GAS2* mRNA and protein levels in lenti-HBxΔ35 and lenti-CTRL-infected MIHA cells were examined by RT-PCR and Western blot analyses, respectively. We found that *GAS2* mRNA (Fig. 3.10A) and protein (Fig. 3.10B) were down-regulated by HBxΔ35 in MIHA cells. Besides, no GAS2 protein expression was detected in LO2 cells (Fig. 3.11). Overall, these results demonstrated that overexpression of HBxΔ35 directly repressed *GAS2* expression via promoter binding in hepatocytes.

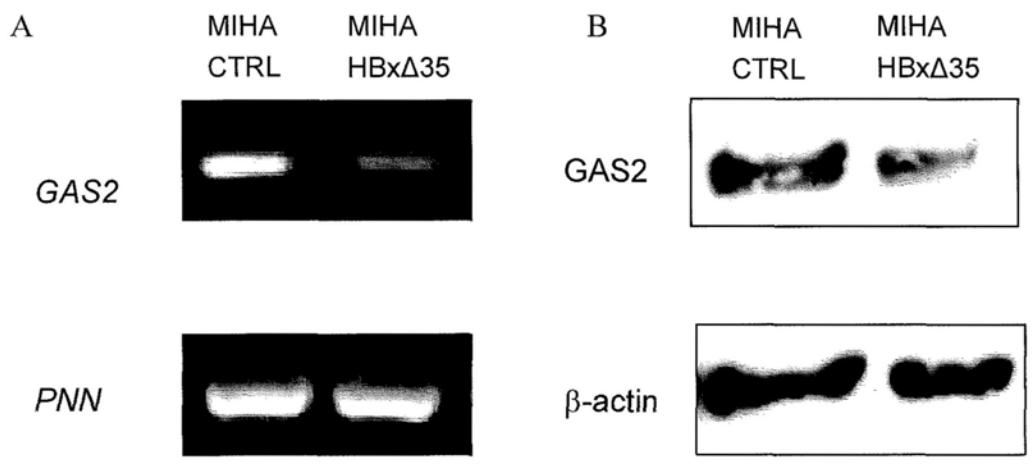

Fig. 3.10 Expression of *GAS2* mRNA and protein in lenti-HBxΔ35 and lenti-CTRL -infected MIHA cells. (A) Quantitative RT-PCR of *GAS2* mRNA expression in MIHA cellsusing *PNN* as loading control. (B) Western blot analysis of GAS2 protein in MIHA cells. β-actin was used as the loading control.

3.4 Functional characterization of GAS2 in HCC development

3.4.1 Ectopic overexpression of GAS2 suppresses HCC cell proliferation

To investigate the functions of GAS2 in HCC development, we first examined the GAS2 expression in liver and HCC cell lines. GAS2 was found to highly express in normal liver tissue and MIHA hepatocytes (Fig. 3.11). In hepatoma cell lines, GAS2 was expressed in Hep3B and HepG2 but not in Huh7, PLC5 and SK-hep1 cells (Fig. 3.11).

To investigate the effect of GAS2 on HCC cell growth, we transfected pDEST40-*GAS2* and pDEST40-CTRL plasmids into SK-hep1 cells and then analyzed cell viability by MTS assay. Ectopic overexpression of GAS2 in SK-hep1 cells (Fig. 3.12A) significantly suppressed cell proliferation (Fig. 3.12B).The growth suppressive effect of GAS2 in SK-hep1 HCC cells was further confirmed by colony formation assay. Ectopic overexpression of GAS2 caused a significant reduction in the number of colonies when compared with the control cells (Fig. 3.12C).

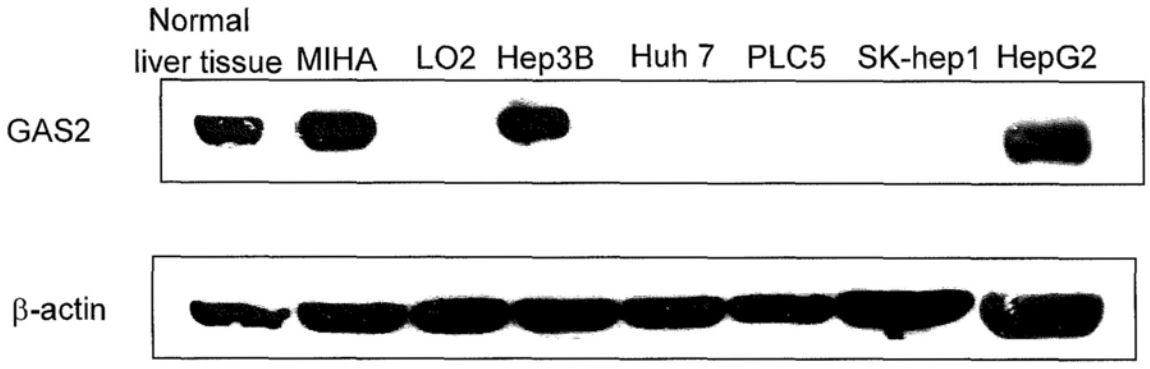

Fig. 3.11 Western blot analysis of GAS2 expression in liver and HCC cell lines. β-actin was used as the loading control.

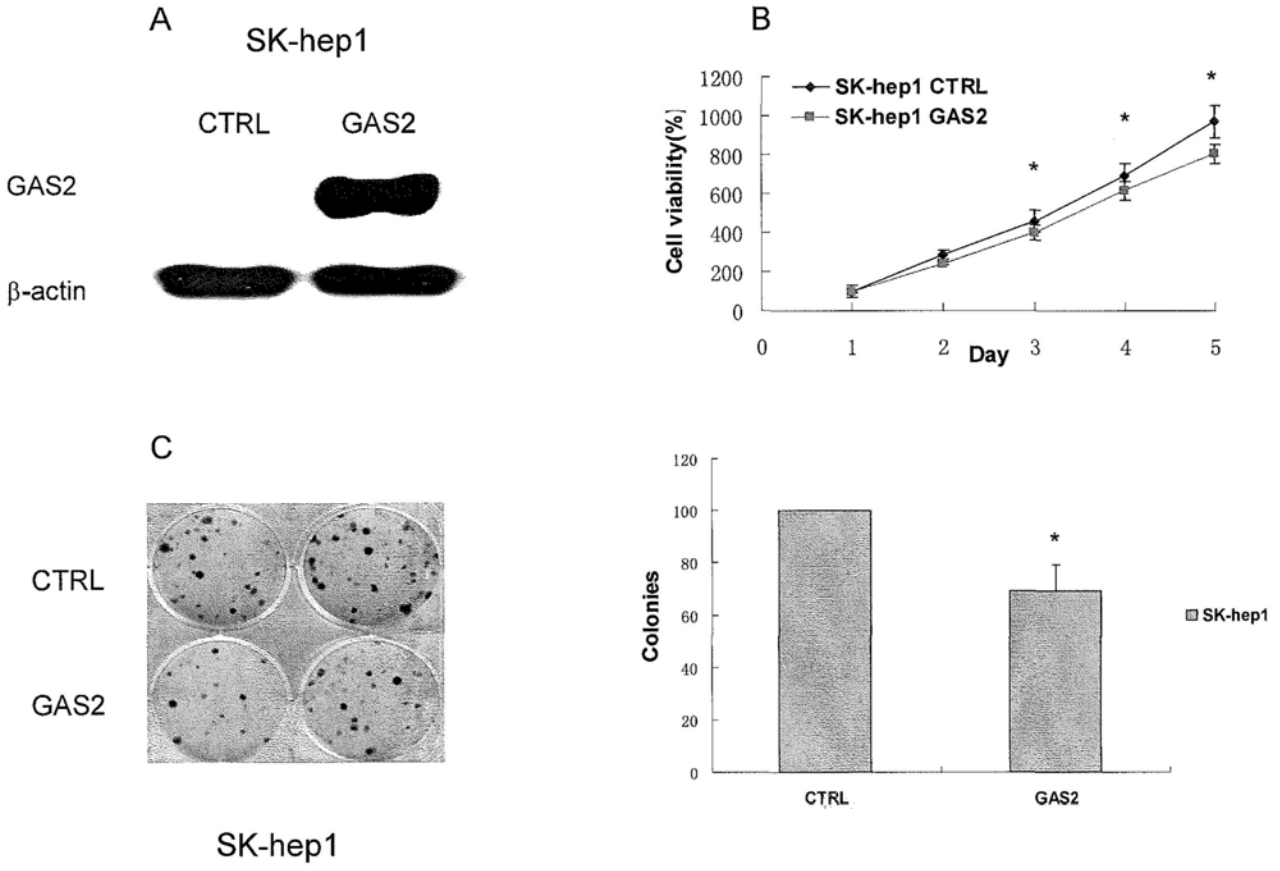

Fig. 3.12 Effect of GAS2 overexpression on HCC cell growth. (A) Western blot analysis of GAS2 expression in SK-hep1 cells transfected with pDEST40-CTRL and pDEST40-*GAS2* plasmids. β-acting was used as the loading control. (B) Cell viability of SK-hep1 cells transfected with pDEST40-CTRL and pDEST40-*GAS2* plasmids as determined by MTS assay. *P <0.05. (C) Colony formation assay of SK-hep1 cells transfected with pDEST40-CTRL and pDEST40-*GAS2* plasmids. Two weeks after G418 selection, drug-resistant colonies were stained and scored. Data are means ± SD (n=6).

3.4.2 Ectopic overexpression of GAS2 alters cell cycle progression in HCC cells

The growth-suppressive effect of GAS2 may depend on its activity to cell cycle progression and apoptosis. Fluorescence-activated cell sorting (FACS) analysis of GAS2-transfected SK-hep1 cells revealed a significant increase in the population of G_0/G_1 phase cells compared to the control cells ($P<0.01$; Fig.3.13A and 3. 13B). Moreover, there was also a significant decrease in the population of S phase cells although the extent appears minimal ($P<0.05$). More importantly, the population of subG1 phase in GAS2-transfected SK-hep1 cells was significantly larger than (more than 2-fold) that in the control SK-hep1 cells (Fig. 3.13C), suggesting that the growth inhibition by GAS2 was primarily related to apoptosis.

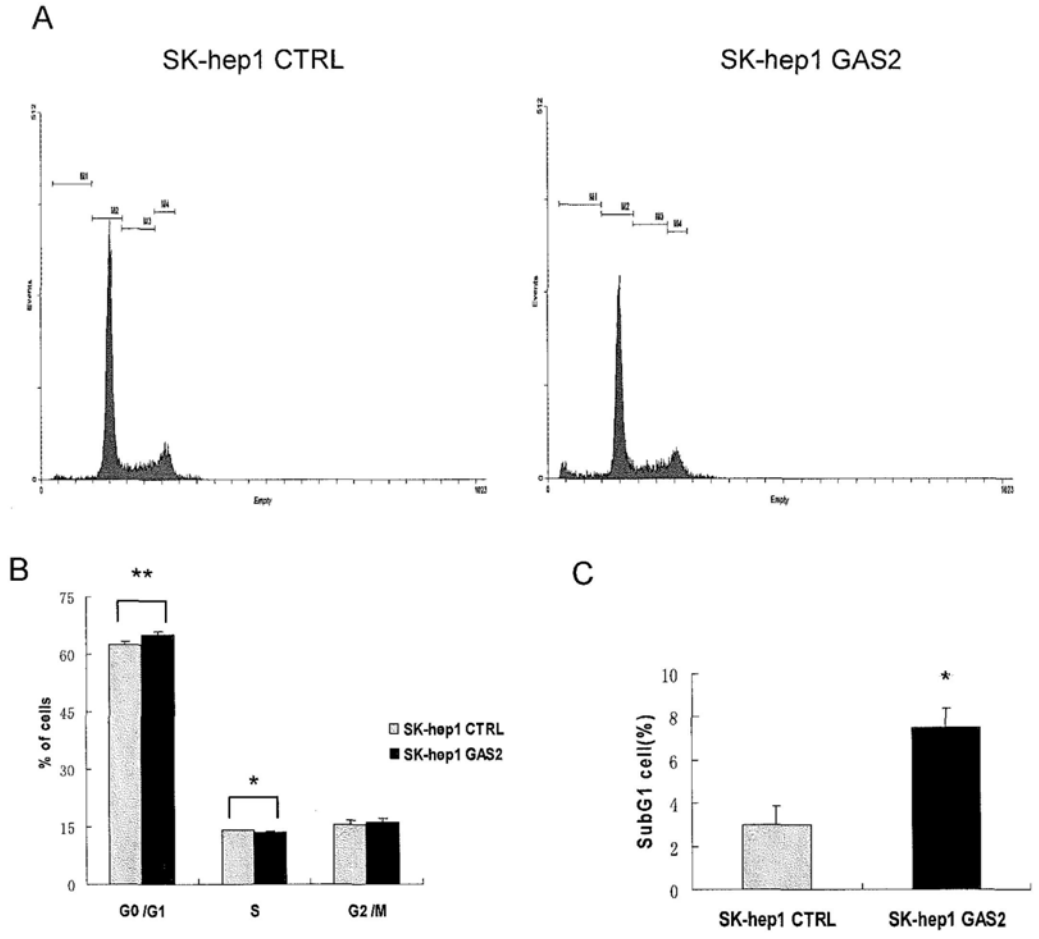

Fig.3.13 Effect of GAS2 on cell cycle progression. SK-hep1 was transfected with pDEST40-GAS2 and pDEST40-CTRL plasmids followed by FACS analysis. (A) Representative histogram plots of the flow cytometry analysis (FITC/PI). (B) Cell populations in different fractions of cell cycle phase were plotted. (C) The cell population in subG1 phase was determined by flow cytometry. M_1: subG1; M_2: G_0/G_1 phase; M_3: S phase; M_4: G_2/M phase. $^{**}P<0.01$, $^{*}P<0.05$.

3.4.3 Ectopic overexpression of GAS2 enhances susceptibility to apoptosis

In order to ascertain whether the observed decrease in cell proliferation by GAS2 was due to induction of apoptosis, the cellular apoptosis was determined using annexin V-APC by flow cytometry. Since GAS2 has been demonstrated to increase susceptibility to p53-dependent apoptosis (Benetti et al., 2001), we first determined the expression of P53 in HCC cell lines. P53 protein was expressed in the most HCC cell lines expect Hep3B (Fig. 3.14A).

We then treated P53-expressing SK-hep1 cells with or without etoposide, an anti-tumor drug dependent on a functional P53, to investigate the potential apoptotic effect of GAS2 in HCC cells. Annexin V flow cytometric analysis demonstrated that ectopic overexpression of GAS2 significantly increased the population of apoptotic cells ($P<0.05$; Fig. 3.14 B and 3.14 C). The number of early apoptotic SK-hep1 cells was increased by treatment with etoposide for 24 hours and the number of apoptotic cells was further significantly enhanced by GAS2 overexpression ($P<0.05$; Fig. 3.14 B and 3.14 C).

To validate the apoptotic effect of GAS2 in HCC cells, we assessed the apoptosis markers, cleaved caspase-3 and nuclear enzyme poly (ADP-ribose) polymerase (PARP), in SK-hep1 cells by Western blot. While overexpression of GAS2 did not induce the level of cleaved caspase-3 and cleaved PARP, these apoptosis markers

were induced by etoposide and further enhanced by GAS2 overexpression (Fig. 3.15). These findings corroborated with the flow cytometric data, demonstrating that the growth-suppressive effect of GAS2 was at least partially mediated by induction of apoptosis.

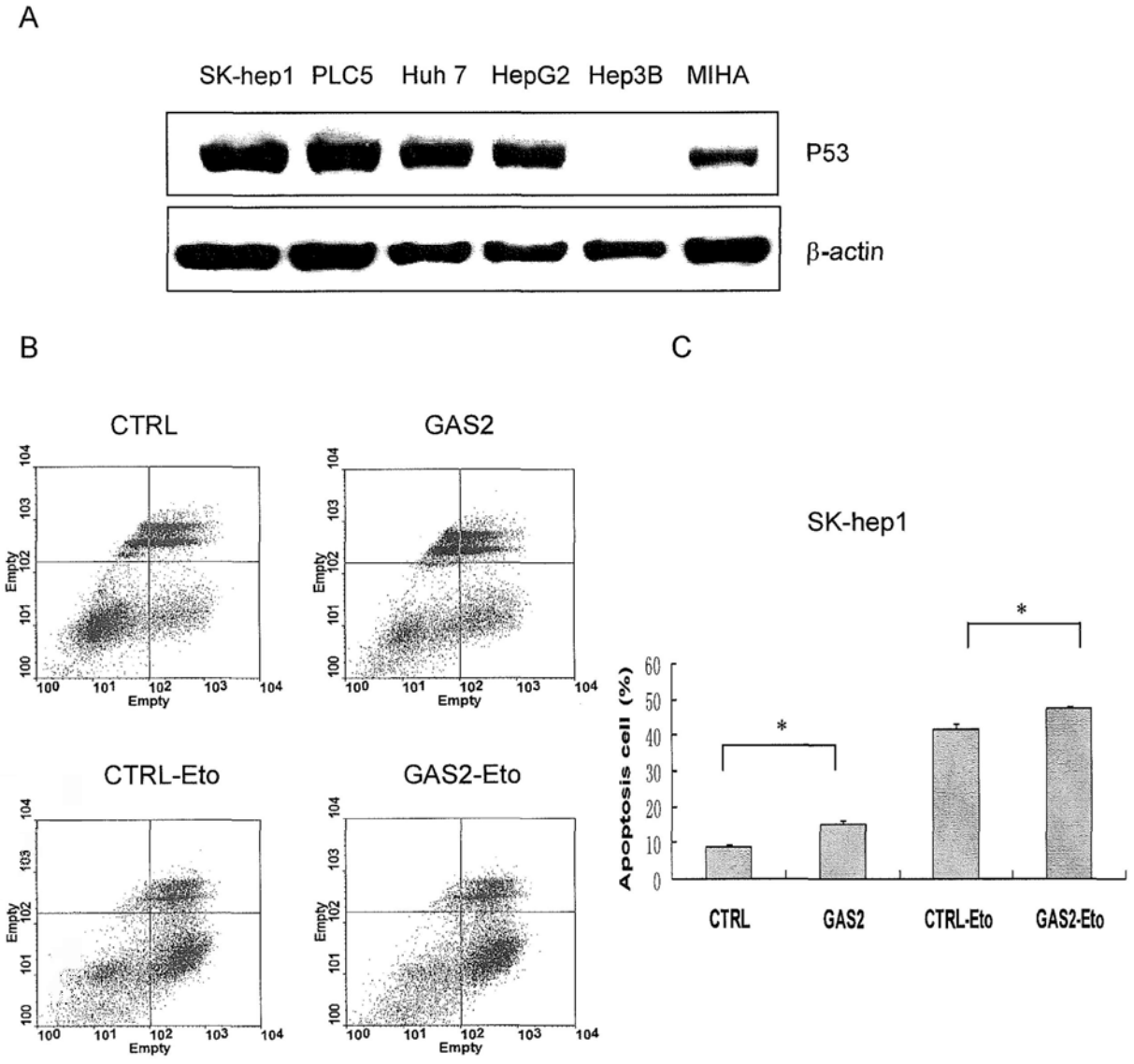

Fig. 3.14 Ectopic overexpression of GAS2 enhanced susceptibility to cell apoptosis. (A) Expression of P53 protein in liver and HCC cell lines was examined by Western blot. β-actin was used as loading control. (B) SK-hep1 cells transfected with pDEST40-GAS2 or pDEST40-CTRL plasmid were treated with or without 100μM of etoposide for 24 hours. Effect of GAS2 overexpression on apoptosis was determined by FACS using annexin V-APC apoptosis assay. (C) Bar chart showing the early apoptosis population in different treatments. Values are mean ± SD from three replicate experiments. *P<0.05. Eto: Etoposide.

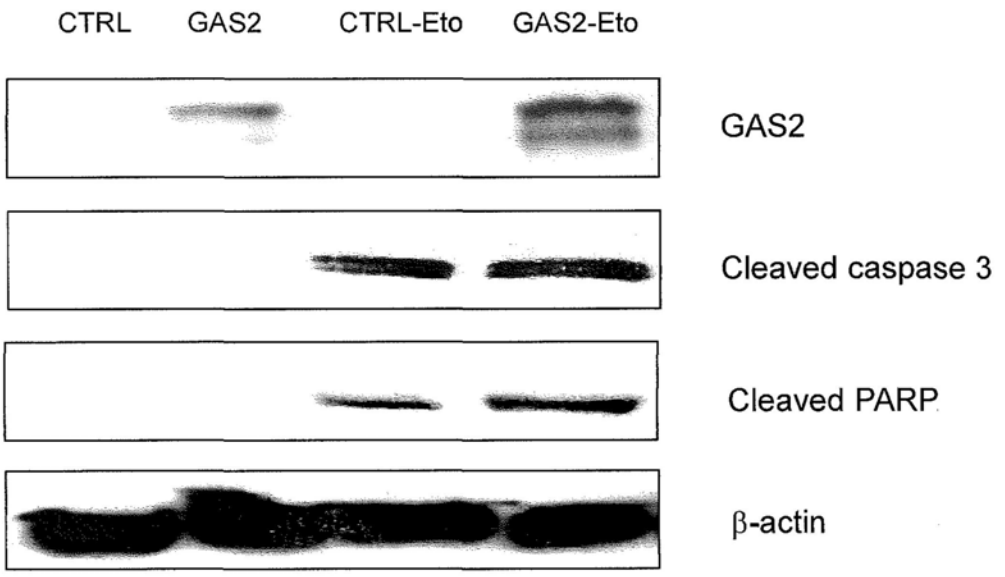

Fig. 3.15 Overexpression of GAS2 increased the expression of apoptosis markers in HCC cells treated by etoposide. Protein expression levels of cleaved caspase 3 and cleaved PARP were detected by Western blot. β-actin was used as loading control.

3.4.4 Knockdown of GAS2 reduces apoptosis

To further confirm the apoptotic effect of GAS2 in HCC cells, we performed siRNA-mediated knockdown followed by apoptosis analysis in GAS2-expressing MIHA and HepG2 cells. Treatment of these cells with siRNA against *GAS2* (siGAS2) dose-dependently decreased the mRNA (Fig. 3.16A) and protein (Fig. 3.16B) levels of GAS2 as determined by real-time RT-PCR and Western blot analyses, respectively, when compared to the cells treated with siRNA against a non-specific control sequence (siCTRL). Thus, we used 100μM siGAS2 or siCTRL in the following knockdown experiments.

As expected, etoposide treatment increased levels of cleaved caspase 3 and PARP in MIHA and HepG2 cells (Fig. 3.17). Notably, knockdown of GAS2 decreased the levels of these apoptosis markers in both cell lines (Fig. 3.17).

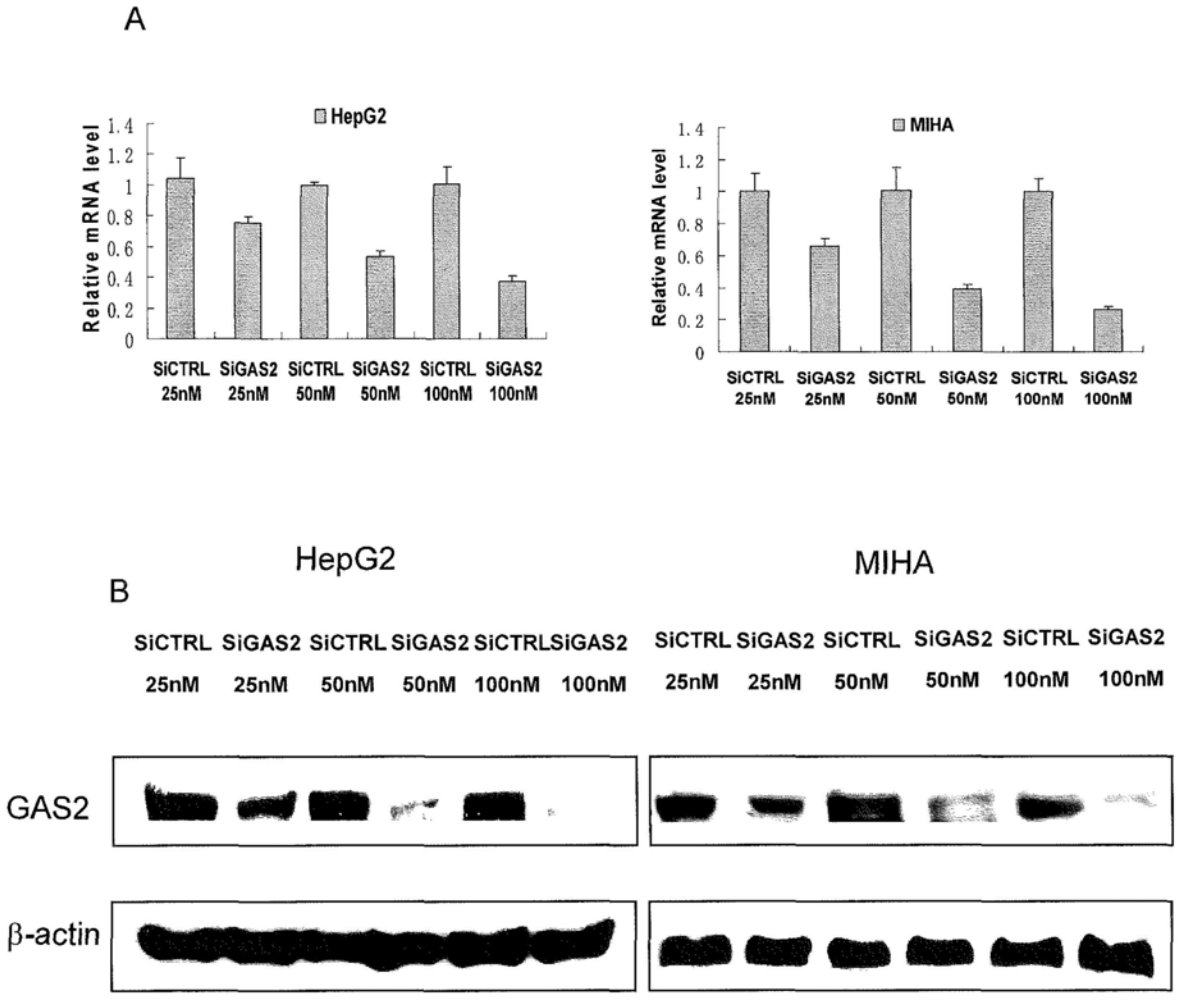

Fig. 3.16 Effect of siRNA on GAS2 expression in MIHA and HepG2 cells. (A) Expression of *GAS2* mRNA level in cells treated with 25, 50 or 100μM of siCTRL or siGAS2 was examined by real-time RT-PCR. (B) Expression of GAS2 protein was assessed by Western blot. β-actin was used as loading control.

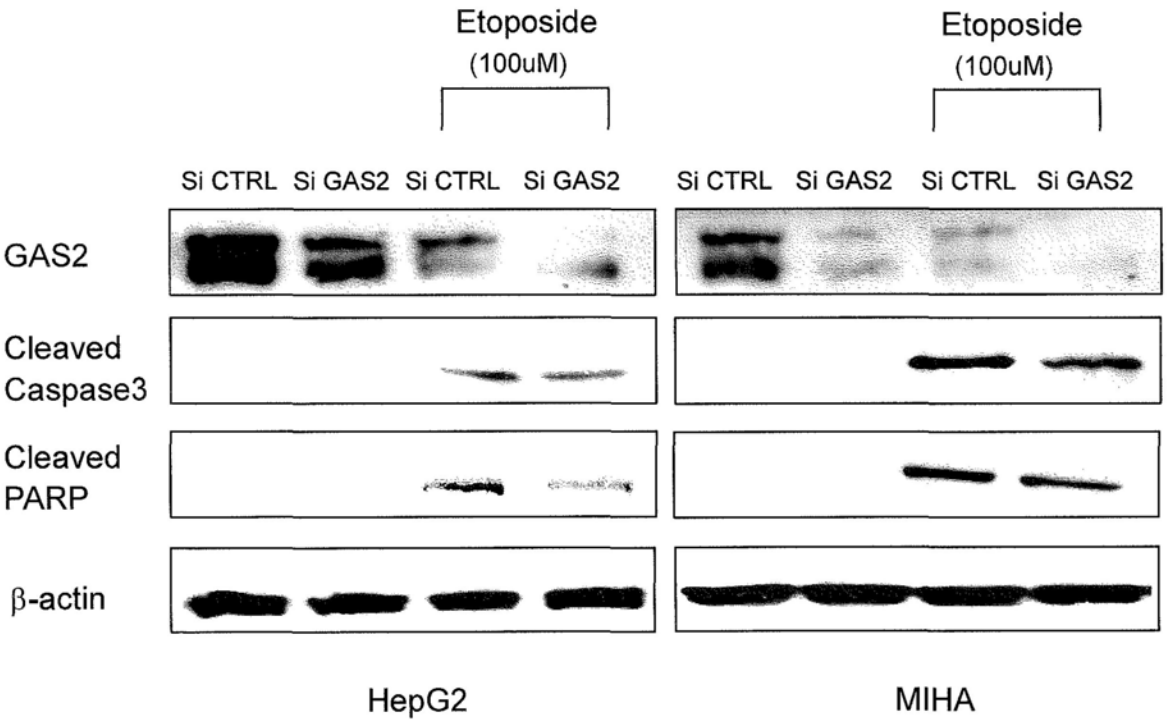

Fig.3.17 siRNA-mediated silencing of *GAS2* decreased the expression of apoptosis markers in MIHA and HepG2 cells treated with etoposide. Protein expression of cleaved caspase 3 and cleaved PARP was detected by Western blot. β-actin was used as loading control.

3.4.5 GAS2-induced apoptosis is P53-dependent

In order to delineate the role of P53 protein in GAS2-induced apoptosis, we evaluated the apoptotic ability of GAS2 after knocking down P53 in SK-hep1 cells. Treatment of siRNA against P53 (siP53) significantly diminished the expression of P53 protein compared to control siRNA (Fig. 3.18). As previously described, ectopic over-expression of GAS2 significantly increased apoptosis in SK-hep1 cells ($P<0.05$; Fig. 3.19A and 3.19B). Notably, knockdown of P53 significantly attenuated the GAS2 apoptosis-inducing effect ($P<0.05$; Fig. 3.19A and 3.19B). This result suggests that GAS2-induced apoptosis is dependent on P53 in HCC cells.

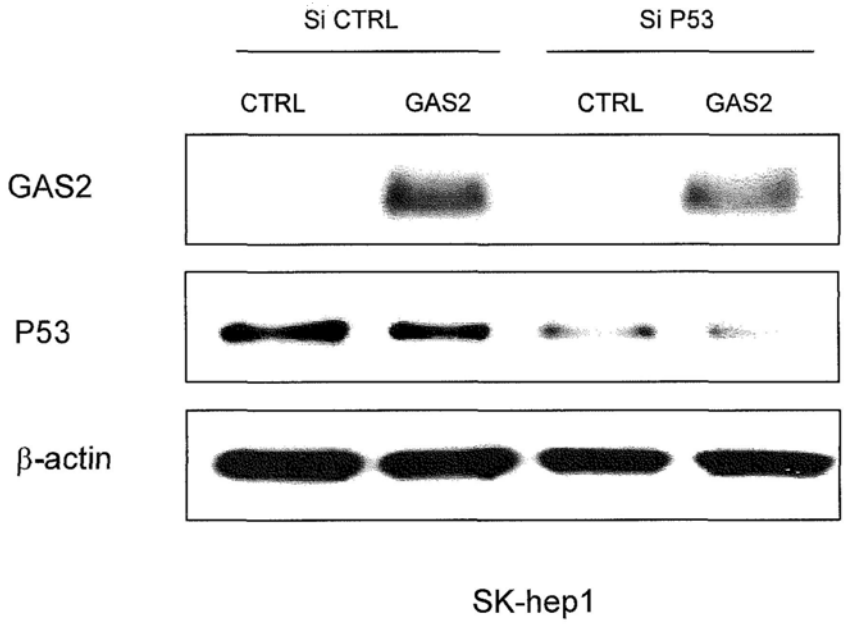

Fig. 3.18 siRNA-mediated knockdown of P53 in SK-hep1 cells. Expression of P53and GAS2 in SK-hep1 cells co-transfected with GAS-expressing or control plasmids and siP53 or siCTRL. β-actin was used as loading control.

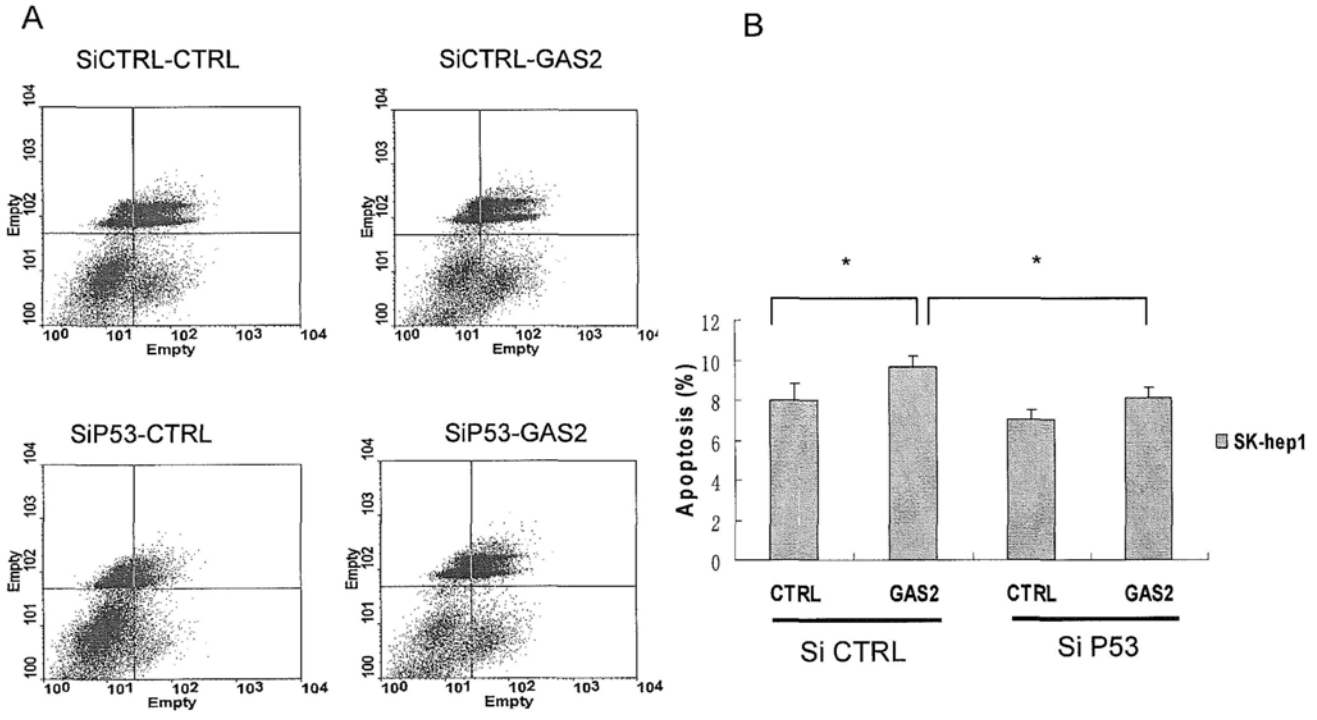

Fig. 3.19 Effect of P53 on GAS2-induced apoptosis in HCC cells. (A) Apoptosis of SK-hep1 cells co-transfected with GAS2-expressing or control plasmids and siP53 or siCTRL (100μM) as determined by annexin V-APC apoptosis assay. (B) Bar chart showing the early apoptosis population in different treatments. Values are mean ± SD from three replicate experiments. *P<0.05.

3.5 Correlation between GAS2 expression and carboxyl-terminal HBx truncation in HCC specimens

To further investigate the clinical relevance of GAS2 repression by C-terminal truncated HBx in human HCC tissues, we first examined the expression of GAS2 in HCCs and their matched adjacent nontumor liver tissues from 39 HBV-associated HCC patients by real-time RT-PCR. Down-regulation of *GAS2* transcripts (defined as 1.5-fold) was detected in 20 of 39 (51.28%) HCCs compared with their adjacent tissues. We next determined the status of HBx integration in these 39 pairs of HCC specimens. Using 2 pairs of PCR primers that distinguished full-length and C-terminal truncated HBx (Fig. 3.20), our PCR results indicated the C-terminal truncated HBx was present in 31 of 39 (79.48%) HCC tumors and 16 of 39 (41.03%) nontumorous liver tissues. Full-length HBx was detected in 4 of 39 (10.26%) HCC tumors and 20 of 39 (51.28%) nontumorous liver tissues. These findings were consistent with those of the previous studies (Ma et al., 2008). Fifteen of 39 HCC cases exhibited C-terminal HBx truncation in tumor tissues and full-length HBx in nontumorous liver tissues. Notably, the expression of *GAS2* was found to be down-regulated (1.5 fold) in 10 of 15 (66.67%) HCC tissues compared to their matched nontumorous liver tissues. Our data suggest that down-regulation of *GAS2* expression was closely associated with C-terminal HBx truncation in HCC tissues. In the remaining 24 pairs of HCC specimens, the expression of *GAS2* was down-regulated in 10 of 24 HCC tissues when compared to their matched nontumorous liver tissues. The *GAS2*

down-regulation in these cases may be due to other undefined causes.

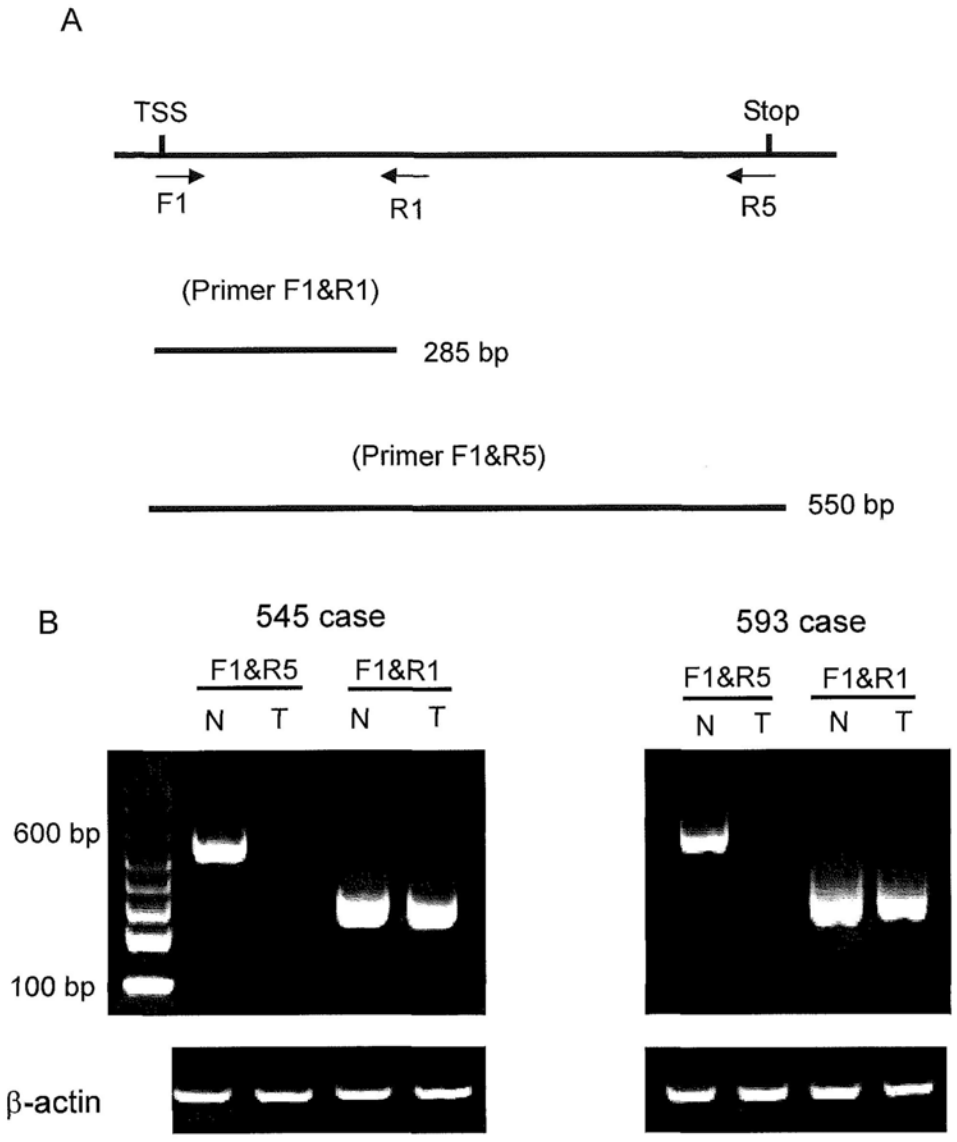

Fig. 3.20 Detection of truncated HBx DNA in HCC specimens. (A) Locations of two pairs of PCR primers encompassing the full-length (F1-R5) and N-terminal (F1-R1) of the HBx gene. (B) Representative examples of HCC cases showing HBx truncation in HCC tumors. While the short HBx fragments could be amplified from both tumor (T) and nontumor (N) tissues, full-length HBx fragments could only be amplified from adjacent nontumor liver tissues (N) indicative of C-terminal truncation.β-actin was used as loading control.

CHAPTER FOUR- DISCUSSION

4.1 Oncogenic properties of COOH-terminal truncated (Δ35) HBx

Chronic hepatitis B virus infection is strongly associated with HCC, and the viral X-gene product (HBx) has been implicated to play a critical role in the development of HBV-related HCC (Chan et al., 2006; Bouchard et al., 2004; Kwun et al., 2004; Kong et al., 2003; Chung et al., 2003). HBx is a 154-amino acid protein with intricate pleiotropic function. Recently, the role of HBx in HCC carcinogenesis has been debated widely. Some studies have reported that wild-type HBx was detected in most nontumorous liver tissues but only in a paucity of HCC tissues (Ma et al., 2008). A large body of evidence has shown that wild-type HBx induced apoptosis of hepatocytes (Lu et al., 2005; Kim et al., 2005) or sensitized cells to apoptotic death induced by proapoptotic stimuli (Kim et al., 2001; Sirma et al., 1999; Bergametti et al., 1999; Terradillos et al., 1998; Kim et al., 1998) and inhibited the focus formation induced by the cooperation of the *ras* and *mys* oncogenes (Tu et al., 2001). HBx can interrupt host cell DNA repair mechanisms by binding to DNA repair genes and interfere with cell-cycle process including S-phase progression and chromosome stability (Martin-Lluesma et al., 2008). The sensitization of cells to apoptosis by HBx may involve the system of tumor necrosis factor-α-induced apoptosis including mitogen-activated-protein kinase kinase1 and Myc protein (Su et al., 2001; Su et al., 1997).

On the other hand, some studies have elucidated the oncogenic roles of HBx in the development of HCC. HBx and its interaction with signal transduction pathways play a major role in the initiation of hepatocarcinogenesis. HBx can activate protein kinase C, phospholipid-dependent kinase which is associated with the regulation of cell growth and cell cycle progression (Luber et al., 1993). In addition, HBx can up-regulate the stress-activated protein kinases/Jun N-terminal kinase (SAPK/JNK) pathway which provides a survival signal for nontransformed hepatocytes and contributes to the immortalization and transformation of hepatocytes during the process of hepatocarcinogenesis. More importantly, HBx can interact with a variety of transcription factors to regulate the transcription of target genes so as to cause overexpression of cellular oncogenes or alterations of tumor suppressor genes. (Qadri et al., 1996; Cheong et al., 1995; Haviv et al., 1995; Wang et al., 1994). For example, HBx can up-regulate the pathway of nuclear factor-κB that prevents hepatocyte apoptosis and has a positive role in liver regeneration (Kekulé et al., 1993). Moreover, HBx can increase the recruitment of the CREB-binding Protein /p300 co-activators to endogenous cellular target genes which participate in the many functions of survival, proliferation, and glucose metabolism (Cougot et al., 2007).

How to explain the dual yet opposite roles of HBx in hepatocarcinogenesis? One key clue can be provided by the studies of HBV integration in HCC tissues, where the 3'-end of X gene was frequently deleted resulting in the formation of carboxyl-terminal truncated forms of HBx protein (Wang et al., 2004; Iavarone et al., 2003).

Some studies revealed that most of the deletion of the integrated HBx sequences derived from HCC tissues were longer than 16 amino acids at the COOH terminus, which had previously been reported to abrogate the growth-suppressive function (Tu et al., 2001). More importantly, a recent study has elucidated a mechanism of the generation of carboxyl-terminal truncated HBx, where the human APOBEC3 protein can produce G-to-A mutations at positions 359 and 360 (TGG to TAA) leading to a premature stop codon at position 120 amino acid and thus missing the last 35 amino acid in the carboxyl-terminal of HBx protein (Xu et al., 2007). In vitro experiments demonstrated that the carboxyl-terminal truncated HBx promoted liver cell growth (Xu et al., 2007; Ma et al., 2008) and the focus transforming ability of *ras* and *myc* (Tu et al., 2001). In vivo studies also showed that truncated HBx increased the tumorigenicity of liver cells in the nude mice (Ma et al., 2008; Tu et al., 2001). However, the molecular mechanism underlying carboxyl-terminal truncated HBx-induced hepatocarcinogenesis is not clear.

In our study, in order to investigate the oncogenic effect of carboxyl-terminal truncated HBx in the human normal hepatocyte, we overexpressed truncated HBx (tHBx) in the non-tumorigenic liver cell lines MIHA and LO2 using lentivirus expressing HBxΔ35 (lenti-HBxΔ35) or empty vector control. We chose to study HBxΔ35 because this carboxyl-terminal truncated HBx is naturally occurring in HCC tissues due to a well-defined mechanism. Our results further confirmed that carboxyl-terminal truncated HBx (lenti-HBxΔ35) increased liver cell growth and

promoted the colony formation. In order to explore the molecular mechanism of tHBxΔ35-mediated oncogenicity, we have applied a genome-wide approach called ChIP-chip to identify the direct target genes of tHBxΔ35. Since HBx does not bind directly to DNA, its transcriptional activity may thus be mediated via a protein-protein interaction (Unger et al., 1990; Haviv et al., 1995). The transactivated function of HBx may be exerted both in the cytoplasm, via mitogenic signaling pathways, and in the nucleus, via DNA-binding proteins, e.g. specific transcription factors to modulate gene expression (Andrisani et al., 1999). Chromatin immuno-precipitation (ChIP) has become a widely used method for the study of protein-DNA interaction. When coupled with DNA microarray, we can identify the novel genomic regions from indirect protein-DNA binding as well as transcriptional factors directly interacting with HBx (Kirmizis et al., 2004; Van Steensel et al., 2005).

According to our ChIP-chip data, there were 42 common target genes identified in both MIHA and LO2 cell lines. Growth arrest specific 2 (*GAS2*) is the common target gene in the two cell lines that was confirmed by quantitative and conventional ChIP-PCR. We further demonstrated that GAS2 was down-regulated by COOH-terminal truncated HBx (HBxΔ35) by quantitative RT-PCR and Western blot. The reason why only 1 common target gene was transcriptionally regulated in both cell lines may be due to cell-line specificity. Given the potential tumor-suppressive function of GAS2, we next investigated its function in HCC development, which has not been previously explored.

4.2 Anti-oncogenic properties of Growth arrest specifc 2 (GAS2) in HCC

GAS2 is a caspase-3 substrate that plays a role in regulating microfilament and cell shape changes during apoptosis (Schneider et al., 1988; Brancolini et al., 1992). Although it has potentially important role in cell survival, the role of GAS2 in cancer is largely unexplored. We hypothesized that GAS2 possesses anti-oncogenic properties in HCC cells. As a direct target gene of COOH-terminal truncated HBx (tHBxΔ35), we found that ectopic overexpression of tHBxΔ35 can suppress GAS2 expression. While we found that GAS2 expression was abundant in normal liver tissue and liver cell line, only one of the 4 examined HCC cell lines, Hep3B and the HepG2 hepatoblastoma cell line expressed GAS2. This result was consistent with the GAS2 expression pattern in the other cancer cell lines such as prostate and breast (Kondo et al., 2008). In order to better define the effect of GAS2 in HCC development, we examined the functional consequences of GAS2 overexpression in an null-expressing HCC cell line, SK-hep1 which carries functional p53. Although the lack of GAS2 and the presence of p53 were also found in the PLC5 and Huh7 cells as in SK-hep1, p53 mutation was reported in these two cell lines. PLC5 displayed Arg249Ser mutations in p53, while Tyr220Cys mutation of p53 was observed in Huh7 (Puisieux et al., 1993; Hsu et al., 1993; Sayan et al., 2001; Cagatay et al., 2002).

GAS2 has been shown to modulate cell susceptibility to p53-dependent apoptosis by inhibiting calpain activity (Benetti et al., 2001). In our study, overexpression of GAS2

in wild-type p53-expressing SK-hep1 cells led to the inhibition of cell growth, proliferation and colony formation. These findings suggest a possible mechanism by which GAS2 can suppress HCC growth. To further investigate the mechanism by which GAS2 regulated cell growth, we performed FACS. Cell cycle distribution analysis revealed significantly more cell arrest in the G_0/G_1 phase and less cell population in the S phase, which may result in decreased cell proliferation (Baserga et al., 1985; Pardee et al., 1987; Zetterberg et al., 1985). Similar findings were observed in murine keratinocytes and NIH 3T3 cells (Manzow et al., 1996; Brancolini et al., 1994).

The unbalance between cellular proliferation and apoptosis may contribute to the carcinogenesis (Evan et al., 2001). The interruption of apoptosis is likely one of the key mechanisms in promoting the transition from benign cells to cancer cells. The induction of apoptosis in SK-hep1 cells by GAS2 was also accompanied with the inhibition of cellular proliferation. It had been reported that GAS2 is a death substrate cleaved by caspase-3 and can efficiently increase cell susceptibility to apoptosis following UV irradiation, etoposide and MMS treatments, which were dependent on increased p53 stability and transcription activity (Benetti et al., 2001). Therefore, in order to investigate the association between GAS2 and p53-induced apoptosis, we overexpressed GAS2 SK-hep1 cells in the presence or absence of etoposide and found that the combined GAS2 overexpression and etoposide treatment had an additive effect in promoting apoptosis in SK-hep1 cells compared with cells treated with

etoposide alone. This result was in agreement with the previous reports (Brancolini et al., 1997c; Benetti et al., 2001, Kondo et al., 2008). The presence of etoposide may accelerate the proteolysis of GAS2 (Benetti et al., 2001, Kondo et al., 2008). The molecular basis of p53-dependent apoptotic pathway in HCC cells was also analyzed by the expression of apoptosis markers, such as cleaved caspase-3 and cleaved PARP functioned in the execution of the intrinsic mitochondrial apoptotic pathway. The proteolytic cleavage of PARP facilitates cellular disassembly and undergoes apoptosis (Nicholson et al., 1995). According to our data, the over-expression GAS2 alone could not induce the level of cleaved caspase-3 and cleaved PARP in MIHA and HepG2 cells, indicating that other factors are needed to induce the apoptotic pathway. In this regard, over-expression of GAS2 can increase the level of cleaved caspase-3 and cleaved PARP induced by etoposide. To further confirm the GAS2-induced apoptosis in HCC cells, we knocked down *GAS2* gene in MIHA & HepG2 cells carrying wild-type p53 gene, with or without etoposide treatment. Consistent with our overexpression experiment, silencing *GAS2* decreased the expression of caspase protein induced by etoposide.

In order to further ascertain whether the apoptosis induced by GAS2 is dependent on p53, we evaluated the ability of GAS2-induced apoptosis after knocking down p53. Down-regulation of p53 protein significantly attenuated the GAS2-induced apoptosis as shown by annexin V-APC apoptosis assay. These results suggest that GAS2-induced apoptosis is dependent on p53 protein in HCC cells, which was compatible

with previous findings in other systems (Benetti et al., 2001; Petroulakis et al., 2009).

4.3 Clinical significance of GAS2 down-regulation by COOH-terminal truncated HBx in HCC

The clinical relevance of GAS2 down-regulation in HCC was further examined by quantitative RT-PCR analysis in 39 pairs of HCC and their matched adjacent nontumor liver tissues from HBV-related HCC patients. We found down-regulated GAS2 expression in 51.28% of HCC tissues. In the 39 pairs HCC and nontumor tissues with available DNA, COOH-terminal HBx truncation was detected in 79.48% of HCC tissues, while full-length HBx was expressed in the major of nontumorous liver tissues (51.28%), which was consistent with previous reports that showing that C-terminal truncated HBx was frequently expressed in HCC tissues and full-length HBx was frequently expressed in the majority of nontumorous liver tissues (Ma et al., 2008).

To further ascertain whether the association of GAS2 down-regulation and COOH-terminal truncated HBx was involved in human HCC development, we found that in the 15 HCC cases showing COOH-terminal truncated HBx in tumor tissues and full-length HBx in nontumorous liver tissues, majority (66.67%) of the cases demonstrated GAS2 down-regulation in HCC tissues compared with their matched nontumorous liver tissues. On the other hand, in the remaining 24 pairs of HCC specimens, the expression of *GAS2* was down-regulated in 10 of 24 HCC tissues when compared to their matched nontumorous liver tissues, which may be due to

other factors e.g. transcriptional repressors.

4.4 Future Studies

We have investigated the function of GAS2 in liver and HCC cell lines without truncated HBx expression. In further study, we will explore the functional interaction between GAS2 and truncated HBx35. First, we will examine the (anti-)apoptotic effect of truncated HBx35. Secondly, in cells transfected with truncated HBx35 and thus having GAS2 down-regulated, we will investigate whether re-expression of GAS2 can abrogate the potential anti-apoptotic effect of HBx35. In addition, we will also further confirm the growth inhibition of GAS2 in HCC cell lines *in vivo*.

On the other hand, since HBx does not bind directly to DNA, it is conceivable that HBx physically interacts with transcription factors partner to modulate gene transcriptional activity. Our preliminary transcription factor binding site analysis based on the ChIP-chip dataset revealed that 15 transcription factor binding motifs were significantly enriched in the bound promoter regions of tHBxΔ35 direct target genes. Particularly, we observed highly significant over-representation of POU factor N-Oct3 (POU3F2 or Brn2) binding sites in tHBxΔ35-bound loci (p<1E-53) including the *GAS2* promoter. Transcription factor POU3F2 possessed consensus sequence (T/ATATGT/CTAAT) over-represented in HBxΔ35 binding regions that was found in the proximal promoter of *GAS2* (Fig.4.1).

POU3F2 is one of the POU family factors containing six classes, which is a POU-

Homeo-domain transcription factor expressed in neurons and melanoma cells. POU domain transcription factors are able to interact with a variety of other proteins required for the nucleation site in the generation of a transcription unit (Cook et al, 2008). In the mammalian two-hybrid experiments and GST-fusion protein pulldown assays, POU3F2 has also been shown to interact with TBP, which revealed direct protein-protein contacts between BRN2 and each of the TBP and TFIIB proteins (Smit et al., 2000). POU3F2 functions as transcriptional repressor and represses VP16-mediated transcription activation of herpesvirus immediate-early genes (Hagmann et al., 1995). Therefore, POU3F2 may act as a previously unidentified transcription factor partner of C-truncated HBx in exerting its oncogenic properties via direct repression of potential tumor-suppressor gene like *GAS2*. Further bio-chemical and genetic studies will be needed to verify the relationship among POU3F2, HBx and GAS2 as well as their functional interaction in HCC.

A

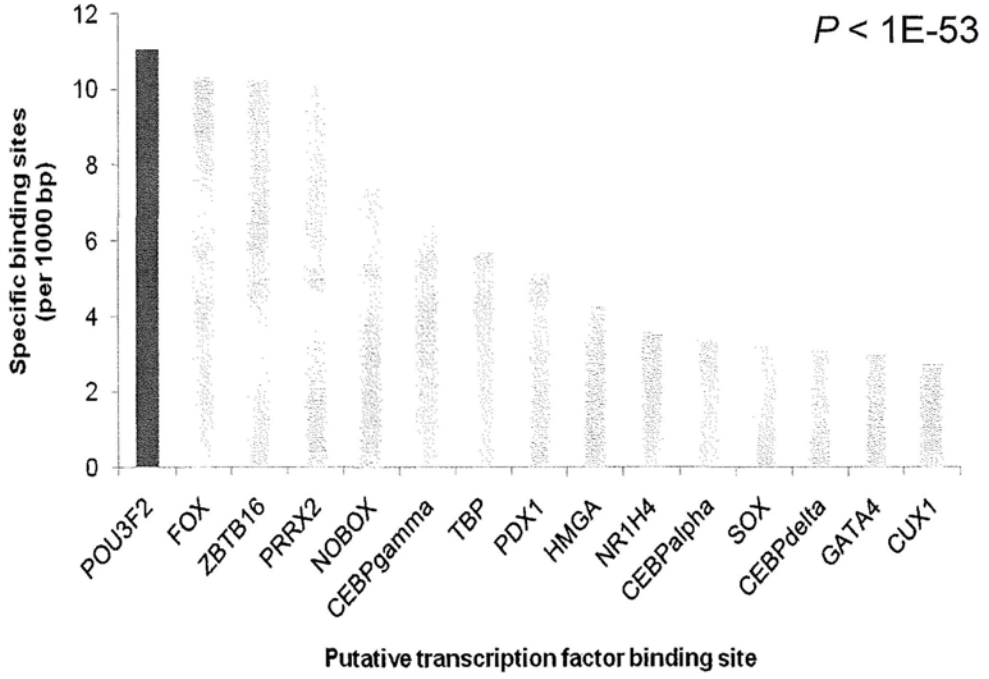

B

Fig.4.1 Identification of potential transcription factor partners of HBxΔ35 by promoter binding site analysis. (A) Enrichment of 15 transcription factors in C-truncated HBx binding regions as denoted by their highly significant binding *p*-values. (B) Picture showing POU3F2 consensus sequence over-represented in HBxΔ35 binding regions including *GAS2* promoter.

4.5 Limitation of the present study

In the course of studying direct target genes of tHBxΔ35 that characterize oncogenic properties in HCC, we compared the direct target genes of truncated lenti-HBxΔ35 with that of lenti-ctrl without examination of direct target genes of full-length HBx. Technically, it is necessary to collect abundant transfected cells ($3x10^6$ $\sim 1x10^7$ cells) in the ChIP-chip experiment. However, in our study, we found that it was very difficult to establish stable full-length HBx-expressing human immortalized non-tumorigenic cell lines (MIHA and LO2), since full-length HBx gene can induce apoptosis as discussed above. Hence, the growth rate of cell lines expressing full-length HBx was much slower than those of cell lines expressing truncated HBx during the early passages (five passages for MIHA-HBx and seven passages for LO2-HBx). Moreover, these cells were rapidly growing after six passages for MIHA-HBx and eight passages for LO2-HBx, which were associated with lack of expression of full length HBx (lost of expression construct). Such phenomenon was similar to the previous report (Ma et al., 2008). Then, in order to further explore whether there were common target genes between truncated and full-length HBx, we compared carefully our target gene list of truncated HBx with that of full-length HBx that was identified in HepG2 hepatoblastoma cells (Sung et al., 2009). We found that there were no overlapping target genes, suggesting that truncated and full-length HBx regulate distinct sets of transcriptional targets. However, we can't exclude the possibility that there is cell type specificity of HBx target genes, since the previous study used

HepG2 HCC cells whereas our study used normal liver cells. Therefore, further studies will be required to compare their direct target genes in the same cell line under identical culture condition.

In addition, detection of COOH-terminal truncated HBx in HCC tissues and their matched adjacent nontumor liver tissues was carried out by semi-quantitative PCR amplification using 2 sets of primers. The results were interpreted by the presence or absence of PCR product bands after gel electrophoresis. However, in this way, we could not compare exactly the amount of truncated HBx or even determine the exact truncation sites of HBx in tissues, when truncated HBx lied in both tumor tissues and nontumorous tissues. Quantitative RT-PCR might be used to analyse the level of truncated HBx expression, but this approach could not differentiate from full-length HBx when 2 forms co-existed in the specimens. This situation might be improved by immunohistochemical staining in liver tissue sections using two different anti-HBx antibodies, one targeting on the COOH terminal and the other on the middle region of the HBx protein. Differentiation of HBx forms is possible by using these 2 antibodies. However, this immunohistochemical approach suffers from lack of accurate quantification. Ideally, one should detect and measure different forms of HBx using integrated approaches that evaluate the DNA, RNA and protein levels. Nevertheless, it is difficult to detect the minority population of HBx mutants. To overcome the limitation, a high-throughput massive-parallel sequencing called pyrosequencing technology can be performed (Thomas et al., 2006). By this technology, the

examination of truncated HBx and the accurate sites of truncation could be determined and quantified in tissue specimens.

CHAPTER FIVE- CONCLUSION

In order to explore the molecular mechanism underlying carboxyl-terminal truncated HBx-induced hepatocarcinogenesis, we have applied an integrated approach of genome-wide binding and expression analysis to illustrate for the first time that truncated HBx down-regulated the transcription of *GAS2* by indirectly binding to its promoter. We further characterized the function of this direct truncated HBx-dependent target gene in hepatocarcinogenesis and showed that GAS2 inhibited HCC cell proliferation possibly via enhancing the susceptibility to p53-dependent apoptosis. Normal GAS2-expressing hepatocytes acquire balance of cell survival through p53-dependent apoptosis. In truncated HBx-expressing hepatocytes with GAS2 down-regulation, such balance will be lost and the premalignant cells might be able to escape from apoptosis even in the presence of the p53 guardian. Taken together, COOH-terminal truncated HBx, via its repressed mRNA and miRNA targets, may cause uncontrolled growth placing large numbers of cells susceptible to neoplastic transformation. .

Finally, the enrichment of POU3F2 in promoter regions of tHBxΔ35 direct target genes revealed by the transcription factor binding site analysis uncovers a previously unidentified transcription factor partner of COOH-terminal truncated HBx in exhibiting its oncogenic characteristics (Fig.5.1). Further studies will be executed to verify their expression, relationship and functions in HCC.

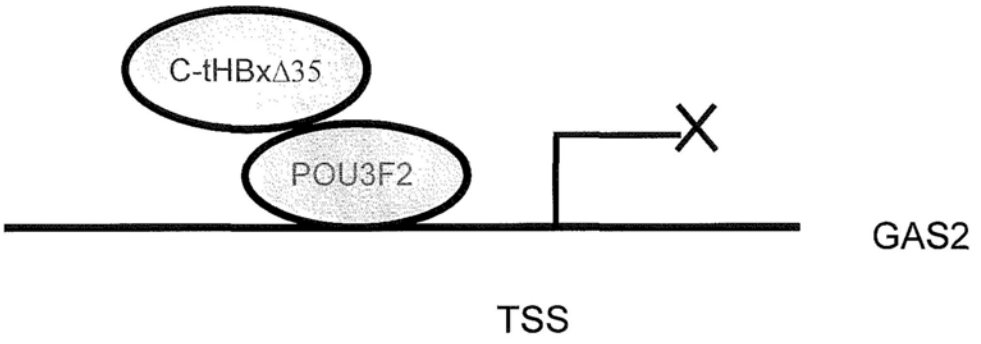

Fig.5.1 A working model of transcriptional repression by C-terminal truncated HBx. C-tHBxΔ35 may physically interact with DNA-binding POU3F2 transcription factor in the promoter of target genes e.g. *GAS2* and inhibit the gene transcription.

REFERENCES

Adams LA, Angulo P, Lindor KD. (2005). Nonalcoholic fatty liver disease. CMAJ. 172:899 –905

Ahmed F, Perz JF, Kwong S, Jamison PM, Friedman C, Bell BP. (2008). National trends and disparities in the incidence of hepatocellular carcinoma, 1998–2003. Prev Chronic Dis. 5:A74

Allegrucci C, Rushton MD, Dixon JE, Sottile V, Shah M, Kumari R, Watson S, Alberio R, Johnson AD. (2011) Epigenetic reprogramming of breast cancer cells with oocyte extracts. Molecular Cancer. 10:7

Andrisani OM, Barnabas S. (1999).The transcriptional function of the hepatitis B virus X protein and its role in hepatocarcinogenesis (Review). Int J Oncol. 15: 373–379

Angulo P, Keach JC, Batts KP, Lindor KD.(1999). Independent predictors of liver fibrosis in patients with nonalcoholic steatohepatitis. Hepatology. 30: 1356–1362

Anthony PP. (2001).Hepatocellular carcinoma: An overview. Histopathology. 39: 109 –118

Arii M, Takada S, and Koike K. (1992). Identification of three essential regions of hepatitis B virus X protein for trans-activation function. Oncogene. 7: 397–403

Atencio I, Ramachandra M, Shabram P and Demers G. (2000). Calpain inhibitor 1 activates p53-dependent apoptosis in tumor cell lines. Cell Growth Differ. 11: 247–253

Barry SC, Harder B, Brzezinski M, Flint LY, Seppen J, Osborne WR. (2001). Lentivirus vectors encoding both central polypurine tract and post-transcriptional regulatory element provide enhanced transduction and transgene expression. Hum Gene Ther. 12:1103–1108

Baserga R. (1985). The biology of cell reproduction. Harvard University Press, Cambridge, Mass.

Bedogni G, Miglioli L, Masutti F, Tiribelli C, Marchesini G, Bellentani S.(2005). Prevalence of and risk factors for nonalcoholic fatty liver disease: The Donysos nutrition and liver study. Hepatology.42: 44 –52

Benetti R, Del Sal G, Monte M, Paroni G, Brancolini C, Schneider C. (2001).The death substrate Gas2 binds m-calpain and increases susceptibility to p53-dependent apoptosis. EMBO J. 20:2702–2714

Benetti R, Copetti T, Dell'Orso S, Melloni E, Brancolini C, Monte M, Schneider C. (2005). The calpain system is involved in the constitutive regulation of beta-catenin signaling functions. J Biol Chem. 280:22070-22080

Benn J and Schneider RJ. (1995). Hepatitis B virus HBx protein deregulates cell cycle checkpoint controls. Proc Natl Acad Sci USA. 92: 11215–11219

Bergametti F, Prigent S, Luber B, Benoit A, Tiollais P, Sarasin A, and Transy C. (1999).The proapoptotic effect of hepatitis B virus HBx protein correlates with its transactivation activity in stably transfected cell lines. Oncogene. 18: 2860–2871

Bergsland EK. (2001). Molecular mechanisms underlying the development of hepato-cellular carcinoma. Semin Oncol. 28: 521-531

Bergametti F, Prigent S, Luber B, Benoit A, Tiollais P, Sarasin A, and Transy C. (1999). The proapoptotic effect of hepatitis B virus HBx protein correlates with its transactivation activity in stably transfected cell lines. Oncogene. 18: 2860–2871

Block TM, Mehta AS, Fimmel CJ, Jordan R.(2003). Molecular viral oncology of hepa-tocellular carcinoma. Oncogene. 22: 5093-5107

Bosch FX, Ribes J, Cléries R, Díaz M.(2005) Epidemiology of hepatocellular carcinoma. Clin Liver Dis. 9:191–211

Bouchard MJ and Schneider RJ. (2004). The enigmatic X gene of hepatitis B virus. Virol. 78: 12725–12734

Boyle P, Levin B. (2008).World Cancer Report. 5:351-357

Brancolini C, Bottega S and Schneider C. (1992) Gas2, a growth arrest specific protein, is a component of the microfilament network system. J. Cell Biol. 117:1251–1261

Brancolini C, and Schneider C. (1994) Phosphorylation of the growth arrest-specific protein Gas2 is coupled to actin rearrangements during Go-->G1 transition in NIH 3T3 cells. J. Cell. Biol. 124:743–756

Brancolini C, Benedetti M. and Schneider C. (1995) Microfilament reorganization during apoptosis: the role of Gas2, a possible substrate for ICE-like proteases. EMBO J.14: 5179–5190

Brancolini C, Lazarevic D, Rodriguez J, and Schneider C. (1997a). Dismantling cell–cell contacts during apoptosis is coupled to a caspase dependent proteolytic cleavage of betacatenin. J. Cell Biol. 139:759–771

Brancolini C, Marzinotto S, and Schneider C. (1997b). Susceptibility to p53-dependent apoptosis correlates with increased levels of Gas2 and Gas3 proteins. Cell Death Diff. 4:247–253

Brancolini C and Schneider C (1997c) Cut and die: proteolytic cascades regulating apoptosis. Adv. Clin. Pathol. 3:177–189

Brechot C. (2004).Pathogenesis of hepatitis B virus-related hepatocellular carcinoma: old and new paradigms. Gastroenterology.127: S56–61

Bruix J. & Sherman M. (2005). Management of hepatocellular carcinoma. Hepatology 42:1208–1236

Bugianesi E, Vanni E, Marchesini G. (2007). NASH and the risk of cirrhosis and hepatocellular carcinoma in type 2 diabetes. Curr Diab Rep.7:175–180

But DYK, Lai CL, Yuen MF.(2008). Natural history of hepatitis-related hepato-cellular carcinoma. World J Gastroenterol.14:1652–1656

Cagatay T, Ozturk M. (2002). P53 mutation as a source of aberrant beta-catenin accumulation in cancer cells. Oncogene. 21:7971 - 7980

Calle EE, Rodriguez C, Walker-Thurmond K, Thun MJ.(2003). Overweight, obesity, and mortality from cancer in a prospectively studied cohort of U.S. adults. N Engl J Med.348:1625–1638

Campisi J, and d'Adda di Fagagna F. (2007). Cellular senescence: when bad things happen to good cells. Nat. Rev. Mol. Cell Biol. 8:729 –740

Cao GW.(2009). Clinical relevance and public health significance of hepatitis B virus genomic variations. World J. Gastroenterol. 15: 5761–5769

Carafoli E. and Molinari M. (1998) Calpain: a protease in search of a function? Biochem. Biophys. Res. Commun. 247:193–203

Centers for Disease Control and Prevention [CDC]. (1995). Hepatitis surveillance report no. 56.Atlanta, GA: U.S. Department of Health and Human Services, Public Health Service, CDC.

Centers for Disease Control and Prevention [CDC]. (2006). Estimates of disease burden from viral hepatitis.

Cha MY, Ryu DK, Jung HS, Chang HE and Ryu WS. (2009).Stimulation of hepatitis B virus genome replication by HBx is linked to both nuclear and cytoplasmic HBx expression. J Gen Virol. 90: 978–986

Chan HL, Hui AY, Wong ML Tse AM, Hung LC, Wong VW, Sung JJ. (2004). Genotype C hepatitis B virus infection is associated with an increased risk of hepatocellular carcinoma. Gut. 53: 1494–1498

Chan HL, Tse CH, Mo F, Koh J, Wong VW, Wong GL, Lam Chan S, Yeo W, Sung JJ, Mok TS.(2008). High viral load and hepatitis B virus subgenotype ce are associated with increased risk of hepatocellular carcinoma J Clin Oncol. 26:177-182

Chan HL, Sung JJ.(2006). Hepatocellular carcinoma and hepatitis B virus. Semin Liver Dis. 26:153-161

Chang MH, You SL, Chen CJ, Liu CJ, Lee CM, Lin SM, Chu HC, Wu TC, Yang SS, Kuo HS, Chen DS; Taiwan Hepatoma Study Group.(2009). Decreased incidence of hepatocellular carcinoma in hepatitis B vaccinees: a 20-year follow-up study. J. Natl Cancer Inst. 101:1348–1355

Chen CL, Yang HI, Yang WS, Liu CJ, Chen PJ, You SL, Wang LY, Sun CA, Lu SN, Chen DS, Chen CJ.(2008). Metabolic factors and risk of hepatocellular carcinoma by chronic hepatitis B/C infection: a follow-up study in Taiwan. Gastroenterology. 135:111–121

Chen Y, Lin MC, Yao H, Wang H, Zhang AQ, Yu J, Hui CK, Lau GK, He ML, Sung J, Kung HF. (2007). Lentivirus-mediated RNA interference targeting enhancer of zeste homolog 2 inhibits hepatocellular carcinoma growth through down-regulation of stathmin. Hepatology. 46:200-208

Cheong JH, Yi M, Lin Y, Murakami S. (1995). Human RPB5, a subunit shared by eukaryotic nuclear RNA polymerases, binds human hepatitis B virus X protein and may play a role in X transactivation. EMBO J.14:143–150

Chirillo P, Pagano S, Natoli, G, Puri, PL, Burgio VL, Balsano C, and Levrero M. (1997). The hepatitis B virus X gene induces p53-mediated programmed cell death. Proc. Natl. Acad. Sci. USA. 94: 8162–8167

Chung TW, Lee YC, Ko JH, Kim CH. (2003). Hepatitis B Virus X protein modulates the expression of PTEN by inhibiting the function of p53, a transcriptional activator in liver cells. Cancer Res. 63:3453-3458

Cohen GM. (1997) Caspases: the executioners of apoptosis. Biochem. J. 326: 1–16

Colgrove R, Simon G, Ganem D.(1989).Transcriptional activation of homologous and heterologous genes by the hepatitis B virus X gene product in cells permissive for viral replication. J Virol.63:4019–4026

Collado M, Blasco MA, and Serrano M. (2007). Cellular senescence in cancer and aging. Cell. 130: 223– 233

Colombo M, de Franchis R, Del Ninno E, Sangiovanni A, De Fazio C, Tommasini M, Donato MF, Piva A, Di Carlo V, Dioguardi N. (1991). Hepatocellular carcinoma in Italian patients with cirrhosis. N Engl J Med. 325:675–680

Cook AL and Sturm RA. (2008). POU domain transcription factors: BRN2 as a regulator of melanocytic growth and tumourigenesis. Pigment Cell Melanoma Res. 21: 611–626

Cougot D, Wu Y, Cairo S, Caramel J, Renard CA, Lévy L, Buendia MA, Neuveut C.(2007).The Hepatitis B Virus X Protein Functionally Interacts with CREB-binding Protein/p300 in the Regulation of CREB-mediated Transcription. J Biol Chem. 282:4277–4287

Datta S. (2008). An overview of molecular epidemiology of hepatitis B virus (HBV) in India. Virol J. 5: 156–168

Davila JA, Morgan RO, Shaib Y, McGlynn KA, El-Serag HB. (2005). Diabetes increases the risk of hepatocellular carcinoma in the United States: A population based case control study. Gut 54:533–539

Di Bisceglie AM. (2002). Epidemiology and clinical presentation of hepatocellular carcinoma. J Vasc Interv Radiol.13:S169 –S171

Donato F, Tagger A, Gelatti U, Parrinello G, Boffetta P, Albertini A, Decarli A, Trevisi P, Ribero ML, Martelli C, Porru S, Nardi G. (2002). Alcohol and hepatocellular carcinoma: The effect of lifetime intake and hepatitis virus infections in men and women. Am J Epidemiol.155:323–331

Diao J, Garces R and Richardson CD.(2001). X protein of hepatitis B virus modulates cytokine and growth factor related signal transduction pathways during the course of viral infections and hepatocarcinogenesis. Cytokine Growth Factor Rev. 12: 189–205

DeLuca C, Kwon H, Lin R, Wainberg M, Hiscott J. (1999).NF-kappaB activation and HIV-1 induced apoptosis. Cytokine Growth Factor Rev.10:235–253

Elmore LW, Hancock AR, Chang SF, Wang XW, Chang S, Callahan CP, Geller DA, Will H, and Harris CC.(1997). Hepatitis B virus, X protein and p53 tumor suppressor interactions in the modulation of apoptosis. Proc. Natl. Acad. Sci. USA, 94: 14707–14712

El-Serag HB, Rudolph KL.(2007). Hepatocellular carcinoma: Epidemiology and molecular carcinogenesis. Gastroenterology.132:2557–2576

El-Serag HB, Tran T, Everhart JE. (2004). Diabetes increases the risk of chronic liver disease and hepatocellular carcinoma. Gastroenterology. 126:460–468

Evan GI, Vousden KH. (2001). Proliferation, cell cycle and apoptosis in cancer. Nature. 411:342-348

Falck-Ytter Y, Younossi ZM, Marchesini G, McCullough AJ. (2001). Clinical features and natural history of nonalcoholic steatosis syndromes. Semin Liver Dis. 21: 17–26

Farinati F, Sergio A, Baldan A, Giacomin A, Di Nolfo MA, Del Poggio P, Benvegnu L, Rapaccini G, Zoli M, Borzio F, Giannini EG, Caturelli E, Trevisani F. (2009). Early and very early hepatocellular carcinoma: when and how much do staging and choice of treatment really matter? BMC Cancer 9: 33

Fasani P, Sangiovanni A, De Fazio C, Borzio M, Bruno S, Ronchi G, Del Ninno E, Colombo M.(1999). High prevalence of multinodular hepatocellular carcinoma in patients with cirrhosis attributable to multiple risk factors. Hepatology. 29:1704–1707

Forner A, Reig ME, de Lope CR, Bruix J. (2010). Current strategy for staging and treatment: the BCLC update and future prospects. Semin. Liver Dis. 30: 61–74

Geissler M, Mohr L, Ali MY, Grimm CF, Ritter M, Blum HE. (2003).Immunobiology and gene-based immunotherapy of hepatocellular carcinoma. Gastroenterology. 41: 1101-1110

Giaccia AJ and Kastan MB. (1998). The complexity of p53 modulation: emerging patterns from divergent signals. Genes Dev.12:2973–2983

Lin CL, Kao JH. (2011). The clinical implications of hepatitis B virus genotype: Recent advances J. Gastroenterol. Hepatol. 26 Suppl. 1: 123–130

Goldman CK, Kendall RL, Cabrera G, Soroceanu L, Heike Y, Gillespie GY, Siegal GP, Mao X, Bett AJ, Huckle WR, Thomas KA, Curiel DT.(1998). Paracrine expression of a native soluble vascular endothelial growth factor receptor inhibits tumor growth, metastasis, and mortality rate. Proc Natl Acad Sci USA. 95:8795–8800

Goldstein ST, Zhou F, Hadler SC, Bell BP, Mast EE & Margolis HS. (2005). A mathematical model to estimate global hepatitis B disease burden and vaccination impact. International Journal of Epidemiology. 34:1329–1339.

Gomaa AI, Khan SA, Toledano MB, Waked I, Taylor-Robinson SD. Hepatocellular carcinoma: Epidemiology, risk factors and pathogenesis. World J Gastroenterol.14: 4300–4308

Gonen H, Shkedy D, Barnoy S, Kosower NS and Ciechanover A. (1997). On the involvement of calpains in the degradation of the tumor suppressor protein p53. FEBS Lett. 406:17–22

Gottlob K, Pagano S, Levrero M, and Graessmann A. (1998). Hepatitis B virus X protein transcription activation domains are neither required nor sufficient for cell transformation. Cancer Res. 58: 3566–3570

Greenfield V, Cheung O, Sanyal AJ. (2008). Recent advances in nonalcoholic fatty liver disease. Curr Opin Gastroenterol.24:320 –327

Griscelli F, Li H, Bennaceur-Griscelli A, Soria J, Opolon P, Soria C, Perricaudet M, Yeh P, Lu H.(1998). Angiostatin gene transfer: inhibition of tumor growth in vivo by blockage of endothelial cell proliferation associated with a mitosis arrest. Proc Natl Acad Sci USA. 95:6367–6372

Hagmann M, Georgiev O, Schaffner W, Douville P.(1995). Transcription factors interacting with herpes simplex virus alpha gene promoters in sensory neurons. Nucleic Acids Res. 23:4978-4985

Han J, Yoo HY, Choi BH and Rho HM. (2000). Selective transcriptional regulations in the human liver cell by hepatitis B viral X protein. Biochem Biophys Res Commun. 272: 525–530

Hassan MM, Hwang LY, Hatten CJ, Swaim M, Li D, Abbruzzese JL, Beasley P, Patt YZ.(2002).Risk factors for hepatocellular carcinoma: synergism of alcohol with viral hepatitis and diabetes mellitus. Hepatology 36:1206–1213

Haviv I, Vaizel D, Shaul Y. (1996). pX, the HBV-encoded coactivator, interacts with components of the transcription machinery and stimulates transcription in a TAF-independent manner. EMBO J.15:3413–3420

Haviv I, Vaizel D, Shaul Y. (1995).The X protein of hepatitis B virus coactivates potent activation domains. Mol Cell Biol.15:1079–1085

Henkler F, Hoare J, Waseem N, Goldin RD, McGarvey MJ, Koshy R and King IA. (2001) Intracellular localization of the hepatitis B virus HBx protein. J Gen Virol 82: 871–882

Hiwasa T. Arase Y, Kikuno K, Hasegawa R, Sugaya S, Kita K, Saido T, Yamamori H, Maki M, Suzuki N. (2000). Increase in ultraviolet sensitivity by over-expression of calpastatin in ultraviolet-resistant UVr-1 cells derived from ultraviolet-sensitive human RSa cells. Cell Death Differ.7:531–537

Hollinger FB. (1987). Serologic evaluation of viral hepatitis. Hosp Pract (Off Ed). 22:101–114

Hsu IC, Tokiwa T, Bennett W, Metcalf RA, Welsh JA, Sun T, Harris CC. (1993) p53 gene mutation and integrated hepatitis B viral DNA sequences in human liver cancer cell lines. Carcinogenesis.14:987–992

Iavarone M, Trabut JB, Delpuech O, Carnot F, Colombo M, Kremsdorf D, Bréchot C, Thiers V. (2003).Characterisation of hepatitis B virus X protein mutants in tumour and non-tumour liver cells using laser capture micro dissection. J. Hepatol 39:253–261

Ikeda K, Marusawa H, Osaki Y, Nakamura T, Kitajima N, Yamashita Y, Kudo M, Sato T, Chiba T. (2007). Antibody to hepatitis B core antigen and risk for hepatitis C-related hepatocellular carcinoma: a prospective study. Ann. Intern. Med. 146:649–656

Jacobson MD, Weil M, and Raff M. (1997). Programmed cell death in animal development. Cell 88:347–354

Janssen JJ, Klaver SM, Waisfisz Q, Pasterkamp G, de Kleijn DP, Schuurhuis GJ, Ossenkoppele GJ.(2005). Identification of genes potentially involved in disease transformation of CML. Leukemia 19: 998–1004

Kane M. (1995). Global program for control of hepatitis B infection. Vaccine, 13: S47–S49

Kao JH. (2002). Hepatitis B viral genotypes: clinical relevance and molecular characteristics. J. Gastroenterol. Hepatol.17: 643–650

Kao JH, Chen DS. (2006).HBV genotypes: epidemiology and implications regarding natural history. Curr. Hepat. Rep.5: 5–13

Kao JH, Chen PJ, Lai MY, Chen DS. (2000). Hepatitis B genotypes correlate with clinical outcomes in patients with chronic hepatitis B. Gastroenterology.118: 554–559

Kao JH, Chen PJ, Lai MY, Chen DS. (2003). Basal core promoter mutations of hepatitis B virus increase the risk of hepatocellular carcinoma in hepatitis B carriers. Gastroenterology. 124: 327–334

Kao JH, Wu NH, Chen PJ, Lai MY, Chen DS. (2000). Hepatitis B genotypes and the response to interferon therapy. J. Hepatol. 33: 998–1002

Kekulé AS, Lauer U, Weiss L, Luber B, Hofschneider PH. (1993). Hepatitis B virus transactivator HBx uses a tumour promoter signalling pathway. Nature. 361:742-745

Kim H, Lee H, and Yun Y. (1998). X-gene product of hepatitis B virus induces apoptosis in liver cells. J. Biol. Chem. 273: 381–385

Kim KH and Seong BL. (2003). Pro-apoptotic function of HBV X protein is mediated by interaction with c-FLIP and enhancement of death-inducing signal. EMBO J. 22: 2104–2116

Kim WH, Hong F, Jaruga B, Zhang ZS, Fan SJ, Liang TJ, Gao B. (2005).Hepatitis B virus X protein sensitizes primary mouse hepatocytes to ethanol- and TNF-alpha-induced apoptosis by a caspase-3-dependent mechanism. Cell Mol Immunol. 2:40–48

Kim YC, Song KS, Yoon G, Nam MJ, and Ryu WS. (2001). Activated ras oncogene collaborates with HBx gene of hepatitis B virus to transform cells by suppressing HBx-mediated apoptosis. Oncogene. 20: 16–23

Kim YS, Ahn YO & Kim DW. (1994). Familial clustering of hepatitis B and C viruses in Korea. Journal of Korean Medical Science. 9:444–449

Kirmizis A, Farnham PJ. (2004). Genomic approaches that aid in the identification of transcription factor target genes. Exp Biol Med (Maywood). 229: 705–721

Koike K, Moriya K, Yotsuyanagi H, Shintani Y, Fujie H, Tsutsumi T, and Kimura S. (1998). Compensatory apoptosis in preneoplastic liver of a transgenic mouse model for viral hepatocarcinogenesis. Cancer Lett. 134: 181–186

Kondo Y, Shen L, Cheng AS, Ahmed S, Boumber Y, Charo C, Yamochi T, Urano T, Furukawa K, Kwabi-Addo B, Gold DL, Sekido Y, Huang TH, Issa JP. (2008). Gene silencing in cancer by histone H3 lysine 27 trimethylation independent of promoter DNA methylation. Nat. Genet. 40:741–750.

Kong HJ, Park MJ, Hong S, Yu HJ, Lee YC, Choi YH, Cheong J.(2003). Hepatitis B virus X protein regulates transactivation activity and protein stability of the cancer-amplified transcription coactivator ASC-2. Hepatology. 38:1258–1266

Kumar V, Jayasuryan N, and Kumar R. (1996). A truncated mutant (residues 58–140) of the hepatitis B virus X protein retains transactivation function. Proc. Natl. Acad. Sci. USA, 93: 5647–5652

Kurbanov F, Tanaka Y, Mizokami M. (2010). Geographical and genetic diversity of the human hepatitis B virus. Hepatol Res.40: 14–30

Kwun HJ, Jang KL. (2004).Natural variants of hepatitis B virus X protein have differential effects on the expression of cyclin-dependent kinase inhibitor p21 gene. Nucleic Acids Res. 32: 2202–2213

Lau WY. and Lai EC (2008). Hepatocellular carcinoma: current management and recent advances. Hepatobiliary Pancreat Dis Int. 7: 237–257.

Lavanchy D. (2004). Hepatitis B virus epidemiology, disease burden, treatment, and current and emerging prevention and control measures. Journal of Viral Hepatitis. 11: 97–107.

Lee WM. (1997). Hepatitis B virus infection. N Engl J Med. 337: 1733–1745.

Leto TL, Fortugno-Erikson D, Barton D, Yang-Feng TL, Francke U, Harris AS, Morrow JS, Marchesi VT, Benz EJ Jr. (1988).Comparison of nonerythroid alpha- spectrin genes reveals strict homology among diverse species. Mol Cell Biol. 8 : 1–9

Levine AJ. (1997). p53, the cellular gatekeeper for growth and division. Cell. 88: 323–331.

Liu Q, Chen J, Liu L, Zhang J, Wang D, Ma L, He Y, Liu Y, Liu Z, Wu J.(2011).The X protein of hepatitis B virus inhibits apoptosis in hepatoma cells through enhancing the methionine adenosyltransferase 2A gene expression and reducing S-adenosyl-methionine production. J Biol Chem. 286:17168–17180

Lok AS, Seeff LB, Morgan TR, di Bisceglie AM, Sterling RK, Curto TM, Everson GT, Lindsay KL, Lee WM, Bonkovsky HL, Dienstag JL, Ghany MG, Morishima C, Goodman ZD; HALT-C Trial Group. (2009). Incidence of hepatocellular carcinoma and associated risk factors in hepatitis C-related advanced liver disease. Gastroenterology 136:138–148.

Lowe SW, Cepero E, and Evan G. (2004). Intrinsic tumour suppression. Nature, 432: 307– 315

Lu YW, Chen WN. (2005).Human hepatitis B virus X protein induces apoptosis in HepG2 cells: role of BH3 domain. Biochem Biophys Res Commun. 338: 1551-1556

Luber B, Lauer U, Weiss L, Hohne M, Hofschneider PH, Kekule AS.(1993). The hepatitis B virus transactivator HBx causes elevation of diacylglycerol and activation of protein kinase C. Res Virol.144:311–321

Maki M, Ma H, Takano E, Adachi Y, Lee W, Hatanaka M, and Murachi T, (1991). Calpastatins: biochemical and molecular biological studies. Biomed. Biochim. Acta, 50: 509–516

Ma NF, Lau SH, Hu L, Xie D, Wu J, Yang J, Wang Y, Wu MC, Fung J, Bai X, Tzang CH, Fu L, Yang M, Su YA, Guan XY.(2008).COOH-Terminal Truncated HBV X Protein Plays Key Role in Hepatocarcinogenesis. Clin Cancer Res. 14: 5061–5068

Manfioletti G, Brancolini C, Avanzi G, and Schneider C. (1993). The protein encoded by a growth arrest-specific gene (gas6) is a new member of the vitamin K-dependent proteins related to protein S, a negative coregulator in the blood coagulation cascade. Mol. Cell. Biol. 13:4976–4985

Manzow S, Brancolini C, Marks F and Richter KH. (1996). Expression of growth arrest-specific (Gas) genes in murine keratinocytes: Gas2 is specifically regulated. Exp. Cell Res. 224: 200–203

Martin SJ and Green DR.(1995). Protease activation during apoptosis: Death by a thousand cuts? Cell. 82:349–352

Martin-Lluesma S, Schaeffer C, Robert EI, van Breugel PC, Leupin O, Hantz O, Strubin M. (2008).Hepatitis B virus X protein affects S phase progression leading to chromosome segregation defects by binding to damaged DNA binding protein 1. Hepatology. 48:1467–1476

McMahon BJ.(2009). The influence of hepatitis B virus genotype and subgenotype on the natural history of chronic hepatitis B. Hepatol. Int. 3: 334–342

Meredith JJ, Mu Z, Saido T and Du X. (1998). Cleavage of the cytoplasmic domain of the integrin b3 subunit during endothelial cell apoptosis. J. Biol. Chem. 273: 19525–19531

Mohr L, Geissler M, Blum HE. (2002). Gene therapy for malignant liver disease. Expert Opin Biol Ther; 2: 163–175

Mohr L, Yeung A, Aloman C, Wittrup D, Wands JR.(2004). Antibodydirected therapy for human hepatocellular carcinoma. Gastroenterology. 127: S225–231

Møller H, Mellemgaard A, Lindvig K, Olsen JH. (1994) Obesity and cancer risk: a Danish record-linkage study. Eur J Cancer. 30A:344–350

Montalto G, Cervello M, Giannitrapani L, Dantona F, Terranova A, Castagnetta LA.(2002). Epidemiology, risk factors, and natural history of hepatocellular carcinoma. Ann N Y Acad Sci.963:13–20.

Na S, Chuang TH, Cunningham A, Turi TG, Hanke JH, Bokoch GM, Danley DE. (1996). D4-GDI, a substrate of CPP32, is proteolyzed during Fas-induced apoptosis. J. Biol. Chem. 271:11209–11213

Neuschwander-Tetri BA, Caldwell SH. (2003).Nonalcoholic steatohepatitis: summary of an AASLD Single Topic Conference. Hepatology.37:1202–1219

Nicholson DW, Ali A, Thornberry NA, Vaillancourt JP, Ding CK, Gallant M, Gareau Y, Griffin PR, Labelle M, Lazebnik YA, Munday NA, Paju SM, Smulson MK, Yamin TT, Yu V& Miller DK(1995).Identification and inhibition of the ICE/CED-3 protease necessary for mammalian apoptosis. Nature. 376: 37–43

Ni YH, Chang MH, Huang LM, Chen HL, Hsu HY, Chiu TY, Tsai KS, Chen DS.(2001).Hepatitis B virus infection in children and adolescents in a hyperendemic area: 15 years after mass hepatitis B vaccination. Ann. Intern. Med. 135, 796–800

Noh EJ, Jung HJ, Jeong G, Choi KS, Park HJ, Lee CH and Lee JS.(2004). Subcellular localization and transcriptional repressor activity of HBx on p21(WAF1/Cip1) promoter is regulated by ERK-mediated phosphorylation. Biochem Biophys Res Commun. 319: 738–745

Nuoffer C, Jeno¨ P, Conzelmann A and Riezman H. (1991). Determinants for glycophospholipid anchoring of the Saccharomyces cerevisiae GAS1 protein to the plasma membrane. Mol. Cell. Biol. 11: 27–37

Ohishi W, Fujiwara S, Cologne JB, Suzuki G, Akahoshi M, Nishi N, Takahashi I, Chayama K. (2008).Risk factors for hepatocellular carcinoma in a Japanese population: A nested case-control study. Cancer Epidemiol Biomarkers Prev.17:846–854

Ohki T, Tateishi R, Sato T, Masuzaki R, Imamura J, Goto T, Yamashiki N, Yoshida H, Kanai F, Kato N, Shiina S, Yoshida H, Kawabe T, Omata M. (2008). Obesity is an independent risk factor for hepatocellular carcinoma development in chronic hepatitis C patients. Clin. Gastroenterol. Hepatol. 6: 459–464

Olinger CM, Jutavijittum P, Hübschen JM, Yousukh A, Samountry B, Thammavong T, Toriyama K, Muller CP. (2008). Possible new hepatitis B virus genotype, southeast Asia. Emerg. Infect. Dis.14: 1777–1780.

Ono Y, Sorimachi, H. and Suzuki K. (1998) Structure and physiology of calpain, an enigmatic protease. Biochem. Biophys. Res. Commun. 245: 289–294.

Ozturk M. (1999).Genetic aspects of hepatocellular carcinogenesis. Semin Liver Dis 19: 235-242

Pardee, AB. (1987). The yang and yin of cell proliferation: an overview. J. Cell. Physiol. Suppl. 5:107-110

Parkin DM, Bray F, Ferlay J Pisani P. (2005). Global cancer statistics, 2002.CA Cancer J Clin.55:74 –108

Parkin DM. (2006). The global health burden of infection-associated cancers in the year 2002. Int J Cancer. 118:3030–3044

Pariat M, Carillo S, Molinari M, Salvat C , Debussche L, Bracco L, Milner J and Piechaczyk M. (1997). Proteolysis by calpains: a possible contribution to degradation of p53. Mol. Cell. Biol.17: 2806–2815

Pei Z, Chu L, Zou W, Zhang Z, Qiu S, Qi R, Gu J, Qian C, Liu X. (2004).An oncolytic adenoviral vector of Smac increases antitumor activity of TRAIL against HCC in human cells and in mice. Hepatology.39: 1371–1381

Petricoin EF 3rd, Espina V, Araujo RP, Midura B, Yeung C, Wan X, Eichler, GS, Johann DJ, Jr, Qualman S, Tsokos M, Krishnan K, Helman LJ, Liotta LA. (2007). Phospho protein pathway mapping: Akt/mammalian target of rapamycin activation is negatively associated with childhood rhabdomyosarcoma survival. Cancer Res. 67:3431–3440

Petroulakis E, Parsyan A, Dowling RJ, LeBacquer O, Martineau Y, Bidinosti M, Larsson O, Alain T, Rong L, Mamane Y, Paquet M, Furic L, Topisirovic I, Shahbazian D, Livingstone M, Costa-Mattioli M, Teodoro JG, Sonenberg N (2009). p53-dependent translational control of senescence and transformation via 4E-BPs. Cancer Cell. 16:439-446

Poon D, Anderson BO, Chen LT, Tanaka K,Lau WY, Van Cutsem E, Singh H, Chow WC, Ooi LL, Chow P, Khin MW, Koo WH; Asian Oncology Summit. Management of hepatocellular carcinoma in Asia: Consensus statement from the Asian Oncology Summit 2009. Lancet Oncol.10:1111–1118

Porn-Ares M, Samali A, and Orrenius S. (1998). Cleavage of the calpain inhibitor, calpastatin, during apoptosis. Cell Death Differ. 5:1028–1033

Porter A.G. and Janicke RU. (1999). Emerging roles of caspase-3 in apoptosis. Cell Death Differ. 6:99–104

Puisieux A, Galvin K, Troalen F, Bressac B, Marcais C, Galun E, Ponchel F, Yakicier C, Ji J and Ozturk M. (1993). Retinoblastoma and p53 tumor suppressor genes in human hepatoma cell lines. FASEB J. 7: 1407–1413

Qadri I, Ferrari ME, Siddiqui A. (1996). The hepatitis B virus transactivator protein, HBx, interacts with single-stranded DNA (ss-DNA). Biochemical characterizations of the HBx-ssDNA interactions. J Biol Chem. 271:15443–15450

Qian GS, Ross RK, Yu MC, Yuan JM, Gao YT, Henderson BE, Wogan GN, Groopman JD.(1994). A follow-up study of urinary markers of aflatoxin exposure and liver cancer risk in Shanghai, People's Republic of China. Cancer Epidemiol Biomarkers Prev.3:3–10

Quade K, Saldanha J, Thomas H and Monjardino J.(1992). Integration of hepatitis B virus DNA through a mutational hot spot within the cohesive region in a case of hepatocellular carcinoma. J. Gen. Virol., 73: 179–182

Saleh M, Stacker SA, Wilks AF.(1996). Inhibition of growth of C6 glioma cells in vivo by expression of antisense vascular endothelial growth factor sequence. Cancer Res. 56:393–401

Sangro B, Herraiz M, Prieto J. (2003) Gene therapy of neoplastic liver diseases. Int J Biochem Cell Biol. 35:135–148

Sangro B, Qian C, Schmitz V, Prieto J. (2002).Gene therapy of hepatocellular carcinoma and gastrointestinal tumors. Ann NY Acad Sci; 963:6–12

Sanyal AJ, Moyner E, Barghout V. (2009). Retrospective claims database analysis of elderly compared with nonelderly patients (pts) with newly diagnosed hepatocellular carcinoma (HCC) [abstract 9552]. J Clin Oncol. 27:496s

Satoh T, Enokido Y, Aoshima H, Uchiyama Y and Hatanaka H.(1997). Changes in mitochondrial membrane potential during oxidative stress-induced apoptosis in PC12 cells. J Neurosci Res. 50: 413–420

Satyanarayana A, Manns MP, Rudolph KL.(2004). Telomeres and telomerase: a dual role in hepatocarcinogenesis. Hepatology. 40: 276–283

Sayan AE, Sayan BS, Findikli N, Ozturk M. (2001) Acquired expression of transcriptionally active p73 in hepatocellular carcinoma cells. Oncogene. 20:5111–5117

Schneider C, King R. and Philipson L. (1988). Genes specifically expressed at growth arrest of mammalian cells. Cell 54: 787–793

Schneider R, and Sonenberg N. (2007). Translational control in cancer development and progression. In Translational Control in Biology and Medicine, M. Mathews, N. Sonenberg, and J. Hershey, eds. (Cold Spring Harbor, NY: Cold Spring Harbour Laboratory Press).

Schuster R, Gerlich WH, and Schaefer S.(2000). Induction of apoptosis by the trans-activating domains of the hepatitis B virus X gene leads to suppression of oncogenic transformation of primary rat embryo fibroblasts. Oncogene. 19: 1173–1180

Seeger C, Mason WS. (2000). Hepatitis B virus biology. Microbiol Mol Biol Rev. 64: 51–68

Sirma H, Giannini C, Poussin K, Paterlini P, Kremsdorf D, and Brechot C. (1999).Hepatitis B virus, X mutants, present in hepatocellular carcinoma tissue abrogate both the antiproliferative and transactivation effects of HBx.

Oncogene, 18: 4848–4859

Sgorbissa A, Benetti R, Marzinotto S, Schneider C and Brancolini C.(1999). Caspase-3 and caspase-7 but not caspase-6 cleave Gas2 in vitro: implications for microfilament reorganization during apoptosis. J. Cell Sci. 112: 4475–4482.

Smit DJ, Smith AG, Parsons PG, Muscat GE, and Sturm RA (2000). Domains of Brn-2 that mediate homodimerization and interaction with general and melanocytic transcription factors. Eur. J. Biochem. 267:6413–6422

Snipes GJ, Suter U, Welcher AA, and Shooter EM. (1992). Characterization of a novel peripheral nervous system myelin protein (PMP-22/SR13). J. Cell. Biol. 117:225–238

Sorimachi H, Ishiura S, and Suzuki K. (1997). Structure and physiological function of calpains. Biochem. J. 328:721–732

Sto¨ckl L, Berting A, Malkowski B, Foerste R, Hofschneider PH and Hildt E. (2003).Integrity of c-Raf-1/MEK signal transduction cascade is essential for hepatitis B virus gene expression. Oncogene. 22: 2604–2610

Stroffolini T, Andreone P, Andriulli A, Ascione A, Craxì A, Chiaramonte M, Galante D, Manghisi OG, Mazzanti R, Medaglia C, Pilleri G, Rapaccini GL, Albanese M, Taliani G, Tosti ME, Villa E, Gasbarrini G. (1999). Gross pathologic types of hepatocellular carcinoma in Italy. Oncology. 56:189–192

Su F, and Schneider RJ.(1997). Hepatitis B virus HBx protein sensitizes cells to apoptotic killing by tumor necrosis factor alpha. Proc. Natl. Acad. Sci. USA, 94: 8744–8749

Su F, Theodosis CN, and Schneider RJ. (2001).Role of NF-κB and myc proteins in apoptosis induced by hepatitis B virus HBx protein. J. Virol. 75: 215–225

Sung WK, Lu Y, Lee CW, Zhang D, Ronaghi M, Lee CG. (2009). Deregulated Direct Targets of the Hepatitis B Viral (HBV) protein, HBx, identified through chromatin immunoprecipitation and expression microarray profiling. J Biol Chem. 284:21941–21954

Suriawinata A, Xu R. (2004). An update on the molecular genetics of hepatocellular carcinoma. Semin Liver Dis. 24: 77–88

Suzuki K and Sorimachi H (1998). A novel aspect of calpain activation. FEBS Lett., 433, 1–4

Takada S, Shirakata Y, Kaneniwa N, and Koike K.(1999). Association of hepatitis B virus protein with mitochondria causes mitochondrial aggregation at the nuclear periphery, leading to cell death. Oncogene, 18: 6965–6973

Tan X and Wang JY. (1998) The caspase–RB connection in cell death. Trends Cell Biol.8: 116–120

Tarn C, Lee S, Hu Y, Ashendel C and Andrisani OM. (2001).Hepatitis B virus X protein differentially activates RAS-RAF-MAPK and JNK pathways in X-transforming versus non-transforming AML12 hepatocytes. J Biol Chem. 276: 34671–34680

Tatematsu K, Tanaka Y, Kurbanov F, Sugauchi F, Mano S, Maeshiro T, Nakayoshi T, Wakuta M, Miyakawa Y, Mizokami M.(2009). A genetic variant of hepatitis B virus divergent from known human and ape genotypes isolated from a Japanese patient and provisionally assigned to new genotype J. J. Virol. 83: 10538–10547.

Terradillos O, Pollicino T, Lecoeur H, Tripodi M, Gougeon ML, Tiollais P and Buendia MA. (1998). p53-independent apoptotic effects of the hepatitis B virus HBx protein in vivo and in vitro. Oncogene. 17: 2115–2123

Thomas RK, Nickerson E, Simons JF, Jänne PA, Tengs T, Yuza Y, Garraway LA, LaFramboise T, Lee JC, Shah K, O'Neill K, Sasaki H, Lindeman N, Wong KK, Borras AM, Gutmann EJ, Dragnev KH, DeBiasi R, Chen TH, Glatt KA, Greulich H, Desany B, Lubeski CK, Brockman W, Alvarez P, Hutchison SK, Leamon JH, Ronan MT, Turenchalk GS, Egholm M, Sellers WR, Rothberg JM, Meyerson M. (2006). Sensitive mutation detection in heterogeneous cancer specimens by massively parallel picoliter reactor sequencing. Nat Med. 12:852–855

Thorgeirsson SS, Grisham JW.(2002).Molecular pathogenesis of human hepatocellular carcinoma. Nat Genet 31: 339–346

Thuy PT, Alestig E, Liem NT, Hannoun C, Lindh M. Genotype X/C recombinant (putative genotype I) of hepatitis B virus is rare in Hanoi, Vietnam-genotypes B4 and C1 predominate. J. Med. Virol 2010; 82: 1327–1333

Tiribelli C, Melato M, Crocè LS, Giarelli L, Okuda K, Ohnishi K. (1989).Prevalence of hepatocellular carcinoma and relation to cirrhosis: comparison of two different cities of the world – Trieste, Italy, and Chiba, Japan. Hepatology. 10: 998–1002

Tran TT, Trinh TN, Abe K.(2008). New complex recombinant genotype of hepatitis B virus identified in Vietnam. J. Virol. 82: 5657–5663

Tu H, Bonura C, Giannini C, Mouly H, Soussan P, Kew M, Paterlini-Bréchot P, Bréchot C, Kremsdorf D.(2001).Biological impact of natural COOH-terminal deletions of hepatitis B virus X protein in hepatocellular carcinoma tissues. Cancer Res. 61:7803–7810

Unger T, Shaul Y.(1990). The X protein of the hepatitis B virus acts as a transcription factor when targeted to its responsive element. EMBO J. 9:1889–1895

Van Steensel B. (2005). Mapping of genetic and epigenetic regulatory networks using microarrays. Nat Genet. 37 Suppl:S18–24

Wang PC, Hui EK, Chiu JH, and Lo SJ. (2001). Analysis of integrated hepatitis B virus DNA and flanking cellular sequence by inverse polymerase chain reaction. J. Virol. Methods, 92: 83–90

Wang XW, Forrester K, Yeh H, Feitelson MA, Gu JR, Harris CC.(1994). Hepatitis B virus X protein inhibits p53 sequence-specific DNA binding, transcriptional activity, and association with transcription factor ERCC3. Proc Natl Acad Sci USA.91:2230–2234.

Wang Y, Lau SH, Sham JST,Wu MC,Wang T, Guan XY.(2004). Characterization of HBV integrants in 14 hepatocellular carcinomas: association of truncated X gene and hepatocellular carcinogenesis. Oncogene. 23:142–148

Wolk A, Gridley G, Svensson M, Nyrén O, McLaughlin JK, Fraumeni JF, Adam HO. (2001).A prospective study of obesity and cancer risk (Sweden). Cancer Causes Control. 12:13–21

World Health Organization [WHO]. (2000). Hepatitis B fact sheet. Retrieved October 30, 2007, from http://www.who.int/mediacentre/factsheets/ fs204/en/

World Health Organization [WHO]. 2008. Hepatitis B fact sheet.

Xu GW, Sun ZT, Forrester K, Wang XW, Coursen J, Harris CC.(1996). Tissues pecific growth suppression and chemosensitivity promotion in human hepatocellular carcinoma cells by retroviral-mediated transfer of the wild type p53 gene. Hepatology. 24:1264–1268

Xu R, Zhang X, Zhang W, Fang Y, Zheng S, Yu XF, (2007). Association of human APOBEC3 cytidine deaminases with the generation of hepatitis virus B antigen mutants and hepatocellular carcinoma. Hepatology 46: 1810–1820

Yoshizawa H. (2002). Hepatocellular carcinoma associated with hepatitis C virus infection in Japan: projection to other countries in the foreseeable future. Oncology.62(Suppl 1):8–17

Yu MC, Yuan JM.(2004). Environmental factors and risk for hepatocellular carcinoma. Gastroenterology.127: S72–78

Yuan J. (1997). Transducing signals of life and death. Curr. Opin. Cell Biol. 9: 247–251.

Yuen MF, Tanaka Y, Mizokami M, Yuen JC, Wong DK, Yuan HJ, Sum SM, Chan AO, Wong BC, Lai CL.(2004). Role of hepatitis B virus genotypes Ba and C, core promoter and precore mutations on hepatocellular carcinoma: a case control study. Carcinogenesis. 25: 1593–1598

Zetterberg A, Larsson O.(1985). Kinetic analysis of regulatory events in Gl leading to proliferation or quiescence of Swiss 3T3 cells. Proc. Natl. Acad. Sci. USA 82: 5365–5369

Zhang YJ, Chen Y, Ahsan H, Lunn RM, Chen SY, Lee PH, Chen CJ, Santella RM. (2005).Silencing of glutathione Stransferase P1 by promoter hypermethylation and its relationship to environmental chemical carcinogens in hepatocellular carcinoma. Cancer Lett. 221:135–143

PUBLICATIONS

Accepted manuscript

Yip WK, Cheng ASL, **Zhu R**, Lau SS, Chen Y, Sung JG, Lai PBS, Ng EKO, Yu Y, Wong N, To KF, Wong VWS, Sung JJ, Chan HLY. (2011) Carboxyl-terminal truncated HBx regulates a distinct microRNA transcription program in hepatocellular carcinoma development. PLoS ONE (in press)

Manuscript in preparation

Zhu R, Cheng ASL, Lau SS, Kang W, Chen Y, To KF, Wong VWS, Sung JJ, Chan HLY. (2011) Genome-wide binding analysis of carboxyl-terminal truncated HBx reveals direct repression of a negative growth regulator, *GAS2*, in hepatocellular carcinoma.

Published abstracts

Zhu R, Cheng ASL, Lau SS, Chen Y, Lee TL, Wong VWS, Sung JJ, Chan HLY. (2011) Genome-wide binding analysis of carboxyl-terminal truncated HBx reveals direct repression of a negative growth regulator, *GAS2*, in hepatocellular carcinoma. Gastroenterology (2011 Digestive Disease Week Abstract Supplement) Program 868#, page379 (Selected for oral presentation in AGA Research Forum: Tumor Suppressor Gene in GI cancers, Chicago, USA, May 7-10, 2011).

Cheng ASL, **Zhu R**, Lau SS, Yip WK, Chen Y, Wong VWS, Chan HLY, Sung JJ. (2010) Elucidating gene regulatory network of COOH-terminal truncated HBx associated with hepatocellular carcinoma. Health Research Symposium: Improving health and recognising excellence (Hong Kong SAR, China, September 11, 2011).